IDENTIFYING SEASONAL ENVIRONMENTAL TRIGGER EVENTS AND THEIR INFLUENCE ON SOIL MICROBIAL RESPIRATION AND GREENHOUSE GAS EMISSIONS IN A NOVA SCOTIA AGRICULTURAL SOIL

by

Jaylene Woodworth

Submitted in partial fulfilment of the requirements
for the degree of Master of Science

at

Dalhousie University
Halifax, Nova Scotia
April 2020

TABLE OF CONTENTS

LIST OF TABLES

LIST OF FIGURES

ABSTRACT

N_2O is released from agricultural soils as a result of nitrification and denitrification. These microbial processes are affected by environmental conditions. This study determined a method of predicting trigger environmental events that would induce a response in soil respiration and examined that response under natural field conditions, considering the influence of N-Viro® alkaline biosolid amendment. Additionally, the utility of ^{15}N site preference and the Picarro® Cavity Ring-Down Spectrometer to distinguish the source of N_2O (nitrification or denitrification) from surface flux samples obtained on ^{15}N labelled-NH_4NO_3 sites was investigated. It was confirmed that trigger events influence the magnitude of soil respiration and N_2O emissions from agricultural soils with rewetting events dominating the magnitude of N_2O flux. Indicators of nitrification increased with increasing biosolid amendment rate and NO_3 accumulation was greater at deeper soil depths. The CRDS provided evidence that nitrification was the dominant source of N_2O, based on site preference.

Keywords: nitrous oxide; nitrification; denitrification; trigger event; site preference

LIST OF ABBREVIATIONS USED

°C	degrees Celsius
AEM	anion exchange membrane
ANOVA	analysis of variance
C	carbon dioxide
CH_4^+	methane
CO_2	carbon dioxide
CRDS	cavity ring down spectrometer/spectroscopy
EM50	data logger associated with temp. and VWC
FT	freeze-thaw
GHG	greenhouse gas
GLM	general linear model
HCl	hydrochloric acid
KCl	potassium chloride
N	nitrogen
N_2	dinitrogen
N_2O	nitrous oxide
NH_2OH	hydroxylamine
NH_3^-	ammonia
NH_4^+	ammonium
NO_2^-	nitrite
NO_3^-	nitrate
O_2	oxygen
PAN	plant-available nitrogen
PRS	plant root simulator
RH%	relative humidity
S.P.	site preference
SGWs	soil gas wells
VWC	volumetric water content
WFPS	water-filled pore space

ACKNOWLEDGEMENTS

Academic
Thank-you to my supervisor and committee members, *Dr. David Burton*, *Dr. Gordon Price*, and *Dr. Peter Havard* for their patience and guidance as I navigated my way through soil science; as well as for their support as I explored career opportunities during my studies.

Drucie Janes, *Weixi Shu*, *Yu Zhang*, *Marla McNutt*, and *Abdiraham Haiye*, thank-you for your assistance with this project. Whether it be analysis, spreadsheet lessons, or sampling, your support allowed this project to develop into a capacity I am proud of.

Margaret Savard, *Marilyn Roberts*, and *Dr. Raj Lada* thank-you all for the intermittent life coaching and opportunities to stay involved in the agricultural industry during my studies.

*Family and Frie*nds
My deepest apologies to *Geoff Larkin*, who had to live with me for most of this project; thank you for being unconditionally supportive and keeping me sustained when I often took on more than I could handle.

Thank-you to *Myrna Allen* for being the voice of reason in most of my big life decisions; I treasure our time together because I always leave settled (and well-caffeinated).

Jen Klaus, thank-you for your empathy and confidence in me; your friendship is one of the most valuable things to come out of this degree.

Nannie and Carmen, thank-you for your unconditional pride in me. Your faith and support have allowed me to pursue all my ambitions and I will always be grateful for that.

Mom and Dad, thank-you for your support throughout my academic career; there were many times when I doubted my capabilities, but you never did. Your conviction in my capabilities has always stimulated me to challenge myself and that means the world to me.

Dad, thank-you for reading my entire thesis draft and trying to act genuinely interested in the subject. *Chelsee*, you will not be compensated for helping me sample corn plots in snowstorms; but thank-you for shivering with me and still choosing to pursue a career in agriculture.

CHAPTER 1: INTRODUCTION

1.1 Nitrogen use in Agriculture

Nitrogen (N) is an essential element present in the atmosphere as di-nitrogen gas (N_2). N is present in amino acids and chlorophyll, two components that are vital to plant growth, hence its presence is imperative to primary production. In a natural system, N present in the atmosphere and the soil environment is transformed (mainly by soil microorganisms) to support plant growth. When the plant dies, decomposers return the N to the environment and the cycle is balanced. Leguminous plants can fix N from the atmosphere; but many forage grasses and other crops require additional N, in the form of fertilizers, to supplement their growth. Fertilizers are created by converting atmospheric N (N_2) into plant-available forms through high heat and pressure reactions, i.e. the Haber-Bosch process (Winiwarter et al., 2013). Fertilizers have enhanced our ability to provide N to plants and were one of the main drivers of the Green Revolution, which fed a growing population without increasing land base during the late 1960s.

Common components of agricultural fertilizers, ammonium (NH_4^+) and nitrate (NO_3^-) are both assimilated by plants; however, NO_3^- is highly mobile and can be taken up faster. NH_4^+ tends to bind to clay particles and consequently may be converted to other forms or be lost to the surrounding environment before it is reached by plant roots. Thus, when improperly managed, N is a major pollutant in terms of gaseous emissions (Nevison and Holland, 1997) as well as ground and surface water contamination (Ding et al., 2006). Excess N alters the natural N cycle and will continue to cause global issues over the next century (Rockström et al., 2009).

Nitrous Oxide Emissions

Greenhouse gases (GHG) are gases in the atmosphere that capture radiant energy, contributing to the greenhouse effect and warming the atmosphere. The use of N fertilizer in agriculture accounts for 66% of global nitrous oxide (N_2O) emissions (Winiwarter et al., 2013). N_2O is a GHG and has a global warming potential of up to 298 times greater than carbon dioxide (CO_2) when considered over 100 years (Butterbach-Bahl et al., 2013). Canadian agriculture contributes 8% to total Canadian GHG emissions, mainly in the forms of methane (CH_4^+) and N_2O (Gregorich et al., 2005). Additionally, the use of synthetic N fertilizers on agricultural soils more than doubles N_2O emissions (Butterbach-Bahl et al., 2013) through the excess supply of NO_3^-, which increases the rate of denitrification in saturated soils (International Plant Nutrition Institute, 2019) and the extent to which N_2O is the final product of denitrification in aerobic soils (Burton et al., 2008). Hence, agricultural soils are the greatest single source of N_2O emissions (Risk et al., 2013). As a result, the agricultural sector is being challenged to increase the efficiency of N fertilizer use to reduce environmental impacts, including N_2O emissions (Nol et al., 2012; Soto Golcher et al., 2018).

Water Pollution

Serious N pollution in water (10-50 mg $N.L^{-1}$) has occurred globally as a result of agricultural production. Furthermore, the use of N fertilizers in agriculture is predicted to double, reaching 80-172 Tg $N.yr^{-1}$ over 100 years ending in 2100 (Winiwarter et al., 2013). N contamination of water occurs when excess N becomes mobile and reaches water sources through run-off or leaching. Run-off ensues when soils become saturated and a weather event, i.e. a thaw or a precipitation event, occurs that adds water to saturated soils. Excess N is lost to flooding on frozen ground and is carried away with floodwater, often entering other surface water bodies. Leaching occurs when N

percolates into soils and travels through groundwater routes. A model developed by Agriculture and Agri-Food Canada suggested that the risk of water contamination in Atlantic Canada from agricultural sources had tripled between 1981 and 2006 (De Jong et al., 2009) due to increased use in synthetic fertilizers, an increase in livestock numbers, and increase of legume crop acreage. The Guidelines for Canadian Drinking Water Quality suggest that the maximum acceptable concentrations for NO_3-N and nitrite-N (NO_2-N) in drinking water are 3 $mg.L^{-1}$ and 1 $mg.L^{-1}$ respectively (Health Canada, 2017). Excess N leaving agricultural soil environments threatens water quality by increasing the loading of NO_2^- and NO_3^- to groundwater.

A meta-analysis by Cramer et al. (2001) suggests that 'pre-industrial' (before 1860s) CO_2 would have been 290 ppm. In December of 2018, that number had climbed to 408 ppm (Earth Systems Research Lab, 2018). Rising atmospheric CO_2 promotes global temperature increases, in turn providing ideal environments for microbial respiration. This cycle causes concern globally and emphasizes the need to reduce emissions. Additionally, as atmospheric CO_2 rises, photosynthesis rates increase and thus terrestrial C storage grows (Cao and Woodward, 1998). The rate at which the terrestrial C sink is converted into a C source is dependent on soil respiration at any given time, as a function of temperature. GHG emissions are released by a variety of anthropogenic activities, including agricultural production, as shown in Table 1.

Table 1. Typical greenhouse gas emissions from agricultural practices.

Agricultural practice	**GHG Emissions released**
Biomass burning	CO_2 CH_4 N_2O black C
Ploughing, ridging, mound construction	CO_2
Manuring (heap)	N_2O CH_4 CO_2
Residual removal and burning	N_2O CO_2 black C
Excessive drainage	CO_2 N_2O

Dyson (2008) said that "if we control what plants do with carbon, the fate of CO_2 in the atmosphere is in our hands". Decreasing atmospheric CO_2 enrichment through climate change mitigation strategies increases soil organic carbon, improves soil quality, and increases crop productivity (Ashworth et al., 2014). Improving soil C storage requires adding new C without facilitating mineralization of that C and existing organic matter (van Kessel et al., 2000); retaining residue, applying nutrient (in the form of manures or N fertilizer), establishing cover crops, and implementing conservation tillage practices are all mitigation strategies which increase the soil C content of agricultural lands (Lorenz and Lal, 2005). Best management practices, such as those listed above, are characteristic of grassland production systems because soils are not continually disturbed to accommodate annual cropping. Minimal disruption accommodates greater root penetration and carbon storage (Cui et al., 2014, Soussana et al., 2004).

1.2 Soil Nitrogen Processes

The main N processes occurring in soil systems are fixation, mineralization, nitrification, denitrification, volatilization, and immobilization as described in Table 2.

Table 2. Nitrogen processes in soil systems. Adapted from Johnson et al., 2005.

N fixation: atmospheric N is converted to a plant-available form	$N_2 \rightarrow R\text{-}NH_2$
N mineralization: converts organic N into inorganic forms	$R\text{-}NH_2 \rightarrow NH_3 \Leftrightarrow NH_4^+$
Nitrification: two-step conversion of ammonium to nitrite, and then to nitrate	$NH_4^+ \rightarrow NO_2^- \rightarrow NO_3^-$
Denitrification: Nitrate is converted to nitrous oxide and di-nitrogen	$NO_3^- \rightarrow NO_2^- \rightarrow NO \rightarrow N_2O \rightarrow N_2$
Volatilization: N is lost to the atmosphere through the conversion of ammonium to ammonia	Urea $\rightarrow NH_4^+ \Leftrightarrow NH_3$
N immobilization: uptake of inorganic N forms by soil heterotrophs and its use to make organic N forms	NH_4^+ and /or $NO_3 \rightarrow R\text{-}NH_2$

Mineralization and *immobilization* are controlled mainly by the carbon:nitrogen (C:N) ratio of inputs or the quality of the available C source (Robertson and Groffman, 2007). Microbes, which carry out these processes, utilize organic carbon compounds to obtain C and energy (Coleman et al., 2004). A portion of the C contained in the organic compound is oxidized to obtain energy and released as CO_2. A portion of the organic compound is used to synthesize new organic molecules, many of which are N containing molecules. The release of excess N as NH_4^+ is referred to as mineralization. The use of inorganic N (NH_4^+ and NO_3^-) in the formation of these organic molecules is referred to as *immobilization*. Low C:N organic matter (e.g. manures, legumes) are broken down by microbes faster than lignin-rich inputs (e.g. straw, woodchips) because these are generally simpler organic molecules (e.g., amino acids) and additional N is not needed to support microbial growth (Tisdale, 1993). Thus, lower C:N ratios are usually recommended for crop inputs because N is not tied up in the decomposition process and becomes available as a nutrient source to the crop. C:N ratios below 20:1 support rapid decomposition and thus generate more plant-available N (PAN) for crops. This recommendation is based on the N to crude protein conversion factor of 16.7 (Hoorman, 2010). The ideal C to N ratio of 16.7:1 ensures that adequate N is available to sustain microbial functions without limiting PAN.

Nitrification is an aerobic process, i.e. requires oxygen, that usually occurs in the uppermost part of the soil horizon. This process is inhibited by low soil pH (< 5 pH units), but heterotrophic nitrification (with aerobic denitrification) can take place if adequate C is provided. Heterotrophic nitrifiers are microorganisms that consume organic materials for energy and C and nitrify N solely as a by-product, instead of as an energy source (Robertson and Groffman, 2007). Fungi and some bacteria are the main contributors to this process (Wrange et al., 2001). Autotrophic nitrifiers oxidize NH_4^+ into NO_3^- via NO_2^-

in the presence of oxygen (O_2). Thus, nitrification is regulated mainly by NH_4^+ supply (Robertson, 1989). *Nitrobacteriaceace* carry out autotrophic nitrification and constitute two groups: NH_4^+ oxidizers and the NO_2^- oxidizers (Wrange et al., 2001). Traditionally, it was accepted that these two groups were both needed to carry out stepwise autotrophic nitrification (Winogradsky, 1891) but some organisms can do both steps themselves (comammox) (Koch et al., 2018). Three bacterial species of the genus *Nitrospira* (Daims et al., 2015; and Pinto et al., 2016) have demonstrated the ability to oxidize both NH_4^+ and NO_2^-.

Denitrification is an anaerobic process resulting in the reduction of NO_3^- to N_2O and N_2 and is the dominant N cycle process once soil water content exceeds 60% water-filled pore space (WFPS) (Ruser et al., 2006). Denitrifiers are heterotrophs that use NO_3^- as an electron acceptor in the absence of O_2 (Wrange et al., 2001). When O_2 is present, reduction of NO_3^-, SO_4^-, and N_2 are inhibited (McGill, 2007) and denitrification does not occur. In soil systems, microsites of reduced O_2 concentration are common in soil aggregates (Schlüter et al., 2018) and thus areas of aerobic and anaerobic conditions occur simultaneously very close to each other. A summary of the main environmental conditions driving nitrification and denitrification are shown in Table 3. In unsaturated soils, denitrification occurs within soil aggregates, in plant litter, and the plant rhizosphere (Parkin et al., 1985). Organic substrates (energy) and NO_3^- become important controlling factors for denitrification, stimulated by available organic C and NO_3.

Table 3. Environmental conditions favoring nitrification and denitrification.

Nitrification	Denitrification
High nitrifier population Soil pH >6.0 Temperature >25 °C Oxygen is available Moisture content is approaching field capacity (WFPS= 60%)	Heterotrophic bacteria, fungi WFPS >60% Limited O_2 Available soil organic C (Risk et al., 2013) Availability of NO_3^+ as elector acceptor

1.3 Nitrification and Denitrification as Sources of Nitrous Oxide

Current research focuses on the process of denitrification at varying temperatures in relation to N_2O production (Bonnett et al., 2013; Lai and Denton, 2018Lee et al., 2019; Phillips et al., 2014; Poh et al., 2015; Maggi and Riley, 2015). N_2O production has been identified in several microbial N pathways- nitrification, denitrification, and nitrifier denitrification (Kool et al., 2009). The transition between environmental conditions favouring nitrification (aerobic) and denitrification (anaerobic) boundaries is where the most N_2O production occurs (the presence of both processes) (Wrange et al., 2001). The relationship between nitrifier and denitrifier community composition in terms of N_2O emissions remains unclear (Ma et al., 2008). There is also interest in N_2O release during periods of freezing and thawing due to evidence that denitrifiers remain active at low temperatures (Tatti et al., 2015; Wagner-Riddle et al., 2017; Wertz et al., 2013). On soils in Eastern Canada amended with conventional manures, N_2O emissions were greatest in January and March (Tatti et al., 2014), a reflection of insulation from air temperature fluctuations due to snow cover. Freeze-thaw events were concentrated in November-December and March-April when soil surfaces were vulnerable to environmental fluctuations. It is speculated that warmer and drier conditions may reduce N_2O emissions (Xu et al., 2016) by reducing NO_3^- leaching from soils and elevating the temperature; which combined, overrode the effect of soil moisture on emissions. Since N_2O is linked to

global warming concerns- it is of interest to identify the environmental factors that are affecting emissions of this GHG.

Zhu et al. (2013) tracked N_2O emissions and their sources (via isotopic spectrometry and NH_3 oxidation inhibition) at varying O_2 concentrations in fertilized soils. At 0% O_2, all N_2O production was sourced from heterotrophic denitrifiers. However, at low O_2 concentrations, between 0.5% and 3% (vol/vol), total N_2O production was split between the source processes of heterotrophic denitrification and nitrifier denitrification. Nitrifier denitrification, affected by temperature and carbon availability, potentially dominates N_2O production in soils with limited O_2 or variable O_2 concentrations and high NO_2^- concentrations (Wrange-Mönnig et al., 2018). *Nitrifier denitrification* is another N process in which nitrifiers reduce NO_2^- to N_2 (Wrange et al., 2001 and Baggs, 2011), this process produces N_2O, like denitrification. Hence the specific pathways of released N_2O are difficult to identify.

To identify the source process of N_2O, stable isotope mass spectrometry is used to determine isotopic signatures of ^{15}N and ^{18}O of the produced N_2O (Baggs, 2008, 2011). The ^{15}N isotope can be used as a tracer to determine the extent that each process is contributing to total N_2O emissions. Since N_2O is a linear molecule with two asymmetric N molecules ($N^-=N^+=O$), the difference between the ratio of ^{15}N:^{14}N of the central and terminal positions of the N_2O molecule, referred to as site preference (SP), can be used to distinguish the source (Denk et al., 2017). SP is calculated as the difference between the $\delta^{15}N$ abundance of the central atom (alpha) minus the $\delta^{15}N$ abundance of the terminal N atom (beta). Values for SP differ depending on the process that produced the N_2O (Toyoda et al., 2015). Estimates of SP values for N_2O produced by various N processes still differ widely throughout the literature. In general, fractionation from

nitrification is higher than that of denitrification (Baggs, 2008). Therefore, N_2O produced from the nitrification process will be depleted in ^{15}N relative to N_2O produced from denitrification. This is usually evident by a more negative abundance (δ) in ^{15}N (Butterbach-Balh et al., 2013), which is believed to be due to the N_2O reduction in denitrification. Some reported SPs for $\delta^{15}N$ in N_2O from denitrification range between -5.1 to 23.3 (Toyoda et al., 2005), with values in the mid-range of 6.3, 13.8 (Bol et al., 2003), and 15.3 (Well et al., 2006). Nitrification values have been reported as -8.3 (Sutka et al., 2003), 1.9 (Well et al., 2006), and within the low 30s (Sutka et al., 2006). Different values are reported based on study procedures, soil characteristics, and environmental conditions. Speculations for determining the source of N_2O based on SP assume that high rates of N (which is available due to the application of N fertilizer) will effectively exclude processes that occur at low N availability, i.e. NO_3^- ammonification, immobilization, and remineralization. In this study, processes of nitrification and denitrification were analyzed as N_2O sources through isotope ratio mass spectrometry, i.e. a Picarro® Cavity Ring-Down Spectrometer.

1.4 Role of local climate on soil biology and hydrology

Nitrification slows but continues over the winter months (Mahendrappa et al., 1966), as nitrifiers adapt to temperature and moisture fluctuations. Savard et al. (2007) established the occurrence of nitrification throughout all seasons in Maritime, Canada climate in a groundwater dual-isotope study. They traced ^{15}N and ^{18}O in water samples over two years and quantified winter NO_3^- production, confirming year-round nitrification. High mineralization and low nitrification rates found in a Mueller study confirm that denitrification precedes nitrification following thaw events (Mueller et al., 2003).

Denitrification has been found to increase with temperature, yet microbial activity occurred even when soil temperatures fell below -4 °C (Wertz et al., 2013).

The Climate Action Network of Canada predicts that Atlantic Canada will "experience more storm events, increasing storm intensity, rising sea levels, storm surges, coastal erosion and flooding from warming in global temperatures" (Climate Action Network of Canada, 2017). Freeze-thaw (FT) events, defined as fluctuations in the temperature around the freezing point of the uppermost soil layer reflect fluctuations in air temperature (Tatti et al., 2014) are likely to become more prevalent as climate change increases variability and frequency of events which cause said fluctuations. In temperate regions, more than half of N_2O emissions are released during FT cycles (Butterbach-Bahl et al., 2013), as these rapid changes in temperature provide nutrient availability to soil microorganisms (which remain active at temperatures below 0 °C (Wertz et al., 2013) and spur soil microbial activity. The activity of soil microbes relies mainly on temperature, moisture, and availability of organic material (C). These conditions are most prevalent in Atlantic Canada in the spring and summer, however, as FTs become more frequent- we hypothesize that soil microbial activity will occur throughout the winter resulting in greater annual N_2O emissions.

1.5 Study Objectives

This study had three main objectives that are addressed in the individual chapters.

1. Develop a method of defining weather events (or "trigger events"), and examine the influence of those trigger events, under field conditions, in prompting soil microbial activity, as measured by soil respiration.

2. Examine the influence of the application rate of the N-Viro® alkaline biosolid amendment on seasonal soil respiration and N_2O emissions in a field lysimeter system.
3. Access the utility of ^{15}N site preference and the Picarro® Cavity Ring-Down Spectrometer to distinguish the source of N_2O, i.e. nitrification or denitrification, from the surface flux samples obtained on ^{15}N labelled-NH_4NO_3 modified sites.

CHAPTER 2: SITE DESCRIPTION, INSTRUMENTATION, AND MANAGEMENT

This study was conducted at the Bio-Environmental Engineering Center (BEEC), Faculty of Agriculture, Dalhousie University in Bible Hill, Nova Scotia, Canada. Nine field-based lysimeter cells (Figure 1) were instrumented with auto logging equipment. The cells were constructed from a mixture of A and B horizon soil layers of a Tormentine series, Ortho Humic Podzol with a sandy loam texture (Appendix A).

Figure 1. Lysimeter cells at Dalhousie Faculty of Agriculture Bio-Environmental Engineering Center.

The cells were 5.79 meters in length and 3.35 meters in width. At the center of each cell, a 1.5 m^2 (approximately 8% of the cell) sub-cell was installed which drained into a sampling hut. The sampling hut was equipped with a tipping bucket system for each lysimeter cell, attached to a Campbell-Scientific logger which recorded flow rate by tracking the number of times the bucket was tipped after being filled. Attached to the tipping buckets were Teledyne ISCO 6712 Full-size Portable Samplers, which collected drainage water into 800 millilitre (mL) bottles during a pre-programmed sampling event (planned during heavy rainfall events based solely on local weather forecasting observations).

An alkaline treated biosolid (N-Viro®) from Halifax Biosolid Processing Facility (Walker Industries Inc.), with a 67% moisture content, was applied to each cell at a rate of either "low" (28 Mg. ha^{-1}) or "high" (42 Mg. ha^{-1}). These rates equated to a manual distribution of 2.8 kg (low) or 4.2 kg (high) over the surface of each cell. A sample composition of the material is shown in Table 4.

Table 4. A sample composition of the N-Viro® biosolid amendment.

Parameter (expressed as % unless otherwise stated)	**As applied**	**Dry Basis**
Dry Matter	61.13	-
pH (pH Units)	10.50	-
Nitrogen	0.57	0.94
Ammonium-N	ND	<0.01
Calcium	10.432	17.066
Potassium	0.518	0.847
K_2O	0.627	1.025
Phosphorus	0.386	0.632
P_2O_5	0.885	1.447
Magnesium	0.210	0.344
Sodium	0.051	0.083
Boron (ppm)	12.26	20.05
Copper (ppm)	56.31	92.12
Iron (ppm)	4795.66	7845.02
Manganese (ppm)	133.89	219.03
Zinc (ppm)	128.51	210.22

Three cells were left as controls and received no biosolid amendment. Thus, the treatments were either low (T1), high (T2), or control (C) (Figure 2).

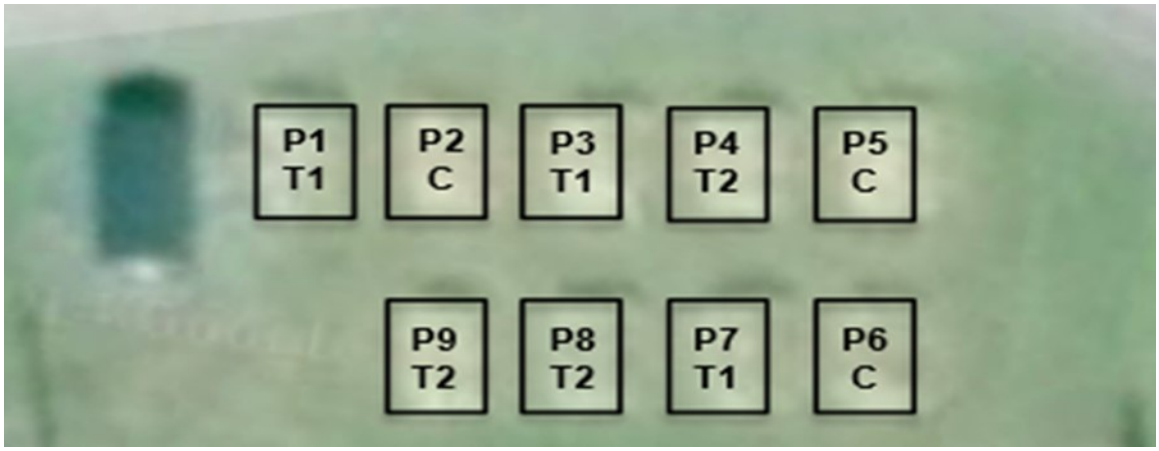

Figure 2. Lysimeter plot layout with biosolid amendment rates T1, T2, and C corresponding to Treatment 1: low, Treatment 2: high, and Control.

The site was cultivated with a rotary hoe after uniformly spreading the biosolid over the surface of each plot, seeded with fall ryegrass (400 g seed.15 m^{-2}) in 2016 and corn (15 000 seeds.$acre^{-1}$) in 2017, and monitored for various parameters throughout the seasons, as described in Table 5.

Table 5. Monitoring devices.

Device	Measurements collected
EM50	Volumetric water content Soil temperature
Weather station	Precipitation Air temperature
Soil gas wells	Carbon dioxide Oxygen
Surface Flux samples	N_2O, CO_2 emissions
ISCOs water sampler	Dissolved nitrous oxide
Cavity ring-down spectrometer	Site preference: $^{15}N^{\alpha}$ and $^{15}N^{\beta}$ Nitrous oxide
Plant root simulator probes and Anion exchange membranes	Soil cumulative nitrate (NO_3^-) Soil cumulative ammonium (NH_4^+)

In December 2016, $^{15}NH_4NO_3$ (1 atom% excess; 25 kg N ha^{-1}) was applied to an m^2 area on the top right-hand side of each cell surrounding the initial location of the soil-gas wells and associated monitoring devices. $^{15}NH_4{}^{15}NO_3$ (5 atom% excess; 25 kg N ha^{-1}) was applied to the entire 1.5 m^2 drainage area at the center of each lysimeter cell. The intent

was that the ^{15}N tracer would assist in determining the source of N_2O production using a Picarro® Cavity Ring-Down Spectrometer. N_2O from nitrification was expected to be quantified by the single-labelled $^{15}NH_4NO_3$, as only the ammonium was labelled, while the double-labelled $^{15}NH_4{}^{15}NO_3$ tracer was added to account for general N_2O and NO_3^- loss from NH_4NO_3 fertilizer application. Hence, the potential pathways of ^{15}N after application would be reflected. A summary of management events is presented in Table 6 and the fates of nitrogen traced in the system are shown in Table 7.

Table 6. Management Summary.

Date	Event	Details
June 28, 2016	Biosolid application #1	Rates Controls cells- 2, 5, 6 at 0 Mg N. ha^{-1} Low cells- 1, 3, 7 at 28 Mg N. ha^{-1} High cells- 4, 8, 9 at 42 Mg N. ha^{-1}
July 02, 2016	Seeding	Fall rye
October 12, 2016	Clipped	Whipper snipping throughout Oct, Nov
December 08, 2016	Labelled fertilizer application	Center 5% atom excess $^{15}NH_4{}^{15}NO_3$, 2.5 $g.m^2$ @ 1 L SGW area 1% atom excess $^{15}NH_4NO_3$, 2.5 $g.m^2$ @ 1 L
May 11, 2017	Biosolid application #2	Rates Controls cells- 2, 5, 6 at 0 Mg N. ha^{-1} Low cells- 1, 3, 7 at 28 Mg N. ha^{-1} High cells- 4, 8, 9 at 42 Mg N. ha^{-1}
Mid-May, 2017	Herbicide Spray #1	Unsuccessful, intended to treat wild mustard but growth did not slow following application
May 31, 2017	Seeding #1	Corn, unsuccessful (birds destroyed)
July 29, 2017	Herbicide Spray #2	Second attempt to treat the wild mustard weed growth
August 01, 2017	Seeding #2	Corn was seeded with netting installed to prevent birds from eating the seeds
August 16-18, 2017	Irrigation	Watered 2 hours/day for 3 days
October 2, 2017	Clipping	Corn stalks removed

Table 7. Potential fates of ^{15}N added to the soil system.

$^{15}NH_4^+$ → Organic N →SOIL→ Anion Exchange Membranes, Plant Root Simulators, soil extractions
$^{15}NH_4^+$ → $^{15}NO_3^-$ → $^{15}N_2O$ → AIR → Cavity Ring-Down Spectrometer, Soil Gas Wells, Surface flux
$^{15}NH_4^+$ → $^{15}NO_3^-$ → WATER → ISCOs Water samplers
$^{15}NH_4^+$ → $^{15}N_2O$ → WATER → ISCOs Water samplers

CHAPTER 3: ROLE OF SOIL WATER CONTENT AND SOIL TEMPERATURE IN TRIGGERING SOIL MICROBIAL ACTIVITY

3.1 Introduction

GHGs absorb infrared radiation and reemit it as heat, increasing the overall atmospheric temperature. The main sources of N_2O are fossil fuel consumption and the application of N fertilizers in agriculture (Signor and Cerri, 2013). N_2O and CO_2 are the main GHGs that are produced from agricultural soils; N_2O being the more serious threat due to its greater warming potential (298%) and increasing growth due to the use of N fertilizers. Microbial activity is responsible for the magnitude of GHG emissions produced from a given soil environment. N_2O emissions increase with changes in soil temperature and moisture (Liu et al., 2015), thus most of the N_2O emissions produced from agricultural soils are produced during episodic weather events (Congreves et al., 2018), such as thaws and rewetting events, that result in dramatic fluctuations in soil moisture and temperature. Overlooking the N_2O emissions produced during these events results in an underestimation of global emissions by nearly 28% (Wagner-Riddle et al., 2017).

Soil microbial activity is regulated by environmental factors (Waghmode et al., 2018) including soil temperature, soil moisture content, carbon availability, and oxygen content; which are all influenced by soil structure (Hursch et al., 2017). Soil moisture, C and N availability, and the temperature and duration of a freeze are the most important conditions dictating the magnitude of N_2O production for a freeze-thaw event (Risk et al., 2013). The production of N_2O from soils during freeze-thaws and rewetting events are the result of one of two mechanisms, sometimes occurring simultaneously. The first mechanism is the physical release of N_2O that was produced throughout the freeze but was previously trapped under frozen surface layers or within films of water in the frozen

surface layers. Burton and Beauchamp (1994) described the winter soil profile as an upper layer, which is prone to experiencing intense fluctuations at thaw, a frozen sub-layer, and a deeper, freely drained sub-surface zone which houses N_2O. The second mechanism is referred to as *de novo*, the N_2O that is newly produced at the onset of the thaw due to environmental conditions that are conducive to biological activity (Risk et al., 2013). During a spring thaw, the presence of water in the soil environment is a result of the balance between precipitation and snowmelt relative to drainage and evaporation rates (Congreves et al., 2018). Infiltration and drainage rates are determined by the presence of a continuous frozen layer and thus, the ability of water to penetrate the surface and sub-surface soil layers.

Flushes of gaseous emissions, sometimes referred to as pulses, are dramatic rises in emissions immediately following a thaw or rewetting event, i.e. a trigger event. In a laboratory study on frozen re-packed soil cores, N_2O and CO_2 emissions increased up to three-fold just a few hours following an induced thaw event (raising the core temperature from -15 °C to 4 °C) (Priemé and Christensen, 2001). Emissions peaked at 24 hours into the thaw and eventually dropped after 15 days. Increased N_2O emissions following freeze-thaw events typically only last a short time, usually a couple of days (Matzner and Borken, 2008). In rewetting events, maximum soil respiration has been measured over 10-15 days after wetting (Guo et al., 2012). It has also been observed that the magnitude of N_2O emissions from freeze-thaw events is approximately related to the number of days soil temperature at a 5 cm depth remained below 0° C (Wagner-Riddle et al., 2017).

Soil temperature is the main driver of soil respiration (Hursch et al., 2016), which explains the release of CO_2 during thaw events. Additionally, as soil pore water warms, it

retains less dissolved N_2O, which explains the release of N_2O as it degasses from the soil profile (Risk et al., 2013). Further, these gaseous flushes represent the biological decomposition of newly available C and N from microbial deaths associated with freezing or desiccation, solubilization of soil organic matter, cryosuction, and aggregate disruption (Guo et al., 2012, Priemé and Christensen, 2001, Risk et al., 2013). Though flushes in GHG emissions are observed in both freeze-thaw and rewetting events, the magnitude of emissions as a result of a freeze-thaw event (1 000%) is usually greater than a rewetting event (500%) (Congreves et al., 2018). N_2O fluxes following a thaw are greater and last longer than those following a rewetting event (Teepe et al., 2001); this may be partially due to the presence of ice layers during freeze-thaw events, which temporarily block O_2 diffusion. Soil respiration and N mineralization are greatest in the first few freeze-thaw cycles and then will decrease following multiple events (Herrmann and Witter, 2002), as substrate sources decline with consumption. Lower temperatures at the time of soil freezing and longer duration of freezing conditions will kill off an increasing amount of microbial life, which makes additional C and N available at the time of thaw. C and N turnover after thawing increases with colder freezing temperatures (Matzner and Borken, 2008) and a rise in availability of C and N feeds surviving and new microbial population, resulting in even greater N_2O emissions at thaw (Risk et al., 2013).

N_2O is produced by several processes in different soil environments. In aerobic environments, N_2O is produced as a by-product of hydroxylamine (NH_2OH) oxidation, while in sub-oxic environments, nitrifiers reduce NO_2^- to N_2O through a process termed nitrifier-denitrification. In anaerobic environments, denitrification produces N_2O as a result of the respiration of nitrogen oxides such as NO_3^- and in acidic soils, N_2O can be produced via chemodenitrification (Risk et al., 2013). Denitrification is usually the main pathway for production following a freeze-thaw event (Priemé and Christensen, 2001),

however, in the absence of a substrate for denitrifiers (NO_3^- and organic C), other pathways may also be involved. Nitrification is active in N_2O production when soil pH and organic matter is high (Bremner, 1997). Seasonal variation has the greatest influence on the diversity of microbial populations and interacts in combination with other factors characterizing a freeze-thaw or rewetting event to influence the magnitude of N_2O emitted. When soil water-filled pore space (WFPS) reaches between 70-90%, N_2O emissions are greatest (Risk et al., 2013, Zhu et al., 2013). The limitation of O_2 supply at high WFPS creates conditions conducive to denitrification and this process dominates at WFPS exceeding 60% (Ma et al., 2008).

Snow cover acts as an insulator, which limits the diurnal fluctuations (daily fluctuations in radiation flux), resulting in less fluctuation in soil moisture and temperature overall and less frost penetration (Congreves et al., 2018). Under thick snow covers, the temperature rarely falls below -10 °C (Henry, 2007), even when the air temperature is much colder (-30 °C). Winters that provide early snowfall and a resulting snowpack will result in shallow freezing depths, while snowfall mid-winter, following soil freezing, deepens the frost depth. Thus, the magnitude of emissions emitted is highly dependent on the preceding weather conditions.

This study was designed to develop a method for categorizing weather events (or "trigger events") that would induce a response in soil respiration, by defining "event thresholds" (thaw events and rewetting events) based on the magnitude of change in soil temperature and soil volumetric water content, respectively. This study further investigates the influence of those trigger events by examining specific "dates of interest" (trigger events that occurred over multiple cells) and their impact on soil respiration (as measured by CO_2 and O_2 within the soil environment) and N_2O flux.

3.2 Materials and Methods

3.2.1 Soil Monitoring

Eosense Soil Gas Wells (SGWs; Eosense, Dartmouth, NS) combined with EM50 dataloggers (for temperature and soil volumetric water content) were installed at a 15 cm depth in each of the nine lysimeter cells at the BEEC research site. The Eosense SGWs were prototype sensors involving an on-board infra-red gas analyzer to detect CO_2 and a chemical sensor to detect O_2, and a data logger to store the readings. The CO_2 sensors were 20 mm nondispersive infra-red sensors with a custom calibration from 0 to 50 000 ppm CO_2 and operating temperature range from -20 to 40 °C. The O_2 sensors were galvanic sensors (Alphasense Ltd, Great Notley, UK). Together these sensors provided continuous measurement of CO_2 ppm, O_2 %, soil temperature (°C), and soil relative humidity (RH%) in the soil profile. Soil water content (vol/vol with an associated error of ±0.08%) and air temperature (°C, with an associated error of ±0.1 °C) were measured continuously at 15 and 30 cm depths and reported on 15-minute intervals using Decagon 5TE soil moisture probes attached to an EM50 datalogger throughout 2015-2017 (Meter Group, Pullman, WA). Equipment functioning was not constant across all cells, and consequently, the dates of available data are not inclusive of the entire season in all cells (Table 8).

Table 8. Dates included in SGW/EM50 monitoring by the cell.

Cell	Dates available
1	11/14/15 – 11/29/17
2	7/08/15 – 11/23/17
3	7/22/15 – 5/13/17
4	7/08/15 – 5/13/17
5	7/08/15 – 11/30/17
6	7/22/15 – 3/23/17
7	7/22/15 – 5/13/17
8	7/22/15 – 5/13/17
9	7/22/15 – 7/07/17

3.2.2 Surface Flux Sampling

Surface CO_2 and N_2O flux samples were collected manually using vented static chambers. For flux measurements, chambers were deployed on permanently placed collars, each being constructed from PVC piping, fitting together to form a closed system over the soil surface. Flux samples were collected from each lysimeter cell on 10-minute intervals using a 25 mL syringe inserted through a septum in the chamber top for a total deployment time of 30 minutes, as per the standard operating procedure outlined in Appendix E. The collar part of the system was an open PVC pipe cut to a height of 10 cm. It was set into the ground at near-surface level (maximum of approximately 5 cm above soil surface) and remained in the cells year-round. On sampling dates, the chamber was set on the collar at time 0 and a syringe was inserted into a suba-seal at the top of the chamber to extract the sample. Each chamber remained on the collar during the 30-minute deployment period and gas samples were collected at 10, 20, and 30 minutes. The 20 mL headspace samples were transferred to sealed 12 mL Labco Exetainer® vials and analyzed for CO_2 and N_2O, and ^{15}N SP on a Varian 3800 Gas Chromograph and Picarro® Cavity Ring-Down Spectrometer, respectively. Each cell contained two collars and thus two sampling locations (Figure 3); one in the center of the cell (drainage tile), and one near the soil-gas well sampler.

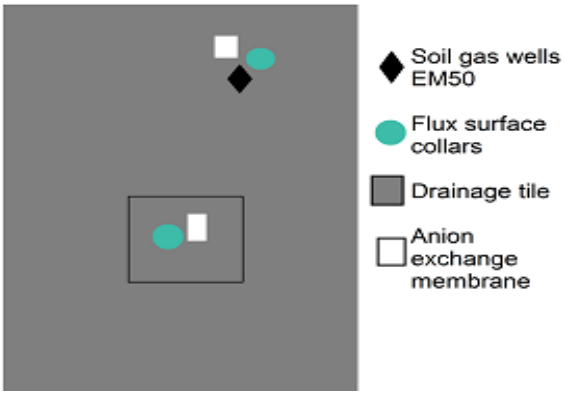

Figure 3. Location of monitoring devices within an individual cell.

3.3 Results

3.3.1 Identifying Influential Weather Events - Rewetting and Thaw Thresholds

Event thresholds were defined in this study based on the magnitude of change in either soil volumetric water content (VWC) or soil temperature that would result in the identification of 10-20 events throughout the observation. Changes in soil temperature relative to the freezing point (0 °C) were used to define thaw events. Changes in soil water content were used to define rewetting events. The impact of each of these events on microbial activity was assessed by measuring the change in CO_2 and O_2 concentrations in the soil. Dates of events were identified based on continuous soil volumetric water content (m^3/m^3) and soil temperature (°C) measurements recorded using auto-logging equipment.

Thaw Events

Thaw events were defined as a 0.1 °C increase in soil temperature above 0 °C. This definition was selected because it resulted in several events that were practical to study, and it reflected an increase in temperature that would result in a thaw (relative to 0 °C). Determining the thaw event threshold that would provide an adequate number of events was similar across all cells, which displayed similar characteristics relative to temperature fluctuation.

Rewetting Events

Defining a rewetting event was somewhat more difficult as it did not reference a specific water content and occurs over the full range of soil temperature. Also, the sensors for detecting soil volumetric water content are somewhat less reliable than those for detecting soil temperature. Individual cells did not behave similarly in terms of change in VWC over time due to variability within the cells and the VWC probes. Thus, obtaining a single rewetting event threshold was more difficult than determining the thawing threshold had been. Appendix B shows rewetting thresholds in increments of a 0.005% change in VWC (m^3/m^3) over 15 minutes and the corresponding number of events expressed in each cell. Rewetting thresholds converged to 0 events (maximum change in water content over 15 minutes) in all plots within a range of 0.05 to 0.185 change in VWC over 15 minutes (Figure 4), disregarding Cell 7 whose convergence represents an outlier in this dataset.

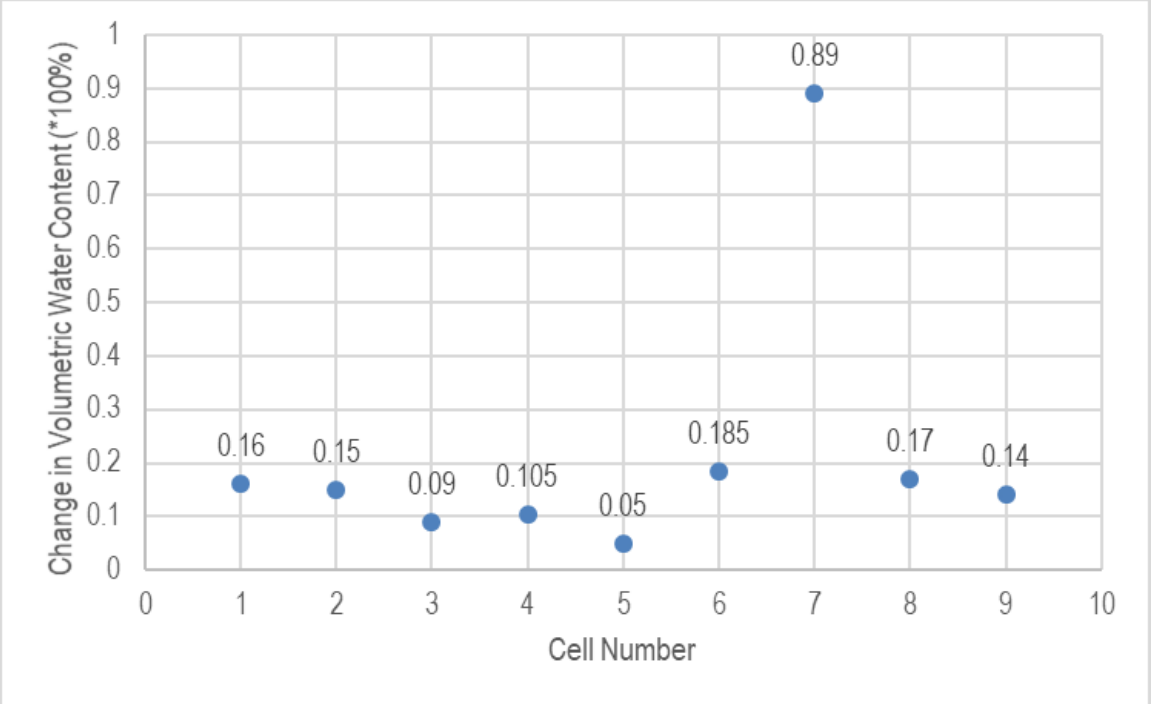

Figure 4. Difference in change in Volumetric Water Content (m^3/m^3) over 15 minutes needed to produce 0 events, i.e. change too large to show events, in each cell.

Rewetting events based on a change of 0.025 (m^3/m^3 VWC) over 15 minutes (Figure 5) produced 10-20 events for most cells however there was considerable variation, even when the amendment rate of alkaline biosolid was considered (4 – 24 events).

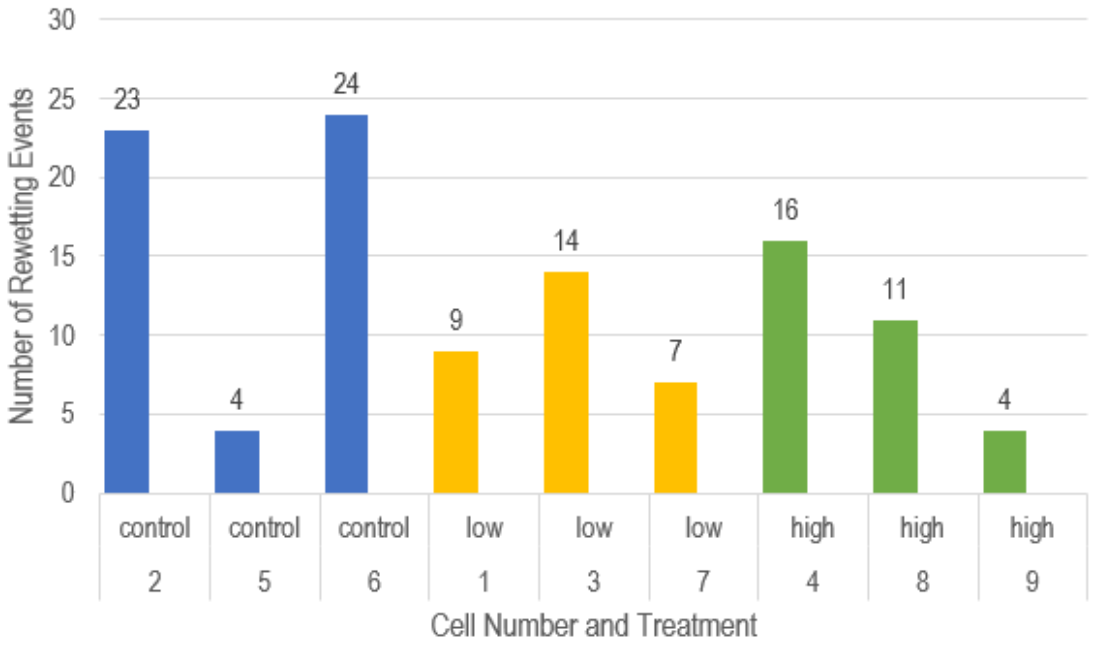

Figure 5. Number of events occurring at 2.5% change in VWC (m^3/m^3) over 15 minutes for each cell. Treatments are displayed in colour.

Individual cells did not show a similar number of rewetting events, thus the individual relationship between rewetting threshold (% change in VWC m^3/m^3 over 15 minutes) and the number of rewetting events was determined (Figure 6). In all cells, the number of events where there was a 0.01% change in VWC over 15 minutes far exceeded 300 (Appendix B), however, the vertical axis has been limited to express a reasonable number of events.

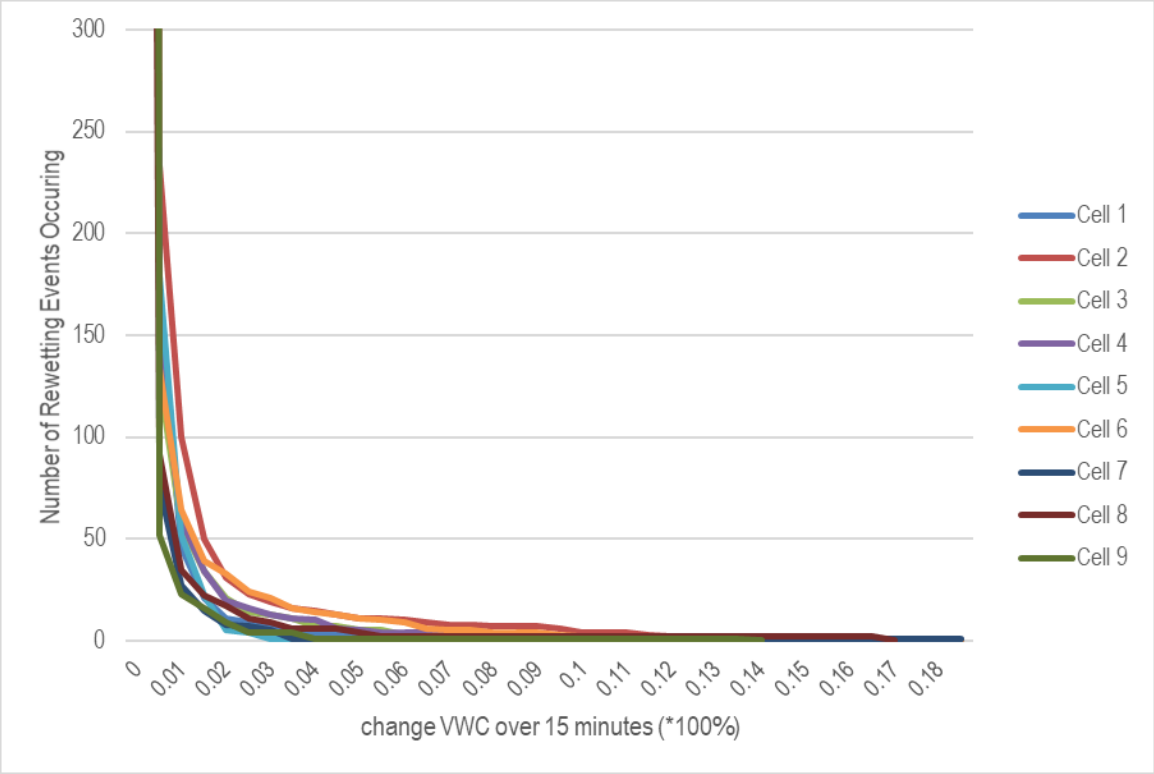

Figure 6. Number of events expressed by rewetting threshold (% change in VWC (m^3/m^3) over 15 minutes) in each cell.

Summary tables of the rewetting thresholds required for the number of events to meet the maximum difference, i.e. no events detected, 5, and 10 events are shown below in Table 9, Table 10, and Table 11. Fluctuations in the number of weather events between small increments (0.005%) were dramatic across cells and thus, not all cells were analyzed for microbial respiration response in the next section.

*Table 9. Rewetting event (change in VWC over 15 minutes (*100%) thresholds of each cell representing relative convergence to the maximum difference (no events detected).*

Threshold at Convergence	Cell								
	1	2	3	4	5	6	7	8	9
Rewetting threshold	0.16	0.15	0.09	0.105	0.05	0.185	0.89	0.17	0.14

*Table 10. Rewetting event (change in VWC over 15 minutes (*100%) thresholds of each cell representing relative convergence to 5 events (defined events occurring).*

Threshold at Convergence	Cell								
	1	2	3	4	5	6	7	8	9
Rewetting threshold	0.03-0.0305	0.095-0.1	0.05	0.05	0.015-0.02	0.07-0.075	0.03	0.3-0.305	0.02-0.025

*Table 11. Rewetting event (change in VWC over 15 minutes (*100%) thresholds of each cell representing relative convergence to 10 events (defined events occurring).*

Threshold at Convergence	Cell								
	1	2	3	4	5	6	7	8	9
Rewetting threshold	0.02-0.025	0.06	0.035-0.04	0.04	0.015-0.02	0.055	0.015-0.02	0.025-0.03	0.015-0.02

Selected Thresholds

The thaw event threshold of 0.1 °C change relative to 0 °C was selected. Thaw trigger events occurred in all but three cells (2, 5, and 8); the average number of thaw events was 19.17. The greatest number of thaw events occurred in Cell 9 (31 events).

A rewetting threshold of 2.5% change in soil VWC (m^3/m^3) over 15 minutes was selected for all cells. The average number of events experienced due to rewetting conditions, as defined, was 10.77 events. Each cell experienced at least four rewetting trigger events,

and the greatest number of rewetting events experienced was 24 in Cell 6. A summary of the number of trigger events occurring in each plot is shown in Figure 7.

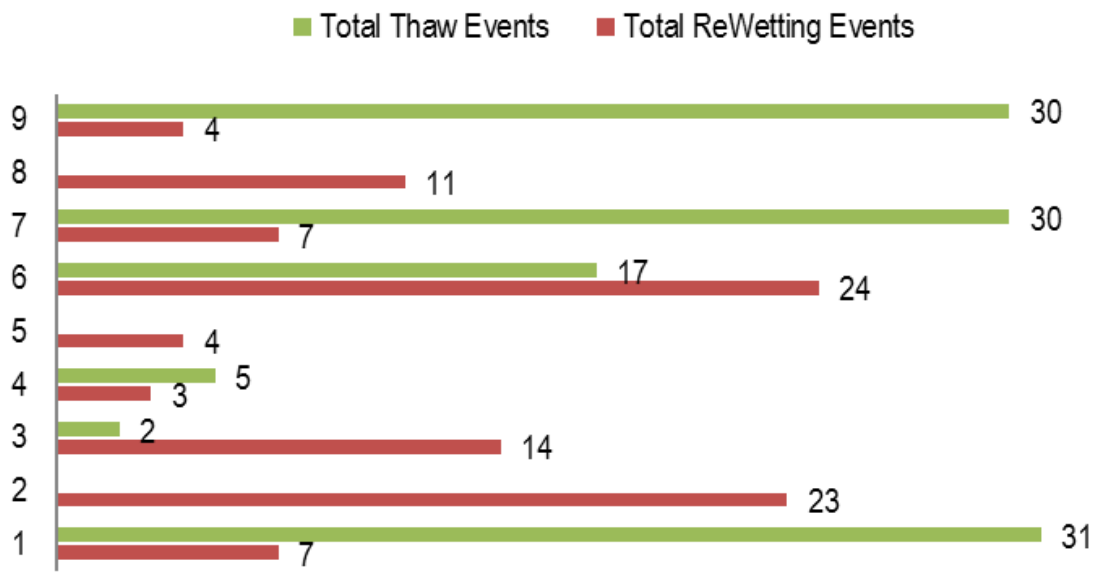

Figure 7. Number of trigger events (thaw and rewetting) as defined occurring by cell.

The relationship between time and volumetric water content (VWC) (with rewetting events), and time and temperature (with thaw events) for individual cells can be found in Appendix C. On each graph, trigger events were identified, and the corresponding dates of those events were recorded. Dates of interest, i.e. those that occurred over multiple cells, for rewetting events were February 26, 2017, August 6, 2017, and September 28, 2017 (Figure 8). Dates of interest for thaw events were March 12-16, 2017 and December 22-26, 2017 (Figure 9).

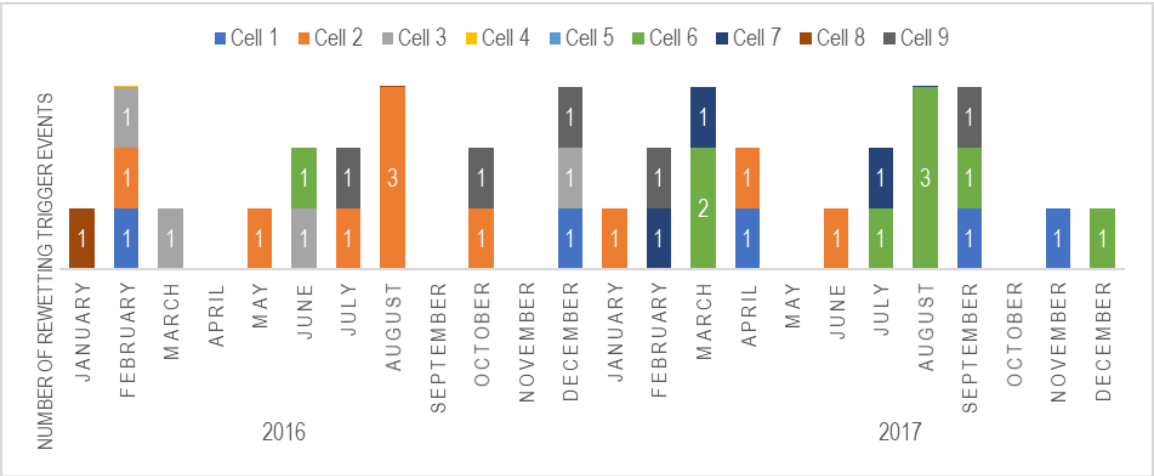

Figure 8. Rewetting trigger event dates across cells. The numbers displayed within bars represent the number of events observed in each cell.

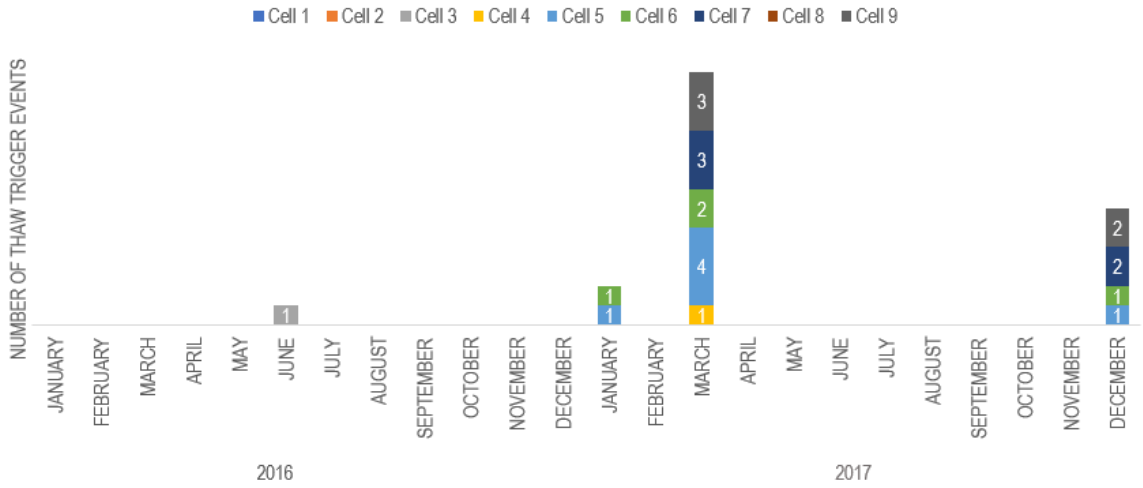

Figure 9. Thaw trigger event dates across cells. The numbers displayed within bars represent the number of events observed in each cell.

3.3.2 Influential Weather Events predicting Soil Microbial Respiration

Event dates from Figure 8 and Figure 9 were used to interpret trends in soil microbial respiration data from the Eosense Soil Gas Wells (SGW). The SGWs collected continuous data on O_2 and CO_2 concentrations at a soil depth of 15 cm. In the second year of the study, data collection from the SGW O_2 sensors showed excessive noise. Several of the O_2 sensors provided what appeared to be erroneous results. Upon

servicing these units, Eosense indicated that several of them had failed. They have since replaced this type of sensor with a more robust O_2 sensor. Between August 22nd, 2016 to late November 2016, the sensors were replaced. Thus, any trigger events identified during this time are not discussed due to the lack of trustworthiness of the datasets.

Responses in CO_2 and O_2 concentrations occurred simultaneously. Lags before a response in CO_2 and O_2 were often present, typically ranging between 0.5 to 2 hours following the detection of the event. We expect that this lag reflects the reaction time of soil microbes to the changing conditions. Lag times were approximately equivalent for both CO_2 and O_2 responses. Relationships between O_2 and CO_2 were often inverse, i.e. as CO_2 increased, O_2 decreased, or vice versa. The application rate of the biosolid amendment did not appear to influence correlations between the two gases. Time of year had the greatest influence on which correlation was expressed but this effect was not consistent. A description of correlations seasonally is shown in Figure 10.

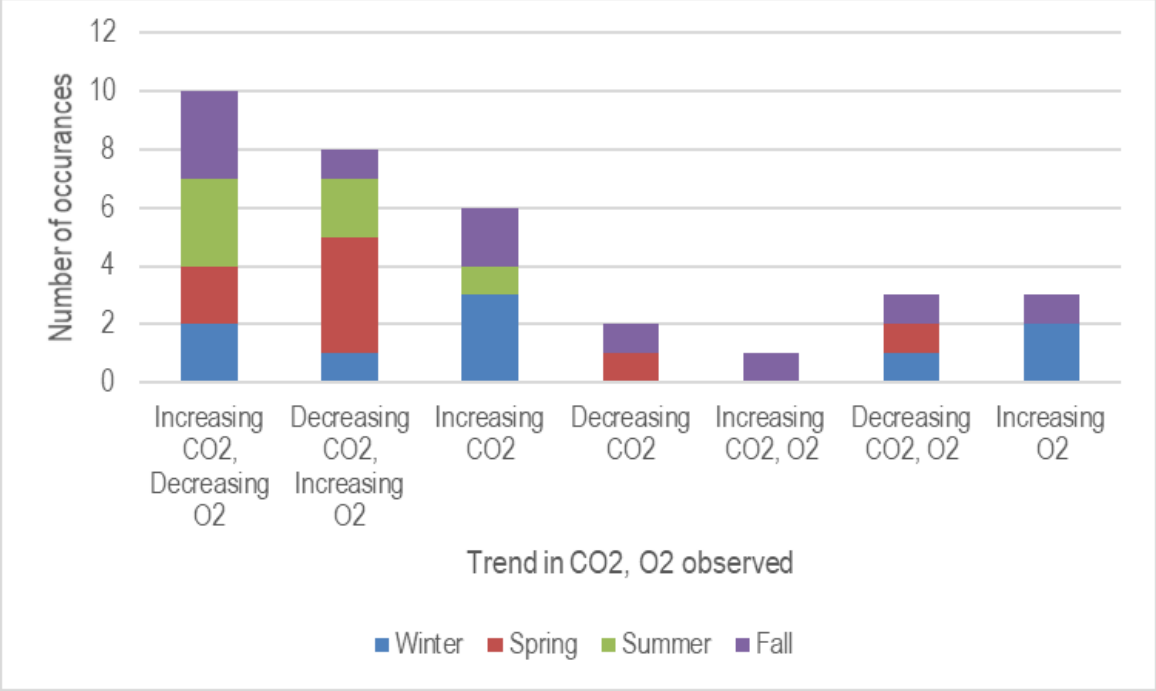

Figure 10. Seasonal distribution of CO_2, O_2 relationships.

Soil water content and soil temperature act as control factors for soil microbial activity, i.e. microbial respiration in the form of CO_2 (Moyano et al., 2013). Generally, these relationships are continuous functions. Here, we propose that the relationship is discontinuous concerning environmental trigger events (Franzluebbers, 1999, Paul et al., 2003). On a global scale, soil respiration is greatest during the summer months (Raich et al, 2002). In our study, during summer rewetting events, CO_2 concentrations generally increased, while soil O_2 concentrations often decreased (Figure 10). Soil O_2 concentrations returned to their original level following soil saturation. Fluctuations in precipitation and temperature are also known to influence microbial respiration (Hursh et al., 2017). Climate change is predicted to result in more intense precipitation events in Atlantic Canada, and global warming will result in warmer winter temperatures resulting in soil respiration over a wider seasonal range, as was observed in our study.

The winter season displayed the most diversity in CO_2-O_2 trends. In December 2016, decreases in CO_2 were most often observed. In February 2017, events mainly resulted in an increased O_2 concentration. Individual events in January, September, and October showed trends of increasing CO_2 concentration without a corresponding measurable change in O_2 concentration. Vargas et al. (2010) also demonstrated that soil temperature and moisture influenced soil respiration. In their study, continuous auto-logging at depths from 2 to 16 cm over two years showed that soil respiration was most substantial following a rainfall. In our study, it was also observed that rewetting events held a greater influence on soil respiration.

Both CO_2 and O_2 concentrations reflected both fluctuations in production and consumption respectively. We expect that these fluctuations were associated with biological activity, as well as changes in gaseous diffusion as a result of changes in

water content as it impacts air-filled porosity and the continuity of air-filled pores. Figure 11, shows a December 2016 response in CO_2 and O_2 concentrations to a rewetting event, as determined by the change in volumetric water content (Figure 11, bottom). During this weather event, soil respiration follows a rapid change in VWC from 18% to 30%, resulting in a rise of the soil CO_2 concentrations by 1 000 ppm (up to 4 000 ppm) over 12 hours and continued to increase up to 5 000 ppm over the following 10 days. The concentrations of O_2 decreased from 10 to 8% during this period.

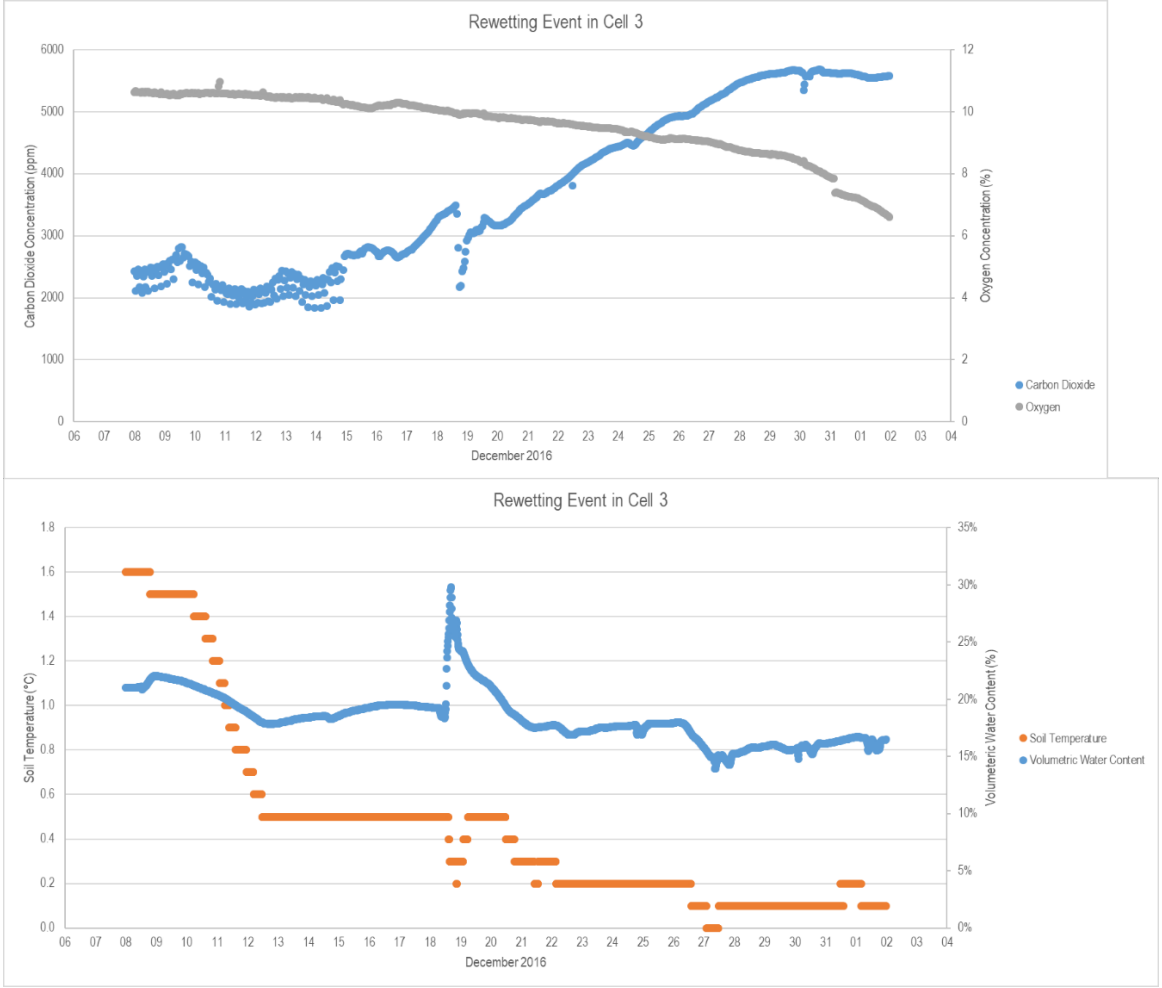

Figure 11. Sample response of CO_2, O_2 in Cell 3 to a December 2016 rewetting event as characterized by soil volumetric water content (%).

Increasing CO_2 and a corresponding decrease in O_2, characteristic of aerobic microbial activity and the decomposition of organic matter, occurred in 6 of the 12 observed

months and all seasons (over 2 years) in this study. In 7 of the 12 observed months, increasing O_2 occurred suggesting that atmospheric O_2 was re-entering the soil system, following a defined event to stabilize the soil O_2 after pulses in microbial activity (following drying or thawing).

Oxygen is used as an electron acceptor by heterotrophic microbes including soil nitrifiers. As O_2 becomes less available, due to soil saturation from a precipitation event and consumption by soil microbes, some organisms switch to denitrification (using NO_3^- as an electron acceptor). The inhibition of aerobic heterotrophic microbial activity, as a result of the lower O_2 concentration, results in reduced CO_2 production. In the December 2016 event shown in Figure 11, soil temperature also dropped as a result of cold water moving through the soil profile. Likely, the decrease in soil temperature also influenced the respiration following the event, as N processes occur more rapidly in warmer temperatures.

Previous studies have documented the accumulation of CO_2 in the sub-surface of frozen soil as a result of the formation of an ice layer, which was followed by a decrease during a thaw event (Burton et al., 1994; Wagner-Riddle et al, 1998). During an event organic C substrate is depleted due to the activity of denitrifiers (a process requiring C as a substrate); thus, the microbial activity would be diminished until the C substrate was replenished.

Figure 12, shows a March 2017 thaw event from our study site. During thaw events, the O_2 content remained stable, however, CO_2 respiration followed a similar trend to soil temperature. As soil temperature increased, soil respiration also increased, but without a depletion in O_2 concentrations. The increase in CO_2 concentrations preceded the thaw

event, occurring as soil temperature increased to greater than -1 °C (Figure 12). The low O_2 concentrations (< 2%) suggests that microbial activity would be primarily the result of denitrification or other anaerobic microbial processes.

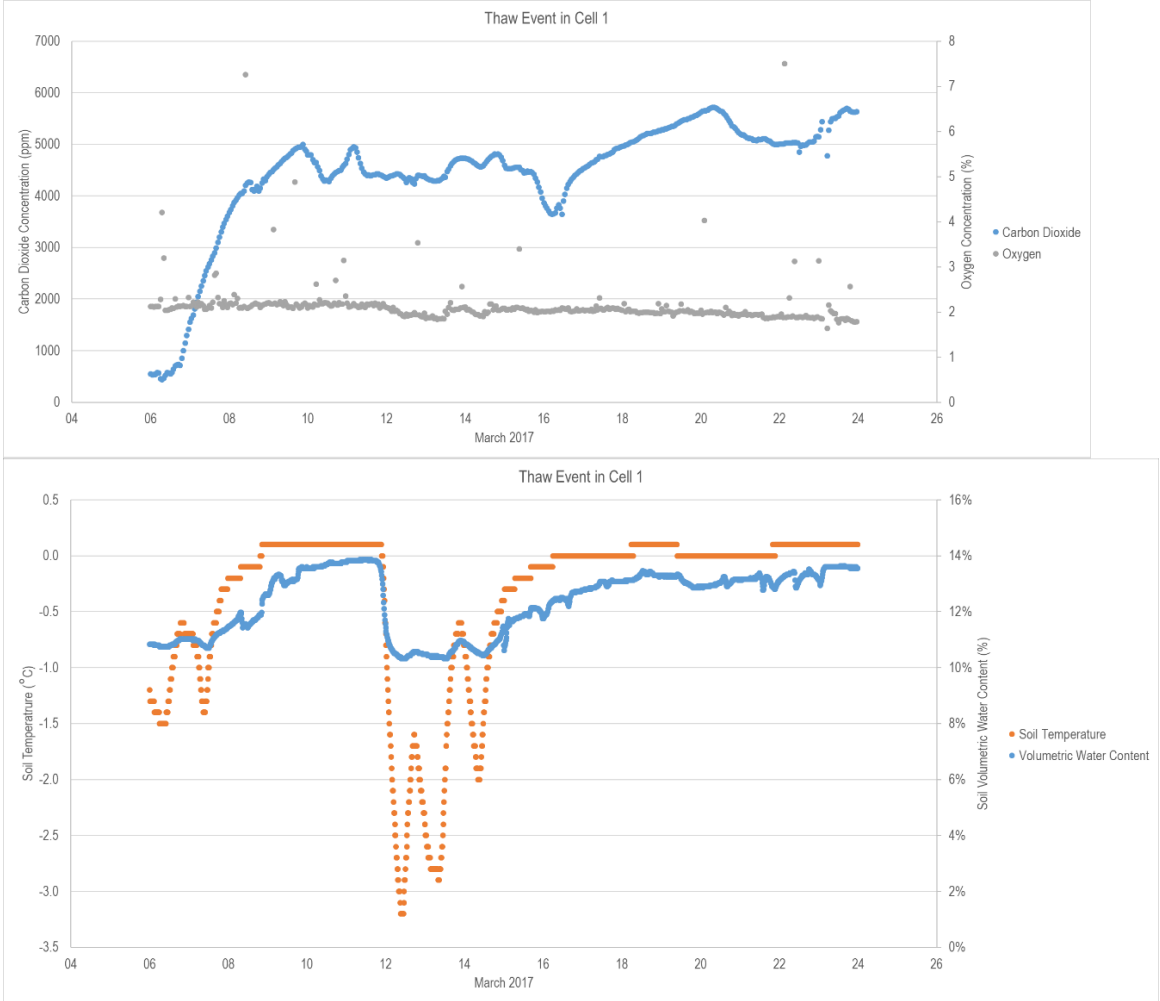

Figure 12. The response of CO_2, O_2 to a March 2017 thaw event as defined by soil temperature.

We speculated that denitrification would be dominating thaw events due to saturated soil conditions associated with thaws. The response in CO_2 concentrations to thaw events was similar across sites, more examples from dates of interest (those that occurred over multiple cells) are presented in Appendix D.

3.3.3 Investigating Influential Factors of N_2O Production from Surface Flux Sampling

The timing and magnitude of N_2O production are dependent on soil moisture and temperature, as is indicated by its episodic nature. Here the impact of pre-defined trigger events (thaw and rewetting) within the soil profile (15 cm) on the surface flux of N_2O is examined. To define the timing of trigger events, air temperature (°C) and precipitation (mm) are shown below in Figure 13 and Figure 14 indicating dates where trigger events occurred. Sampling temperatures and precipitation tended to reflect the seasonal expectations for the region (Province of Nova Scotia, 2019). Surface flux sample dates were selected based on weather events during the winter months and were taken bi-weekly during the summer, fall, and spring when more nitrogen processes were expected to be occurring.

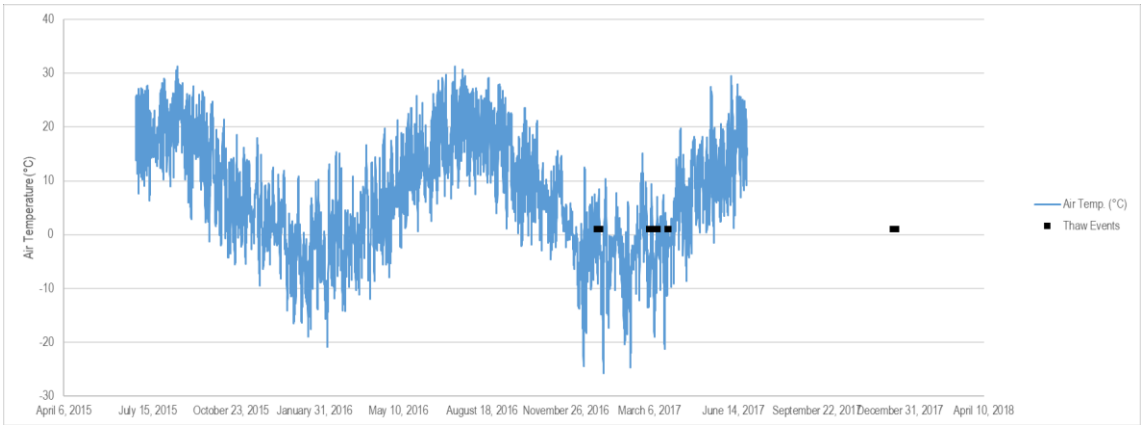

Figure 13. Average air temperature (°C) and defined thaw events during the monitoring period. Adapted from Nova Scotia historical weather data collections.

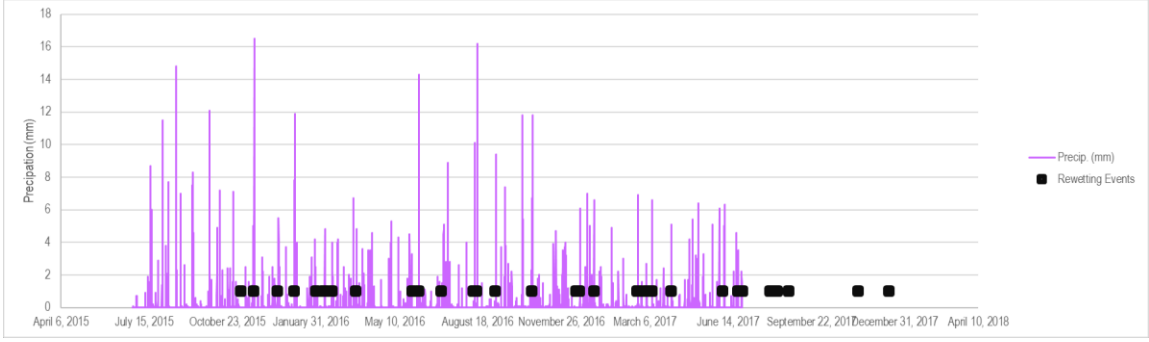

Figure 14. Average precipitation (mm) and defined rewetting events during the monitoring period. Adapted from Nova Scotia historical weather data collections.

Average N_2O emissions (Figure 15) were greatest in late summer and early fall; however, peaks in emissions occurred sporadically throughout the year. Peak N_2O production and soil respiration occurred primarily during rewetting events, as shown by the solid black and black broken lines in Figure 15 and Figure 16.

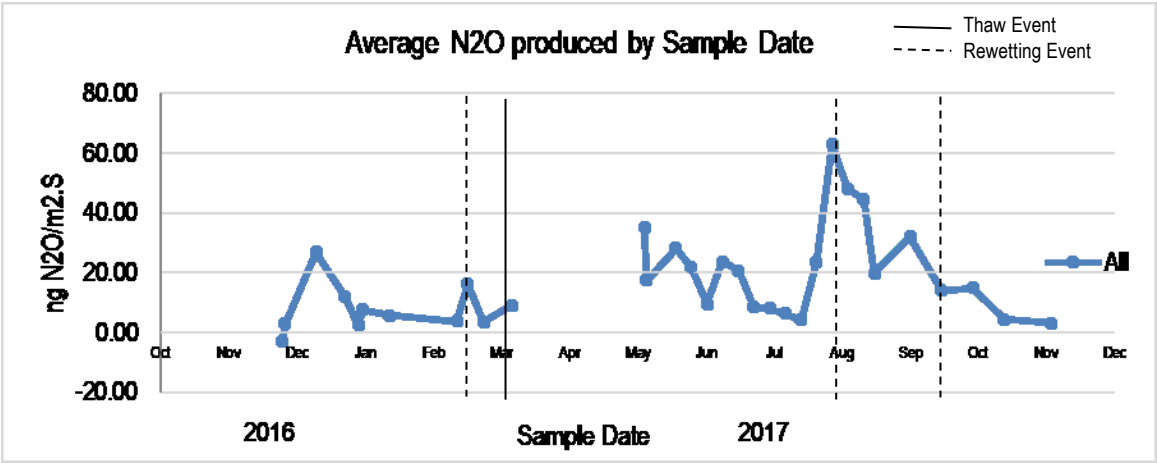

Figure 15. Average N_2O emissions obtained from surface flux samples over all cells; dates of interest (defined event dates that occurred over multiple cells are shown as black lines).

The break in the graph (Figure 15) is attributed to April 2017, in which no sampling occurred due to consistent dry conditions and high air temperatures. The greatest N_2O emissions occurred in August 2017, following an irrigation event; cells were irrigated during a dry period before this sampling date. Application of the NH_4NO_3 and biosolid

amendment may have spiked the emissions in December 2016 and May 2017, as amendments were applied before these sampling events. Summer 2017 was especially dry and reductions in emissions following May were likely due to lower levels of soil moisture. This is further demonstrated by the burst in N_2O flux following the irrigation event on August 16, 2017. Although a trigger event in September 2017 was determined to be a date of interest (occurred over multiple cells), it did not result in a peak in N_2O emissions. We can infer that there was another factor (perhaps temperature) limiting microbial activity during this time.

3.3.4 Investigating Influential Factors of CO_2 Production from Surface Flux Sampling

Average CO_2 emissions (Figure 16), representing soil microbial respiration were greatest during the summer season and decreased in the fall and winter months. No flux sampling occurred in April 2017. Greatest emissions were a result of an irrigation event following a dry period in August 2017. Carbon availability, following a biosolid application in May 2017 shows a spike in soil respiration; carbon substrate was used rapidly and then a decline in emissions was visible until June. Dry conditions throughout the summer were evident from June and July.

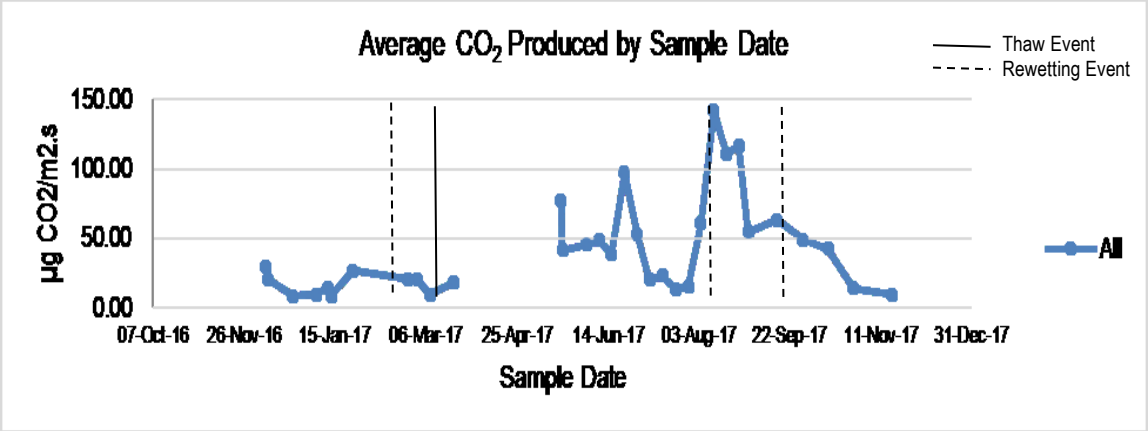

Figure 16. Average CO_2 emissions obtained from surface flux samples over all cells.

Overall, average CO_2 emissions from surface flux sampling were greatest during the summer and dropped over the winter months (Figure 16). Soil respiration tends to increase with soil water content but decreases with prolonged freezing (winter months), seemingly related to dissolved organic carbon content (Haei et al., 2011). However, some microbial respiration was observed year-round.

3.4 Conclusions

Thaw events, defined as a 0.1 °C change in soil temperature provided an average of 19.17 events per cell which was used to assess the impact of thaw events on soil respiration and oxygen concentrations. The thaw event definition was based on a prescribed change in temperature and should be applicable across all nine sites. The rewetting threshold, however, is site-specific, as rewetting dynamics are a result of site characteristics including soil texture, topography, and drainage.

The analysis of continuous soil volumetric water content data revealed that a 2.5% change in soil volumetric water content (m^3/m^3) over 75 minutes resulted in approximately 10-20 events throughout examination at our site, with an average of 9.71 events per cell. Generally, pulses in soil respiration, as indicated by changes in soil CO_2

and O_2 concentrations as measured by Eosense soil gas well chambers, followed a short lag after the trigger event. Following this, peaks in respiration were observed which suggests that the trigger events, as defined by the temperature and moisture thresholds, effectively corresponded with changes in soil microbial activity.

In our study, rewetting events resulted in greater N_2O emissions than thaw events. The greatest average N_2O flux occurred in late summer and early fall, as well as immediately following an irrigation-induced rewetting event. However, sporadic pulses in soil respiration and N_2O flux occurred throughout the year, including over the winter. This confirms that soil respiration occurs year-round and consequently, pulses in GHG emissions are evident even in previously over-looked low temperatures.

CHAPTER 4: ROLE OF BIOSOLID AMENDMENT ON SOIL RESPIRATION AND NITROUS OXIDE EMISSIONS

4.1 Introduction

Nutrient management, including efficient fertilizer use and the addition of manures, contributes to plant growth and improves soil organic C storage by adding biomass and providing soil cover (Conant et al., 2001; Lal 2004). Soils under minimum or no-tillage practices can sequester atmospheric C (West and Post, 2002). Encouraging favorable conditions to optimize C storage in soil not only improves soil health and reduces the implications of global warming by preventing excess nutrient losses, but it also encourages the availability of N to the crop. Table 12 shows strategies applicable to agriculture that improve C sequestration.

Table 12. Strategies for creating a positive ecosystem C budget. Adapted from Soil Carbon, Hardemink and McSweeny (2014).

1. control soil erosion
2. conserve soil water
3. moderate soil temperature
4. enhance soil structure and formation of stable aggregates
5. improve soil fertility (available N, P, S, Ca, Mg)
6. improve the depth distribution of root biomass
7. enhance soil biodiversity or bioturbation
8. improve NPP (net primary productivity)

In systems with excess N (present when amendment rate exceed crop requirements), N becomes mobile. Mobile N can remain in the soil as NO_3^-, travel into the water system as NO_3^- or N_2O in leachate, or into the air or atmosphere as N_2O or N_2 (Groenigen et al., 2015).

Alkaline biosolid is used as a soil amendment, mainly to improve soil pH. The application of biosolid has been shown to raise soil pH by up to 1.5 units in a single application (at rates exceeding 14 $Mg.ha^{-1}$ (Price et al., 2015). Additionally, its use as a soil amendment

provides nutrients and contributes to building soil organic matter at the depth of incorporation. Biosolid use (as described in Chapter 2) has been found to increase seasonal mineral N by up to 42% in similar soils (sandy loam) (Gillis et al., 2014). This chapter investigates the influence of N-Viro biosolids on soil NO_3^- concentrations, NO_3^- leaching in water, and atmospheric N_2O emissions.

4.2 Materials and Methods

4.2.1 Soil

Plant Root Simulator® (PRS; Western Ag. Innovations, Saskatchewan) probes and anion exchange membranes (AEM) were used to identify the amount of NO_3^- and NH_4^+ present in the system throughout the study. During the first season (2016), PRS probes (cation, anion) and AEMs were inserted into each of the nine cells at two locations within each cell (total of 18 of each device). In the second season (2017), PRS probes and AEMs were replaced on a bi-weekly basis over the sampling season.

PRS Procedure

The PRS probes have a membrane area of 17.5 cm^2 per probe and were inserted into the soil at an approximate depth of 5 cm, covering the membrane area. PRS probes (an anion and cation membrane) were inserted side by side at two locations within each cell; the center drainage tile and the top right-hand corner where soil gas well and associated monitoring devices were housed. Both locations were amended with NH_4NO_3 at a rate of 25 $kg.ha^{-1}$. The anion probe's positively charged membrane attracted anions such as NO_3^-, while the cation probe's negatively charged membrane attracted cations such as NH_4^+. Throughout the spring and into the fall of 2017, the probes were changed every two weeks. Probes were removed by being pulled vertically from the ground, rinsed in deionized water to remove debris and wrapped in plastic wrap for transportation back to

the laboratory. Once returned to the laboratory, the probes were washed thoroughly and stored in deionized water in a refrigerator. On the extraction dates, the probes were shaken manually to remove excess water and placed in plastic bags (two to each bag, one anion and one cation membrane from each location) with 35 milliliters of hydrochloric acid (0.5 M HCl). The probes were left soaking at room temperature for one hour and then the eluate was drained and frozen in centrifuge tubes. The extracts were analyzed on a Technicon AutoAnalyzer II for NH_4^+-N and NO_3^--N concentrations.

AEM Procedure

Anion exchange membranes (5.2 cm by 6 cm) with a surface area of 31.2 cm^2 were prepared for insertion at two depths at each location. To insert the membranes, a hole was dug to a depth of 30 cm in the soil. A metal spatula was used to create two slots in the wall of the hole at approximately 15 cm and 30 cm depth. The membranes were situated in the slots and the surrounding soil was loosened to encourage soil-to-membrane contact. The hole was then re-filled and labelled. The membranes were left for two weeks and then removed and replaced by a new set. After removing a set of membranes, they were rinsed with deionized water, wrapped in plastic wrap for transport and cleaned thoroughly with deionized water upon return to the laboratory. AEMs were stored in deionized water in a refrigerator until extraction. Upon extraction, membranes were sorted into individual centrifuge tubes (one membrane per tube) and shaken in potassium chloride (1 M KCl) for one hour. Following shaking, the eluates were gravity filtered and extracts were retained for analysis on a Technicon AutoAnalyzer II.

Mineral Nitrogen (MN)

The mineral N (MN) of the soil was determined as per a standard operating procedure outlined in Appendix E, based on methods described in Soil Sampling and Methods of Analysis (Carter, 1993). A 20 g sample of soil was extracted and 100 mL of 2.0 M KCl was added at a ratio of 1:5. The soil: solution mixture was shaken for one hour and followed by gravity filtration. Eluate was collected and analysed on a Technicon AutoAnalyzer II for NO_3^- and NH_4^+. The mass of N is calculated through the calculation displayed below.

$$\frac{ug\ N}{g\ soil} = \frac{\left(\frac{ug\ N}{mL}extract - \frac{ug\ N}{mL}blank\right) * (mL\ extract + (g\ wet\ soil * GWC))}{\left(\frac{g\ wet\ soil}{1+GWC}\right)}$$

Soil Nitrogen Supply

Dried and sieved (2 mm) soil samples (30 g) were mixed with an equal amount of quartz sand and placed in Büchner funnels fitted with glass fiber filter paper. The soils were leached with a solution of 0.01 M $CaCl_2$ using vacuum filtration. Following filtration, soil samples were incubated in the Büchner funnels for 14 days and were re-filtered following that period. The first leachate provided a measure of soil mineral N while the second leachate was used to determine mineralization after allowing existing microorganisms to convert N within SOM (soil organic matter) through decomposition. The values represent a proxy for N mineralization potential which is related to the mineral N that would be available to a crop or plant.

4.2.2 Atmosphere

Surface flux samples were obtained manually as described in 3.2.2.

4.2.3 Water

Nine Teledyne ISCOs automatic water samplers (Figure 17, models 6700 and 6712) were used to collect water samples from the center drainage tiles (center m^2) of each of the lysimeters. Samplers were programmed to take an 800 mL water sample after ten tips of the bucket corresponding to each lysimeter. Recall, the set-up of the lysimeter cells and tipping bucket system is described in Chapter 2. Each sampler could collect a total of 24 samples during a rain event. During most events, not all sample containers were required. Following an event, the first three bottles were sampled for dissolved N_2O measurements by inserting a spinal-tap needle connected to a 20 mL syringe into a sawed-off pipette (which was present in the bottles during the rain event) and collecting 4 mL of water per container for analysis (Roper et al., 2013). These samples were stored in mercuric chloride ($MgCl_2$) for transport. Upon return to the laboratory, headspace within each vial was analyzed for concentration by gas chromatography. The total dissolved N_2O is calculated by combining the volume of N_2O in the headspace with that presumed to be in the liquid portion (Weiss and Price, 1980).

Figure 17. Teledyne ISCO 6700 model portable water sampler.

4.2.4 Statistical Analysis

Soil, atmosphere, and water datasets were analyzed with the General Linear Model, with fixed factors biosolid amendment rate (at rates 0, low, and high) and location (SGW or Center Drain). Minitab 18 statistical software was used to run the analysis. The assumptions of the normal distribution, constant variance, and independent error were met in each case. Tukey's pairwise comparison letter groupings are displayed to

differentiate means at α ≤ 0.05. Means that are significantly different than each other have different letters.

4.3 Results

Cumulative NO_3^- from AEM Extracts

As shown in Table 13, all factors and the interaction effect were found to be significant for the soil cumulative NO_3^- flux (mg N.10 cm^2), obtained from AEM extracts, over the season (December 8, 2016 – November 3, 2017). Soil cumulative NO_3^- flux increased with the biosolid amendment rate and was nearly 3 times larger at the highest rate than in the control area. Cumulative NO_3^- flux was 39% greater in the Center Drain location than in the SGW location. A significant interaction was noted in the Center Drain location associated with the high biosolid application rate. This interaction reflected a higher cumulative NO_3^- (96.48 mg N.(10 cm^2)$^{-1}$) compared to all other treatments (16-48 mg N.(10 cm^2)$^{-1}$).

Table 13. Analysis of Variance (ANOVA) and Treatment Means for Cumulative NO_3^- from the GLM with factors biosolid amendment rate and location within the cell; letter groupings from Tukey's pairwise comparison.

Source	DF	Adj SS	Adj MS	F-Value	P-Value
Biosolid rate	2	13441	6720.4	14.39	**0.000***
Location within cell	1	14874	14873.7	31.85	**0.000***
Interaction	2	6940	3469.9	7.43	**0.002***
Error	48	22417	467.0		
Total	53	52995			

Biosolid rate N=18	Control	22.22 mg N.10 cm^2 b
	Low	35.32 b
	High	62.41 a

Location N= 18, 36	Center	57.59 mg N.10 cm^2 a
	SGW	22.38 b
Interaction	Interaction Control*Center	27.93 b
	Control*SGW	16.51 b
	Low Rate*Center	48.34 b
	Low Rate*SGW	22.29 b
	High Rate*Center	96.48 a
	High Rate*SGW	28.33 b

Cumulative NO_3^- and Cumulative NH_4^+ flux measured with PRS Probes

As shown in Table 14, the biosolid rate but not location, had a significant impact on Cumulative NO_3^- flux over the monitoring period (December 8, 2016 – November 3, 2017). Higher rates of biosolid addition resulted in higher cumulative NO_3^- flux. Biosolid amendment rate also had a significant impact on cumulative NH_4^+ flux (Table *15*), however, in this case, biosolid application, independent of rate, resulted in lower cumulative NH_4^+ flux relative to the control. The interaction effect of the biosolid rate x location was not significant.

*Table 14. ANOVA for Cumulative NO_3^- from the GLM with factors biosolid rate and location. * denotes factors that are significant at α<0.05.*

Source	DF	Adj SS	Adj MS	F-Value	P-Value
Biosolid rate	2	171.13	85.56	4.42	0.033*
Location within cell	1	17.90	17.90	0.92	0.353
Error	14	271.13	19.37		
Lack-of-Fit	2	61.21	30.61	1.75	0.215
Pure Error	12	209.92	17.49		
Total	17	460.15			

Biosolid rate N = 6	Control	11.79 mg N.10 cm^2 b
	Low	16.50 ab
	High	19.26 a
Location N = 9	Center	16.85 mg N.10 cm^2 a
	SGW	14.85 a

*Table 15. ANOVA for Cumulative NH_4^+ from the GLM with factors C amendment rate and location. * denotes factors that are significant at α<0.05.*

Source	DF	Adj SS	Adj MS	F-Value	P-Value
Biosolid rate	2	0.175691	0.087845	7.22	0.007
Location	1	0.008668	0.008668	0.71	0.413
Error	14	0.170221	0.012159		
Lack-of-Fit	2	0.008726	0.004363	0.32	0.729
Pure Error	12	0.161496	0.013458		
Total	17	0.354580			

Biosolid rate N = 6	Control	0.350 mg N.10 cm^2 a
	Low	0.156 b
	High	0.128 b
Location N = 9	Center	0.233 mg N.10 cm^2 a
	SGW	0.189 a

Dissolved N_2O in Water Samples

As shown in Table 16 below, the sample date had a significant (at α=0.05) influence on the amount of dissolved N_2O found in drainage water. The sample date refers to the date that the ISCO automated water samplers were programmed to collect water samples, which were intermittent based on weather forecasts that predicted heavy rainfalls (these often lined up with the trigger event dates that were identified in Chapter 3). Figure 18 shows the relationship between dissolved N_2O and those predefined trigger events, often the responses were results of management events, i.e. irrigation in August 2017, as described in Table 6, or rewetting trigger events. Minimal amounts of additional precipitation were occasionally enough to induce a rise in N_2O emissions. For example, 27 mm of precipitation on September 7, 2017, resulted in an additional peak in emissions on September 8th. The rate of the biosolid amendment rate did not have a significant impact on the dissolved N_2O concentration in drainage water. The interaction effect of the biosolid amendment rate x location was also not significant.

*Table 16. ANOVA for Dissolved-N_2O from water samples from the GLM with factors sample date and biosolid rate. * denotes factors that are significant at α<0.05*

Source	DF	Adj SS	Adj MS	F-Value	P-Value
Sample date	33	22.644	0.6862	2.85	0.000*
Biosolid amendment rate	1	0.594	0.5944	2.47	0.117
Error	419	100.999	0.2410		
Lack-of-Fit	31	13.212	0.4262	1.88	0.004
Pure Error	388	87.787	0.2263		
Total	453	124.016			

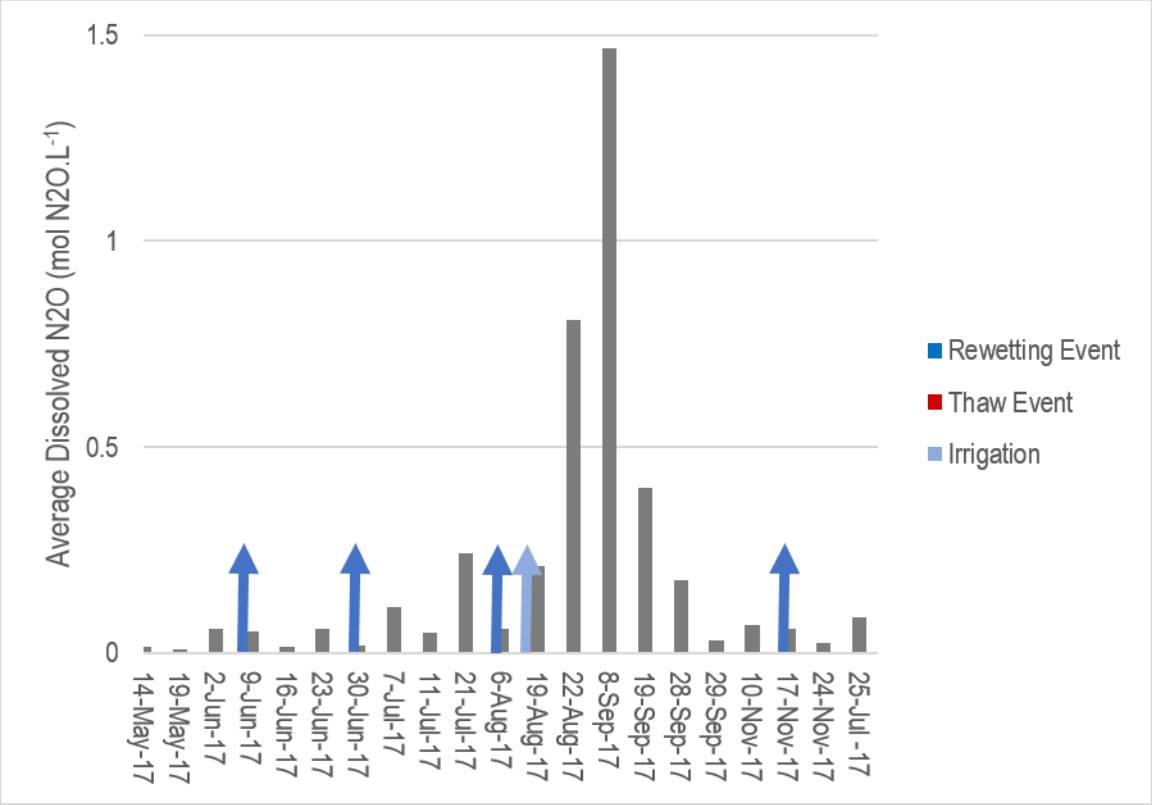

Figure 18. Average Dissolved N_2O (mol $N_2O.L^{-1}$) trends reflected by defined trigger (rewetting and thaw) events that occurred over multiple cells.

Table 17 shows a summary of significant factors. The influence of the biosolid amendment rate on N in the soil system was evident through the AEM and PRS results. However, dissolved N_2O was not influenced by the biosolid amendment rate.

*Table 17. Summary of significant factors. * denotes factors that are significant at α<0.05.*

Factors	AEM Cumulative Nitrate	PRS Cumulative Nitrate	PRS Cumulative Ammonium	Dissolved N_2O in Water
Biosolid rate	*	*	*	
Location	*			

Atmospheric N_2O and CO_2 emissions

Figure 19 and Figure 20 represent the influence of the biosolid amendment rates on N_2O and CO_2 emissions. Biosolid application dates were June 28, 2016, and May 11, 2017. The first application date is not shown in these charts as the collection did not start until December 2016.

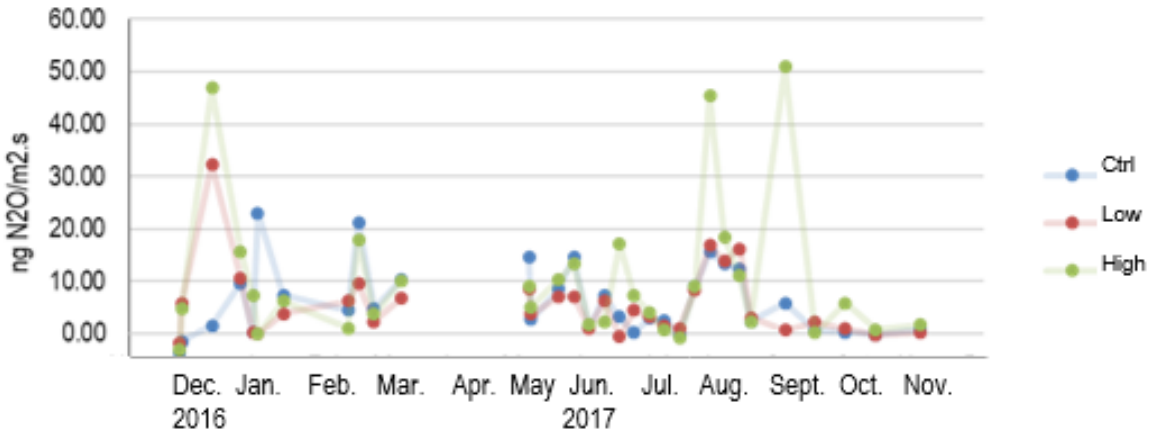

Figure 19. Average N_2O produced from cells amended with biosolid at rates low and high, with control over the flux sampling period (December 2016 to November 2017).

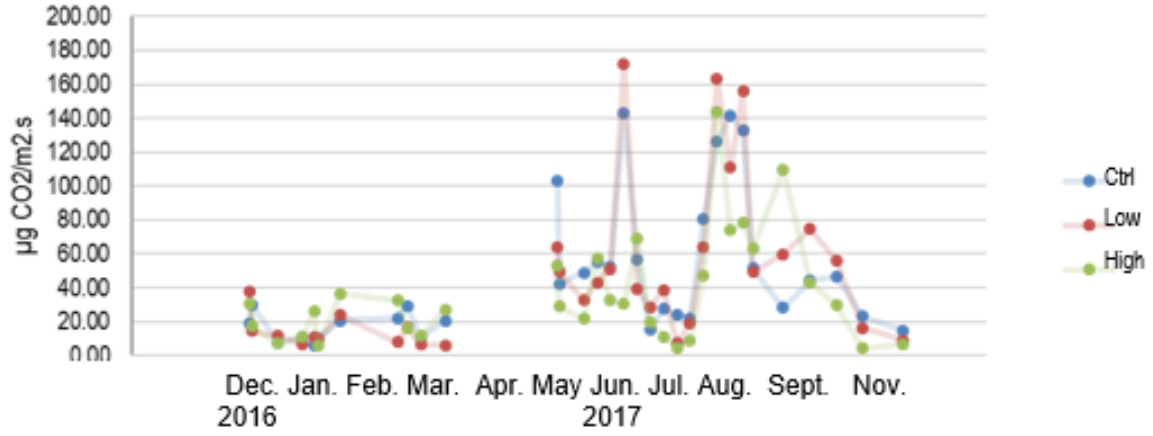

Figure 20. Average CO_2 produced from cells amended with biosolid at rates low and high, with control over the flux sampling period (December 2016 to November 2017).

The greatest N_2O emissions were produced from the high biosolid application rate during summer 2017 when conditions were optimal for microbial activity, i.e. adequate soil

temperature and soil moisture. Higher temperatures in the summer also produced greater CO_2 emissions as a function of increased soil respiration. A 2015 study by Price et al., used the same N-Viro® biosolid product and determined that it was approximately 19% carbon. Their results showed that high rates of biosolid application resulted in increased soil mineral nitrogen and cation exchange capacity. In our study, the biosolid amendment was not as influential on CO_2 flux as weather conditions. The cells with a high rate biosolid application only surpassed the low rate and control plot immediately following an irrigation event in late August 2017. In most instances, the plots that received the low amendment rate surpassed the other plots in the magnitude of soil respiration.

4.4 Discussion

The rate of application of biosolids had a significant impact on all measurements of soil N processes (excluding dissolved N_2O). As discussed, NO_3^- in agricultural soil systems is a concern due to the risk of environmental pollution (Stockdale et al., 2002) from leaching and run-off. Cumulative NO_3 flux, as measured by AEMs showed that biosolids applied at a low rate and in the unamended control (35 and 22 mg N.10 cm^2 respectively) were similar (by Tukey's pairwise comparison) but lower than the high biosolid rate (62 mg N.10cm^2). NO_3^- is a product of nitrification and is a substrate in denitrification. Accumulation of NO_3^- in the cells suggests that nitrification was occurring. Thus, in the high biosolid amendment treatment, it is reasonable to infer that nitrification was occurring more rapidly and/or more frequently (resulting in greater levels of cumulative NO_3^- flux) than in the control and low biosolid rate cells. Therefore, the biosolid amendment helped to facilitate nitrification within the cells (when it was applied at the highest rate). Nitrification would also result in reduced NH_4^+ concentrations, as NH_4^+ is

used as a substrate in nitrification and is quickly converted to NO_3^-. However, the PRS probes, which measured NH_4^+ as well as NO_3^-, showed that cumulative NH_4^+ flux was lower in the amended treatments than in the control cells. The PRS probes, however, were closer to the surface (5 cm depth) than the AEMs (15 cm depth); thus, they should have experienced more fluctuating environmental conditions. Measurements of cumulative NO_3^- flux by PRS probes showed that the low (16.5 mg N.10 cm^2) and high (19.2 mg N.10 cm^2) treatment rates were not significantly different, however, the unamended control (11.8 mg N.10 cm^2) was significantly lower than the high rate and cumulative NO_3^- flux did increase with increasing biosolid application rates. Thus, the biosolid amendment rate enhanced nitrification in the soil surface, which is confirmed by the decline in cumulative NH_4^+ flux, as measured by the PRS probes, with increasing amendment rate.

Large values of NO_3^- (greater than 20 kg N-NO_3.ha^{-1}), like the ones observed in this study, are characteristic of soils in temperate regions (Lasa et al., 1997). The AEMs measured greater values of cumulative NO_3^- (22.2 mg N.10 cm^2 in the control) than the PRS probes (11.8 mg N.10 cm^2 in the control). Since the AEMs were at a deeper depth, much of this NO_3^- is likely leachate from the NH_4NO_3 that was applied to the soil surface. The interaction effect between the biosolid rate and labelled NH_4NO_3 for the AEM measurements was also significant. The high biosolid rate combined with the Center Drain location had significantly greater Cumulative NO_3^- flux (96.5 mg N.10 cm^2) compared to all other combinations (a range of 16 to 48 mg N.10 cm^2). Thus, a combination of the available substrate in the form of NH_4 (from the biosolid) and available NH_4^+ as substrate (decreased NH_4) encouraged nitrification within the soil surface. Increasing NO_3^- with declining NH_4^+ suggests that nitrification was occurring rapidly. Additional NO_3^- from the fertilizer application would make up some of the total

Cumulative NO_3 flux, however, it would not differ from the other cells which received the same product. Additionally, the Center Drain location had received additional biosolid before this study which may have altered the soil structure. The long term effects of biosolid applications include increasing pH and NH_4^+ thus, the presence of nitrification within this location (while providing additional NH_4^+) is not surprising. San Emeterio et al. 2014 also observed a decline in the availability of NH_4^+ with increasing organic carbon source (regardless of the nature of the added C).

The biosolid application did not have a significant impact on dissolved N_2O in tile drainage water. However, there was a significant variation in dissolved N_2O as a function of the sampling date. The greatest average dissolved N_2O was measured in the August and September 2017 samples. Increased dissolved N_2O is typically related to the denitrification process (Reddy and Crohn, 2014), which suggests that the available NO_3^- in the soil system contributed to denitrification occurring during the summer months, spiking following the irrigation event (in August) and during rewetting events (in September). Over the winter months, freezing and thawing would have influenced the regulators of microbial activity (Weintraub and Schimel, 2003, Schimel et al., 2007) by limiting soil microbial activity (Jefferies et al., 2010). The biosolid product used in this study is composed of approximately 19% carbon (Price et al., 2015), which would have provided additional substrate to soil microbes on the treated cells. The availability of N to crops depends on the available C source and the microbial processes that occur (San Emerterio et al., 2014); a result of the C:N ratio which influences decomposition as discussed previously. Therefore, substrate supply (NH_4^+), is one of the main drivers of nitrification and denitrification, which means that its presence contributes to the quantity of N_2O emissions (Schaufler et al., 2010).

4.5 Conclusions

Indicators of the nitrification process, increasing accumulation of NO_3^- and decreasing the accumulation of NH_4^+, were measured as biosolid amendment rate and available NH_4NO_3 at the soil surface increased. Greater accumulation of NO_3^- was found at deeper soil depths, which confirms that a major pathway for the loss of NO_3^- from the root zone was leachate. Cells amended with high rates of biosolid application would have seen increases in soil organic matter, pH, and NH_4^+. As a result, the biosolid amended cells were conducive to the dominance of soil nitrifiers. Additionally, surface flux samples of N_2O and CO_2 were heightened with biosolid application. The biosolid application rate was not a significant factor for the appearance of dissolved N_2O, captured through the center drainage tile by automated water samplers. Most N_2O emissions produced occurred in the summer months (no ice storage), therefore, the majority of N_2O produced by denitrification were *de novo*. Greatest average dissolved N_2O was displayed following an irrigation event and intense rewetting events.

CHAPTER 5: DISTINGUISHING THE SOURCE OF NITROUS OXIDE FROM SURFACE FLUX

5.1 Introduction

Nitrogen (N) occurs naturally as $_7$N, referring to the fact that N has seven protons. $_7$N has two stable isotopes (^{14}N and ^{15}N), meaning that the element can occur with seven neutrons, i.e. seven neutrons plus seven protons equals 14, or with eight neutrons. Usually (99.636% of the time), the element will occur naturally as ^{14}N. Table 18 shows the properties of each isotope.

Table 18. Isotopic N properties.

Symbol	Number of protons	Number of neutrons	Isotopic mass	Isotopic Composition (Mole Fraction)	Range of Natural Variation (Mole Fraction)
^{14}N	7	7	14(6)	0.9963(20)	0.99579–0.99654
^{15}N	7	8	15(7)	0.0036(20)	0.00346–0.00421

^{15}N has been used extensively as a marker to trace N compounds in natural and agricultural environments, as well as in N cycles. The ratio of ^{15}N:^{14}N is referred to as the isotopic ratio (R) of ^{15}N and the abundance or δ^{15}N is calculated as the difference in an isotopic ratio relative to a reference standard.

$$\delta^{15}_{7}\mathrm{N} = \frac{R_{sample} - R_{Standard}}{R_{standard}}$$

The location of the ^{15}N atom on the N_2O molecule is called site preference (SP) (Toyoda et al., 2011). Site Preference is defined as the difference in δ^{15}N of the central (alpha) N and the δ^{15}N of the terminal (beta) N atom in the linear N_2O molecule (Figure 21). The specific δ^{15}N of any individual N element is dictated by the processes that occurred during its formation and

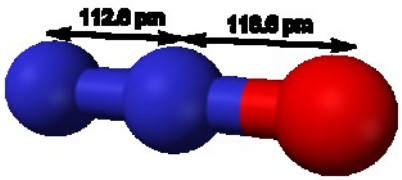

Figure 21. Nitrous oxide molecule. Blue atoms are nitrogen, red is oxygen (Wikipedia).

the place of origin. The isotopic composition and site preference (SP) of a molecule such as N_2O can be determined using Cavity Ring-Down Spectrometry, an optical spectroscopic tool that measures optical extinction by the scatter and absorption of light in samples. Cavity Ring Down Spectrometers (CRDS), such as the Picarro® G5101-i N_2O Isotopic Cavity Ring Down Spectrometer used in this study, can be used to measure and quantify these specific isotopic ratios. These applications have been used in tracking climate history through ice, tracing food origins, and, as in the application of this study, distinguishing sources (nitrification or denitrification) of N_2O production.

Small gas-phase molecules have unique, well-known near-infrared absorption spectrums that can be identified under subatomic pressure with a conventional infrared spectrometer (Picarro, Inc., 2019). Trace gases, however, do not display heights of absorption peaks that are measurable to anything more specific than parts per million (ppm). The CRDS uses a pathlength of many kilometers which increases the sensitivity and allows trace gases to be analyzed in seconds to the parts per billion (ppb) or parts per trillion (ppt) level. The CRDS accomplishes this by sending a single-frequency laser beam through a cavity lined with three mirrors (as opposed to conventional systems with two mirrors); this extra mirror supports the light wave in motion and improves the signal. A photodetector senses the light that leaks through one of the mirrors and a signal (that is proportional to the intensity in the cavity) is produced. Once the photodetector reaches the threshold (in a few seconds), the laser is turned off. The light already present in the cavity will continue to bounce between the mirrors, however, because there is a bit less than 100% reflectivity (99.999%), some of the light escapes and decays to zero exponentially, this is called “ring-down”. The ring-down is measured by the photodetector, and the amount of time that it takes for the ring-down to occur is based on the reflectivity of the mirrors. If the CRDS cavity is just 25 cm in length, the pathlength in

the cavity can be more than 20 km. However, a second escape mechanism for light is introduced if a gas species are present and absorbs the light in the cavity. In this case, the ring-down time would be even faster because more light is being absorbed, leaving less to bounce around the cavity, thus reaching ring-down faster. The CRDS calculates and compares the ring-down time in the cavity with and without this absorption factor which allows highly precise measurements to be obtained.

This chapter addresses the third objective of this study: to access the ability of the Picarro® Cavity Ring Down Spectrometer (CRDS) to distinguish the source of N_2O from surface flux emissions. A preliminary dataset of 764 30-minute surface flux samples was run on the CRDS and analysed to the best of available assumptions.

The addition of isotopically enriched N sources has often been used as a means of identifying the source of reaction products. By enriching the ^{15}N content of the source material the appearance of ^{15}N in the products can be more easily detected.

5.2 Materials and Methods

To determine whether the nitrification of NH_4^+ or denitrification of NO_3^- was the dominant source of N_2O, two different ^{15}N enriched forms of NH_4NO_3 were added to monitoring areas within each cell. In December 2016, $^{15}NH_4NO_3$ (1 atom% excess; 25 kgN.ha^{-1}) was applied to the m^2 area surrounding the soil-gas wells and $^{15}NH_4{}^{15}NO_3$ (5 atom% excess; 25 kg N.ha^{-1}) to the area at the center of the cells (Figure 22). The intent was to determine whether the N_2O produced, immediately following application, from nitrification could be quantified by the addition of $^{15}NH_4NO_3$ increasing SP of the N_2O emitted as only the ammonia was labelled; while the $^{15}NH_4{}^{15}NO_3$ has both ammonium and nitrate

labelled and therefore would result in an increase in ^{15}N in both alpha and beta positions of N_2O and a ^{15}N signature in NO_3^- loss from NH_4NO_3 fertilizer application. Since the label was added to cold soil, it is generally assumed that nitrification would be inhibited and thus the ^{15}N signature of the ammonium should remain until the soil warms in the spring and at that time the signature of the NH_4^+ and N_2O should return to natural abundance levels if nitrification was the primary source of N_2O. The central location within the cell, where the drainage lysimeter was located, received $^{15}NH_4{}^{15}NO_3$ and as a result, it was anticipated that the $^{15}N_2O$ signature would increase as a result of either nitrification or denitrification occurring, with the site preference indicating which process was dominant. Once nitrification had transformed the added NH_4^+ to NO_3^-, the abundance and site preference was anticipated to reflect the production of N_2O from denitrification alone. Another 1 m^2 location on the front left corner of the cell was monitored as a "natural abundance" location to represent the rest of the cell and did not receive any ammonium nitrate or ^{15}N label.

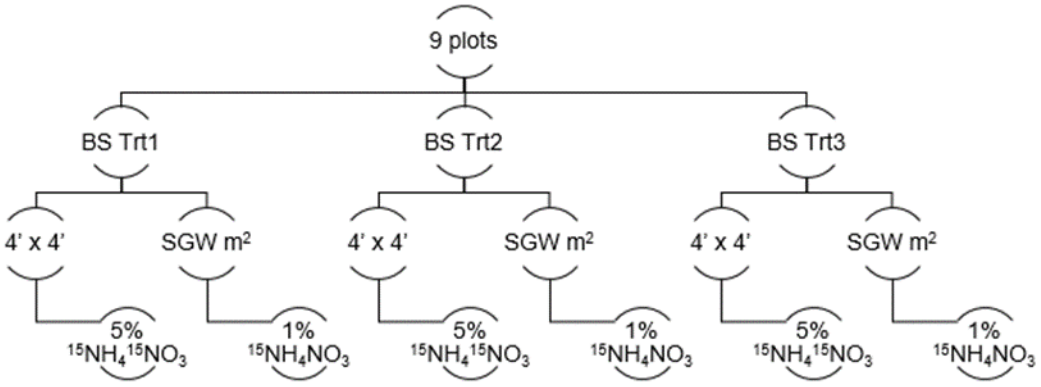

Figure 22. Organizational chart of Marked ^{15}N fertilizer (either $^{15}NH_4NO_3$ 1% a.e. or $^{15}NH_4{}^{15}NO_3$ 5% a.e. at rates of 25 kgN.ha^{-1}) application distribution to cells for tracing purposes in December 2016.

Surface Flux Sampling

Surface flux samples were obtained from the site as previously described in Chapter 2. The 30-minute gas samples were retained for analysis on the CRDS. Samples were

aligned in order of date and were manually run on the CRDS. The surface flux samples were stored as 20 mL gas samples in 12 mL exetainer vials, capped with a rubber seal. To run a sample on the CRDS, a tube with a needle adapter was routed from the inlet valve on the back of the machine. The sample was attached to the needle and placed on a small holding tray to reduce movement of the sample while the CRDS was running and to prevent breakage of the needle due to torque applied by the weight of the vial. For any individual sample, the N_2O concentration, the alpha ^{15}N ($\alpha^{15}N$), and the beta ^{15}N ($\beta^{15}N$) values at steady state (laboratory standards) were recorded along with the time that the sample was introduced. A timer was started as soon as the sample was secure and the CRDS was left to run with the sample in place for ten minutes. Following the ten minutes, the sample was removed, and the system was left to return to steady state for five minutes. A peak appeared on the graph view and estimates of the peak were recorded. The time that the samples were left on the CRDS was determined through manual manipulation and test runs before beginning to run the sample set.

Picarro® Cavity Ring-Down Spectrometer

Site preference refers to the location of ^{15}N labelled atom in the N_2O molecule. A central location of ^{15}N is termed alpha N ($\alpha^{15}N$), while a terminal location is denoted by beta N ($\beta^{15}N$). Site preference is the difference between the two terms, $SP = \int^{15}N^{\alpha} - \int^{15}N^{\beta}$ (Toyoda et al., 1999). Higher (often ~30+ ‰ in natural systems) SPs suggest that $\int^{15}N^{\alpha}$ was greater than $\int^{15}N^{\beta}$, and nitrification was the dominant source of N_2O. If $\int^{15}N^{\beta}$ is larger than $\int^{15}N^{\alpha}$, the SP will be either 0 or a negative integer, which would fall within the range of denitrification as the source. The following equations (Yamamoto et al., 2017) demonstrate how these characteristics are calculated:

$$\int^{15}N^{(i,\ \alpha \text{ or } \beta)} = ({}^{15}R^{i}_{sample})/({}^{15}R^{i}_{standard} - 1)*1000, \textit{ where } R^{i} = \textit{(}^{15}\textit{N)/(}^{14}\textit{N)}$$

$$\int^{15}N^{(bulk)} = (\int^{15}N^{(\alpha)} + \int^{15}N^{(\beta)})/2$$

Here atmospheric N_2O was used as the isotopic standard gas. Given these distinct signatures, it is, therefore, possible, in principle, to use the isotopic signature of emitted N_2O, in combination with N_2O concentration, to partition the N_2O production between nitrification and denitrification in soils with similar ^{15}N in substrates.

For each sample (30-minute flux sample vial), starting readings of N_2O, $\int^{15}N^{\alpha}$ and $\int^{15}N^{\beta}$ were recorded. Graph peak estimates of the same data were also recorded over the 10-minute sample run period. The site preference ‰ was calculated by subtracting the $\int^{15}N^{\alpha}$ from the $\int^{15}N^{\beta}$. In natural abundance studies, SP‰ for nitrification can range between 32 and 35‰, dependent on the nitrifying species. Denitrification SP‰ range between -5‰ (Toyoda et al., 2005) and 0% (Sutka et al., 2006). Nitrification SPs are usually ~33‰ greater than that of denitrification. Since the addition of ^{15}N was used in this study, we expected higher than naturally occurring abundances to be reported by the CRDS. The use of the CRDS to read ^{15}N, in a ^{15}N amended site, characteristics in surface flux samples was a novel approach and therefore, ranges for denitrification and nitrification were not available in the literature. For this study, negative site preference values were considered instances where the dominant source of N_2O was nitrification, and positive site preference values were considered instances where the dominant source of N_2O was denitrification. This is based on the knowledge that site preference is determined as the difference between the abundance of the center and outer atoms within the N_2O molecule (Baggs, 2008) as well as the assumption that fractionation from nitrification is higher than denitrification, therefore, N_2O produced from nitrification is depleted in ^{15}N compared to that produced from denitrification (Butterbach-Bahl et al., 2013).

5.3 Results

The average site preference across all cells was -308‰ and ranged between -3 000‰ and 3 870‰. 48 outliers were identified in the data set based on 25% quartiles. With these 48 outliers removed, the average site preference across all sites was -279‰ and the data distribution is shown in Figure 23.

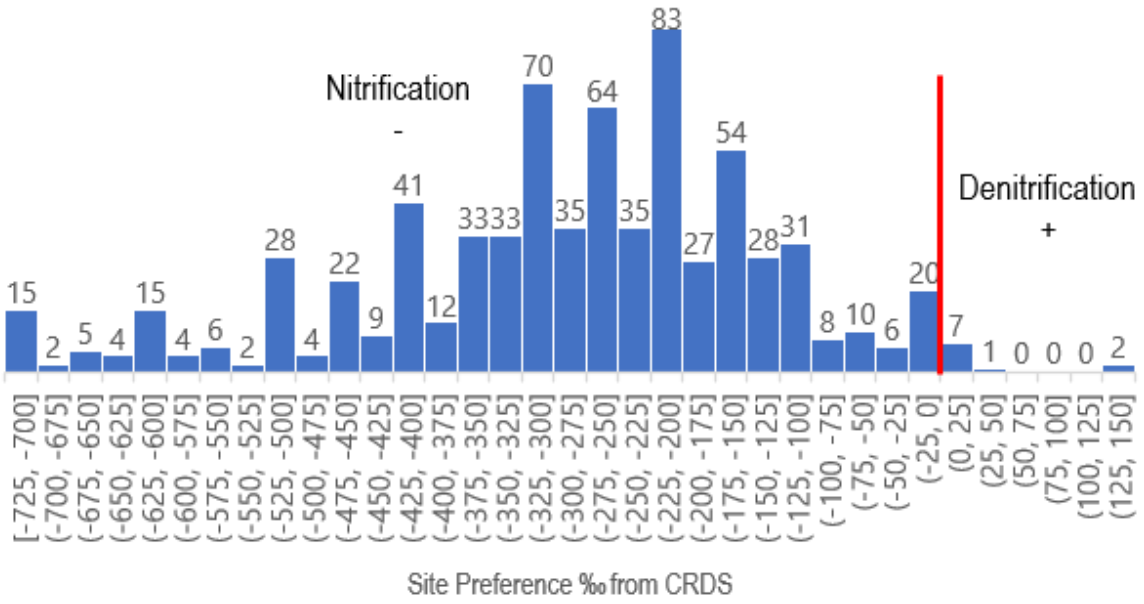

Figure 23. Distribution of site preference ‰ in the 30-minute flux samples from analysis on the Picarro® CRDS, representing instances when nitrification (-) or denitrification (+) were the dominant source of N_2O emissions.

Thirty Minute Flux Samples

The area immediately surrounding the soil gas wells and the center drain tile locations were amended with NH_4NO_3. The SGW location was amended with single-labelled $^{15}NH_4NO_3$. We expected that N_2O produced from the SGW location would reflect the extent to which nitrification was producing N_2O in the soil system because only the NH_4^+ was labelled. The center drainage tile was amended with double-labelled $^{15}NH_4{}^{15}NO_3$ at the same rate. The N_2O being produced at this location was expected to reflect the

combined activities of nitrification and denitrification. N_2O concentration was greater in the center location over the sample sets, which confirms that the double-labelled site may have had environmental conditions more conducive to nitrification, denitrification, or both. The mean SP being negative despite both NH_4^+ and NO_3^- being labelled suggests that the surface flux of N_2O was predominantly from nitrification. Denitrification occurred only 1.4% of the time across all cells (from dataset disregarding outliers), while nitrification appeared to be most often the dominant source of N_2O. Considering the addition of ^{15}N to the plots, it is reasonable that the SP results did not fall within the suggested ranges for natural abundance.

Individual instances where denitrification was the dominant source of N_2O (site preference was positive) occurred on January 13, 2017, May 19, 2017, June 2, 2017, June 9, 2017, June 16, 2017, July 7, 2017, **August 18, 2017**, and **September 29, 2017**. It should be reiterated that multiple events could occur on one day. These dates represent periods of wet soils, in which we expected denitrification to be the dominant source of N_2O. Additionally, two of these dates (in bold) corresponded to significant rewetting events at this site, as defined in Chapter 3. These occurrences were most often in the double (eight instances) or single-labelled (six instances) location and did occur on four instances within the natural location (received no labelled NH_4NO_3). This is consistent with our expectation as N_2O is produced as a by-product of NH_2OH oxidation during the denitrification process, therefore we anticipated that instances, where the source of N_2O was denitrification, would occur mainly within the double-labelled location ($^{15}NH_4{}^{15}NO_3$).

N_2O production from nitrification tends to influence alpha ^{15}N. Results for both alpha ^{15}N (Figure 24) and beta ^{15}N (Figure 25) were relatively steady in the double-labelled

$^{15}NH_4{}^{15}NO_3$ location, even decreasing in the case of beta ^{5}N. However, in alpha and beta ^{5}N for SGW single-labelled $^{15}NH_4NO_3$ location, there was a slight increase in average alpha and beta ^{15}N over time. This suggests that those locations were trending toward natural abundance following the addition of the enriched N sources and therefore the single-labelled $^{15}NH_4NO_3$ location had a greater effect on soil N_2O emissions. The return to natural abundance quantities is likely a result of a decline in the available substrate due to decomposition.

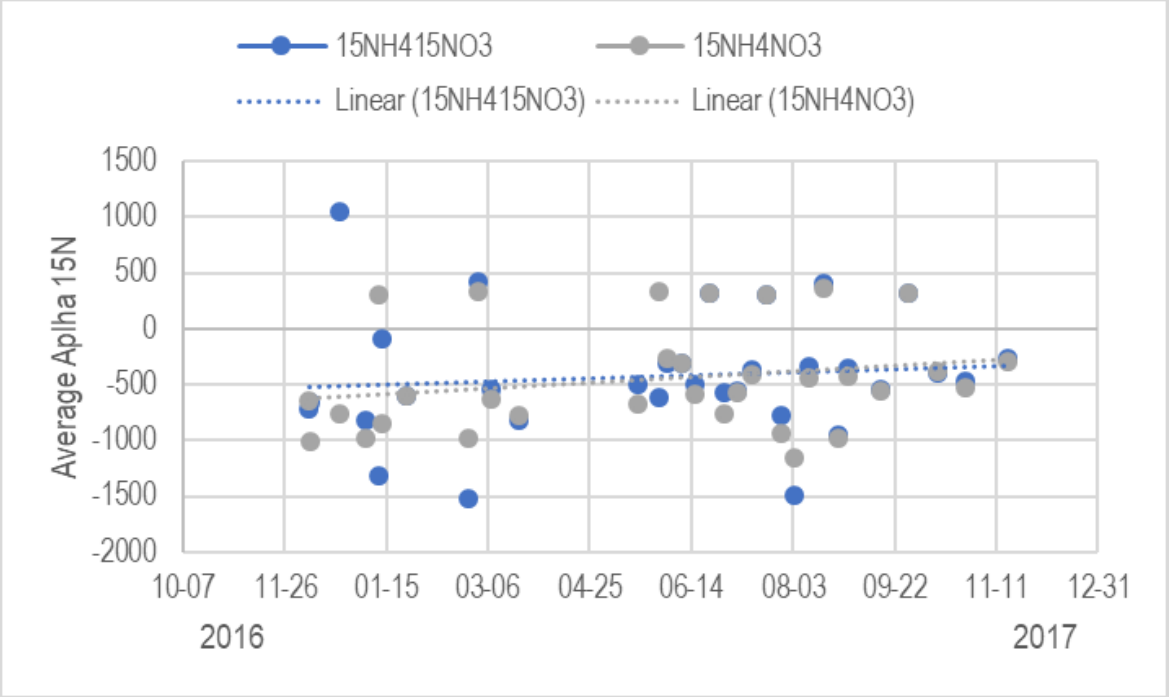

Figure 24. Average peak alpha ^{15}N results from surface flux samples run on the Picarro® Cavity Ring Down Spectrometer.

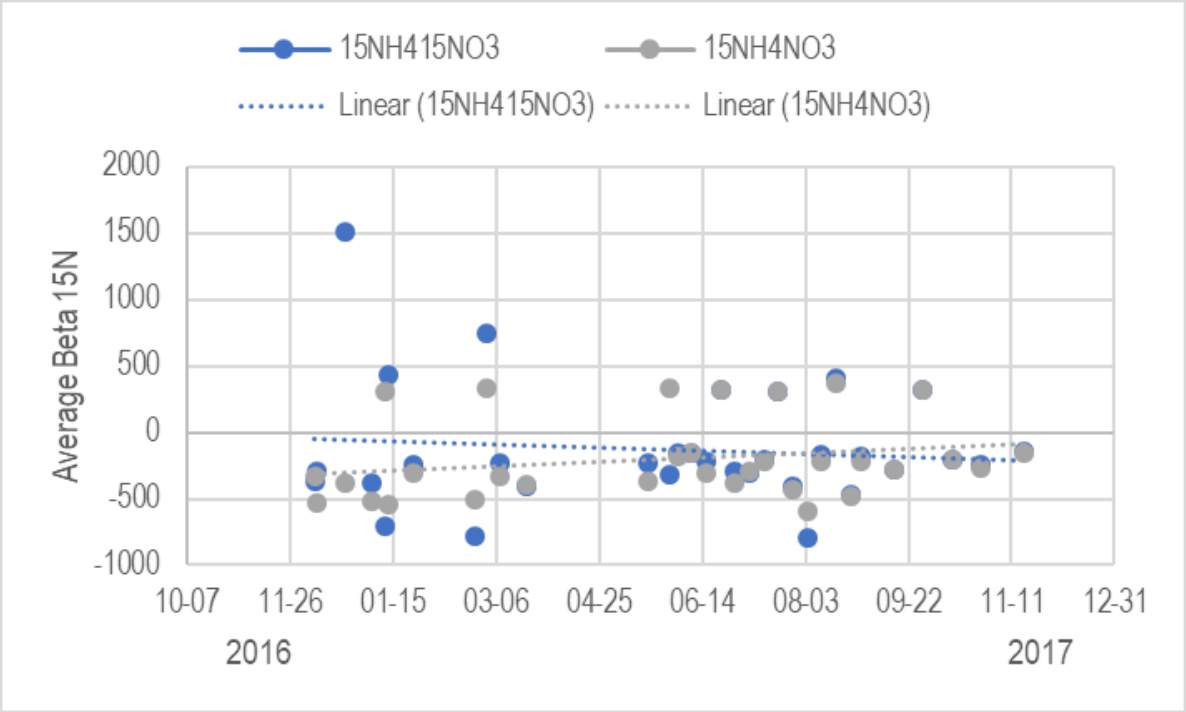

Figure 25. Average peak Beta ^{15}N from surface flux samples run on the Picarro® Cavity Ring Down Spectrometer.

Site preference of the N_2O evolving from the soil surface, in both the double-labelled and single-labelled cells, increased from a strongly negative (-500) value to a more moderate negative value (-150) over the sampling season (Figure 26), but still outside the range values seen in natural abundance studies. The SP values were predominantly negative, which suggests that the beta ^{5}N was greater in magnitude than the alpha ^{15}N and thus, the source of N_2O within the flux samples was predominantly nitrification. The slope of the increase of the double-labelled location was 36% greater than that of the single-labelled location. This suggests that initially denitrification of labelled NO_3^- was having a significant influence on site preference and this decreased as NO_3^- disappeared from the site. Note that the double-labelled center sites also had a greater cumulative NO_3^- flux than did the SGW sites (Table 13).

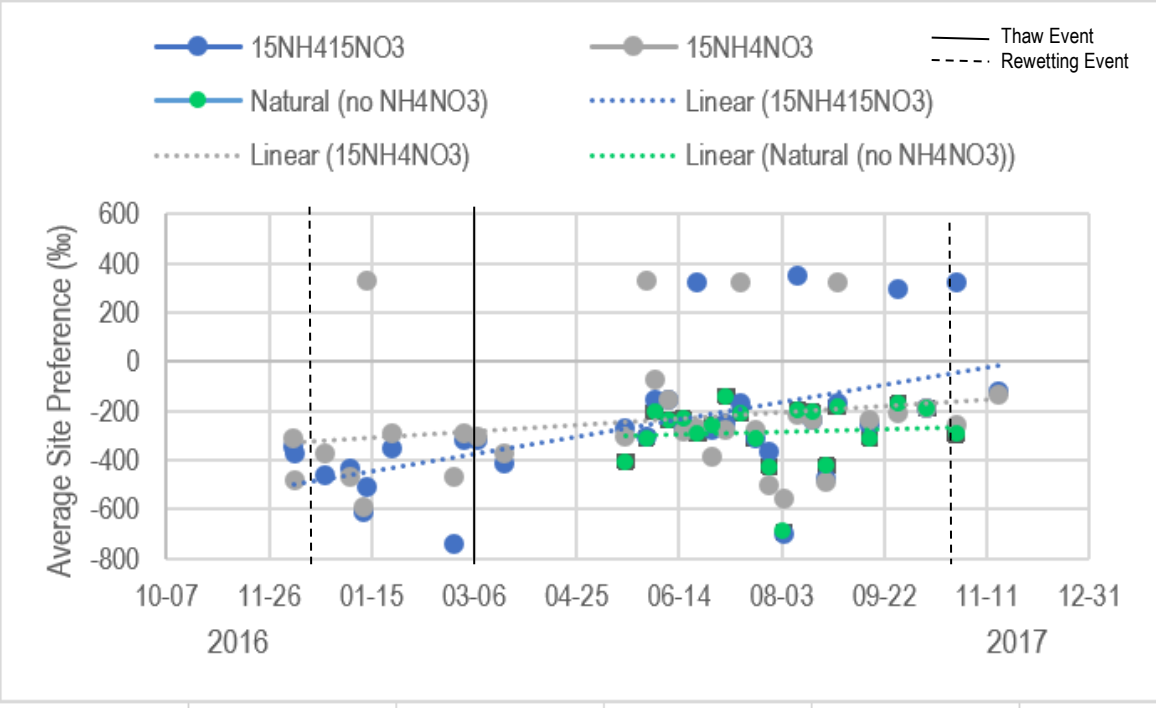

Figure 26. Average site preference over time, with defined events displayed with black lines.

Influence of ^{15}N labeling on CO_2 and N_2O surface flux

Production of CO_2 was not heavily influenced by labeling. In one instance, following August 2017, the single-labelled location produced more CO_2 than the double-labelled or naturalized locations.

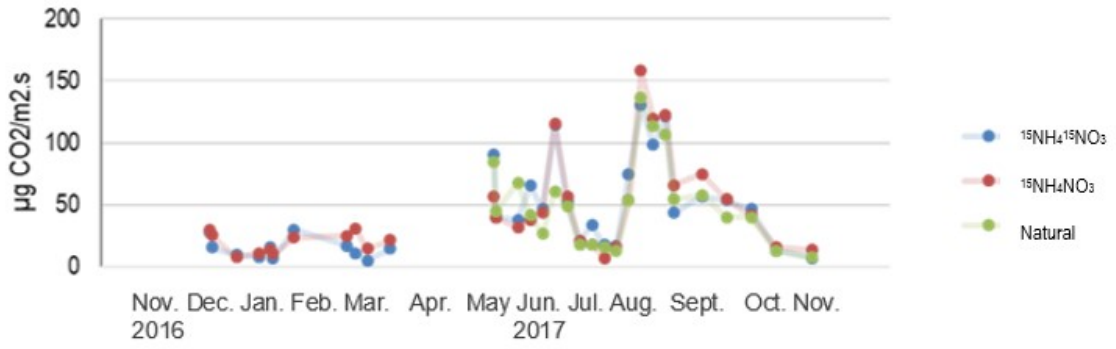

Figure 27. Average CO_2 emissions produced by NH_4NO_3 labelled locations.

More N_2O was produced from the single-labelled $^{15}NH_4NO_3$ SGW location in August 2017 and September 2017, otherwise, the rate of N_2O production was not influenced by location (Figure 28). Interestingly, the natural abundance locations (which were never labelled) consistently produced greater average N_2O than the locations that received either source of labelled NH_4NO_3.

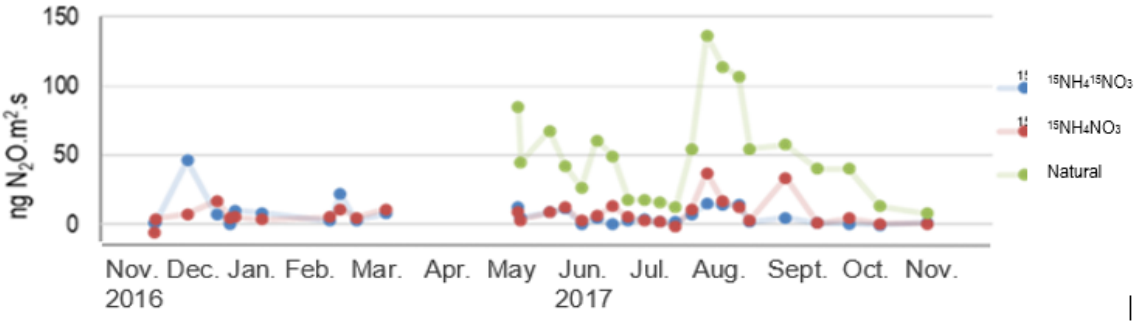

Figure 28. Average N_2O emissions produced by NH_4NO_3 labelled locations.

5.4 Discussion

Morse and Bernhardt, 2013 found relatively low N_2O emissions from nitrification and denitrification in a study that had soil cores amended with labelled NO_3^- or NH_4^+ and were subjected to drying and wetting. The greatest N_2O yield from nitrification was obtained from high soil moisture, and the greatest N_2O yield from denitrification was found during simulated rain events (Morse and Bernhardt, 2013). Similarly, the greatest N_2O emissions in this study occurred in August 2017, following an irrigation event. In another study that looked at influential weather and management factors, denitrification was the main source of N_2O in residue-amended soil even at low moisture conditions (Li et al., 2016). The sample dates in our study produced relatively steady N_2O yields and were not heavily influenced by time of year, i.e. weather fluctuations.

Results for both alpha ^{15}N and beta ^{15}N were relatively constant with time in the center well location where double-labelled $^{15}NH_4{}^{15}NO_3$ was added, even decreasing in the case of beta ^{15}N. However, in alpha and beta ^{15}N for single-labelled $^{15}NH_4NO_3$ locations, there was a slight increase in average ^{15}N over time. This suggests that those locations were working to return to natural abundance as the labelled $^{15}NH_4{}^+$ was nitrified. Another study that labelled field soils with $^{15}NO_3$ or $^{15}NH_4$ found that the main pathway of N_2O release was denitrification; on soils with high or normal organic matter contents, between 54-76 % of N_2O was obtained from denitrification, in agricultural black earth soils under field conditions in Central Germany (Russow et al., 2008).

Site Preference provides a heightened ability to determine the source contribution of N_2O from nitrification and denitrification (Sutka et al., 2006; Zhang et al., 2016). SP is defined as the difference in isotopic ^{15}N content between the central (α position) and the terminal N atom (β position) in the asymmetric N_2O molecule (Wu et al., 2016), as per the equation $SP = \delta^{15}N^{\alpha} - \delta^{15}N^{\beta})$ (Toyoda et al., 1999). In our study, we used only one label or marker (^{15}N). Often the use of dual isotopes, i.e. ^{15}N and ^{18}O are used to trace source partitioning of N_2O; as well as standards for individual sites. General trends in the labelled data reveal that SP in both the double-labelled and single-labelled cells was initially strongly negative and gradually increased over the sampling season (Figure 26). The negative value of site preference suggests that nitrification and not denitrification is the primary source of N_2O. Limitations of the distinguishing ability are largely due to the dynamic and overlapping signatures of nitrogen microbial processes.

5.5 Conclusions

The CRDS was able to read ^{15}N information from surface flux samples. Comparative literature is not available to confirm the quality of the readings based on the process used or applications to agriculture. Alpha ^{15}N and beta ^{15}N trends returned to steady state following application of NH_4NO_3 amendment, which suggests that the substrate was consumed quickly by microorganisms. Site preference, which was used in this study as an indicator of the dominant source of N_2O, showed increasing trends over the sampling season and was expressed at a magnitude of 10-fold when compared to the literature's natural abundance values. Though additional ^{15}N was added to cells, this magnitude is still much greater than expected and is consistent on control sites as well. This may reflect unknowns in the environment from which the surface flux samples were obtained, parameters associated with the lab in which the samples were run, or measurement interpretation on the CRDS itself. There is a need to extend on this work across multiple locations to create a basis of site preference expectations for areas labelled with additional ^{15}N. We assumed negative site preference values were reflective of instances when nitrification was the dominant source of N_2O, and positive integer values were denitrification. Nitrification dominated as the source of N_2O. Denitrification dominated only 1.4% of the time across all cells. In the few instances when denitrification was found to be the dominant source of N_2O, the events lined up with rewetting events defined earlier in Chapter 3. Denitrification events occurred most frequently in the double-labelled cells, consistent with our expectations.

CHAPTER 6: OVERALL CONCLUSIONS

This study monitored several interrelated parameters over a lysimeter field system in Bible Hill, Nova Scotia. The main theme of this work was to describe the magnitude of environmental change that resulted in trigger events for the site. Further, the response of soil microbial activity (in the form of soil respiration), and release of N_2O emissions in response to those events was explored. In the process of addressing this main central theme, the study examined how carbon availability in the system, through N-Viro® alkaline biosolid treatments, affected soil chemical transformations for C and N, as well as exploring the use of a relatively new spectrometry tool (Picarro® Cavity Ring-Down Spectrometer) in ^{15}N labeling of field sites for N_2O source identification.

The three identified objectives of this study were (1) to develop a method of predicting weather events (or "trigger events"); and examine the influence of those trigger events, under natural field conditions, in prompting soil microbial activity as measured by soil respiration and N_2O surface flux; (2) to examine the influence of application rate of N-Viro® alkaline biosolid amendment on soil respiration in a natural field system; and finally (3) to access the utility of ^{15}N site preference and the Picarro® Cavity Ring-Down Spectrometer to distinguish the source of N_2O, i.e. nitrification or denitrification, from surface flux samples obtained on ^{15}N labelled-NH_4NO_3 modified sites.

This study did effectively define trigger event thresholds for thaw events and rewetting events on this site. A thaw event threshold of a 0.1 °C change in soil temperature produced a consistent trigger over 67% of the cells monitored. This thaw trigger event was successful in revealing responses in soil CO_2 and O_2 concentrations following a short lag period. A rewetting trigger event was defined by a 2.5% change in soil

volumetric water content over 15 minutes. The definition of a rewetting trigger was more difficult to obtain consistently across cells; however, all cells did produce a response for the defined rewetting trigger. It is expected that inconsistencies in packing, or other unknown environmental parameters, across cells created high variability in water drainage, resulting in less consistent soil volumetric water content across cells. A parallel study conducted on the same site during the time of our study revealed large variations in drainage rates across cells (data not shown). Trigger events, as defined in this study, do result in responses in soil CO_2 and O_2. Responses are usually negatively correlated relationships between CO_2 and O_2 which appear following a short lag (of 0.5 to 2 hours) after the event was detected and generally result in increases in soil respiration (CO_2) and pulses of N_2O flux.

Most of the trigger events occurred in August and November and the season influenced the nature of the response in CO_2 and O_2 concentrations. Summer trigger events reflected both negatively correlated relationships (CO_2 increased, O_2 decreased and vice-versa), while winter trigger events showed increasing CO_2 and decreasing O_2 patterns. Some instances in March, May, July, and December witnessed only the O_2 increasing and CO_2 decreasing relationship. Rewetting dates of interest, which were defined as rewetting trigger events that occurred over multiple cells, were February 26, 2017, August 6, 2017, and September 28, 2017. Thaw dates of interest occurred on March 12-16, 2017 and December 22-26, 2017. Changes in N_2O flux production were also affected by trigger events, as well as management practices (including the application of biosolid and irrigation). N_2O flux increased immediately following rewetting and irrigation events.

The influence of N-Viro® biosolid, which had a readily available carbon component, also caused a surge in the production of N_2O, regardless of the rate of application. Cumulative NO_3^- and NH_4^+ from anion exchange membranes and plant root simulator probes demonstrated that the biosolid amendment rate was significant to the accumulation of NO_3^- and NH_4^+, i.e. soil N processes. High rates of biosolid application increased average N present in the soil. Cumulative NO_3 was measured via two applications, anion exchange membranes and plant root simulator probes, at two separate depths.

Interestingly, the two devices did not show the same result for labelled ^{15}N locations. The difference between the Center Drain and the monitoring location was only deemed significant to cumulative NO_3 by the anion exchange membranes (which showed a higher NO_3^- content at the double-labelled $^{15}NH_4{}^{15}NO_3$ location, within the center drain tile). This suggests that NO_3^- was a consequence of leaching as the AEMs were at a deeper depth in the soil profile. N_2O production was greater (by 2.5%) in the Center Drain locations. These locations would have received a biosolid amendment over a long-term period before this study, which suggests that the soil structure within the Center Drain location was previously altered. Long term biosolid application increases soil organic matter and pH, conducive to nitrification populations, which were later found to be the dominant source of N_2O.

Further, to meet the last objective, the 30-minute surface flux samples (from the manual samples that were obtained for N_2O analysis) were run on the Picarro® Cavity Ring-Down Spectrometer, a device which can differentiate between sources of characteristics of ^{15}N in N_2O to provide insight on whether the dominant source of N_2O was denitrification or nitrification through site preference measurements. The Picarro® CRDS

did successfully provide data on the small surface flux exetainers however, the quality of that data is highly subject to the machine operator and laboratory conditions on any given day. Additionally, there is limited knowledge of which ranges of site preferences are appropriate to define sources of N_2O in these samples, especially for such a limited site. Nevertheless, site preference in both the double-labelled $^{15}NH_4{}^{15}NO_3$ and single-labelled $^{15}NH_4NO_3$ locations increased over the sampling season. The slope of the increase of the $^{15}NH_4{}^{15}NO_3$ location was 36% greater than that of the $^{15}NH_4NO_3$ location. Site preference was used to infer the dominant source of N_2O. Negative site preferences were attributed to nitrification, while positive site preference values were attributed to denitrification. Denitrification dominance occurred 1.4% of the time over all cells and only during periods of wet weather, as expected. Additionally, the denitrification dominant instances occurred on predefined rewetting events.

Though the influence of the biosolid amendment rate and the tracing of the N_2O source were the most exciting aspects of this study, their importance about the definition of trigger events is far less substantial. The ability to predict soil microbial activity based on instantaneous weather data (soil temperature and soil volumetric water content) is an important tool for agriculture. This study was able to design customized rewetting and thaw triggers that resulted in a response in soil respiration and N_2O emissions. This procedure could be used on infinite sites to provide the agricultural industry with site-specific data monitoring and instantaneous predictions of soil respiration and consequently soil microbial activity, which is the greatest single source of N_2O emissions from agriculture. In furthering the definition of trigger events for Nova Scotia, multiple sites could be evaluated to contribute to the uncovering of the “best trigger event definition” for the region, based on site characteristics, across the province. This information could contribute to the development of a model for forecasting spikes in GHG

emissions, and consequently developing best management practices to limit them and ultimately reduce the agricultural sector's contribution to climate change.

REFERENCES

Ashworth, A., Allen, F., Wright, J., Saxton, A., & Tyler, D. (2014). Long-Term Soil Organic Carbon Changes as Affected. In *Soil Carbon*. doi:10.1007/978-3-319-04084-4.

Baggs, E. (2008). A review of stable isotope techniques for N_2O source partitioning in soils: recent progress, remaining challenges and future considerations. *Rapid Communications in Mass Spectrome*try. 22:1664-1667.

Baggs, E. (2011). Soil microbial sources of nitrous oxide: recent advances in knowledge, emerging challenges, and future direction. *Current Opinion in Environmental Sustainability*. 3:321-327.

Bol, Toyoda, Yamulki, Hawkins, Cardenas, & Yoshida. (2003). Dual isotope and isotopomer ratios of N 2 O emitted from a temperate grassland soil after fertiliser application. *Rapid Communications in Mass Spectrometry, 17*(22), 2550-2556.

Burton, D.L. and Beauchamp, E.G. (1994). Profile nitrous oxide and carbon dioxide concentrations in a soil subject to freezing. *Soil Sci. Soc. Am. J. 58*, 115-122.

Burton, D.L., Zebarth, B.J., Gillam, K.M. and MacLeod, J.M. (2008). Effect of split application of fertilizer nitrogen on N2O emissions from potatoes. *Can. J. Soil Sci. 88*, 229-239.

Bonnett, S., Blackwell, M., Leah, R., Cook, V., O'Connor, M., Maltby, E., & Bonnett, SAF. (2013). Temperature response of denitrification rate and greenhouse gas production in agricultural river marginal wetland soils. *Geobiology, 11*(3), 252-267.

Bremner, J. (1997). Sources of nitrous oxide in soils. *Nutrient Cycling in Agroecosystems, 49*(1), 7-16.

Butterbach-Bahl, K., Baggs, E., Dannenman, M., Kiese, R., and Zechmeister Boltenstern, S. (2013). Nitrous oxide emissions from soils: how well do we understand the processes and their controls?. *Philosophical Transactions of the Royal Society B*. 368:20130102.

Cao & Woodward. (1998). Dynamic responses of terrestrial ecosystem carbon cycling to global climate change. *Nature*, 393(6682), 249-252.

Carter, M. (1993). *Soil sampling and methods of analysis*. Boca Raton: Lewis.

Climate Action Network. (n.d.). Impacts in Canada. Retrieved March 22, 2017, from http://climateactionnetwork.ca/issues/impacts-and-adaptation/learning-cente/impacts-in-canada/.

Coleman D. C., Crossley D. A., Jr., Hendrix P. F. (2004). *Fundamentals of Soil Ecology*, 2nd Edn.Amsterdam: Elsevier [Google Scholar].

Conant RT, Paustian K, Elliott ET (2001). Grassland management and conversion into grassland: effects on soil carbon. *Ecol Appl* 11:343–355

Congreves, K., Wagner-Riddle, C., Si, B., & Clough, T. (2018). Nitrous oxide emissions and biogeochemical responses to soil freezing-thawing and drying-wetting. *Soil Biology and Biochemistry, 117*, 5-15.

Cramer, W., Bondeau, A., Woodward, F., Prentice, I., Betts, R., Brovkin, V., . . . Young Molling, C. (2001). Global response of terrestrial ecosystem structure and function to CO2 and climate change: Results from six dynamic global vegetation models. *Global Change Biology*, *7*(4), 357-373.

Cui, J., Sadegh Askari, M., and Holden, N. (2014). Relating Soil Carbon and Soil Structure to Land Use Management. In *Soil Carbon*. doi:10.1007/978-3-319-04084-4.

Daims, Lebedeva, Pjevac, Han, Herbold,Albertsen, . . . Wagner. (2015). Complete nitrification by Nitrospira bacteria. *Nature,528*(7583), 504-509.

De Jong, Drury, Yang, & Campbell. (2009). Risk of water contamination by nitrogen in Canada as estimated by the IROWC-N model. *Journal of Environmental Management,90*(10), 3169-3181.

Denk, Mohn, Decock, Lewicka-Szczebak, Harris, Butterbach-Bahl, . . . Wolf. (2017). The nitrogen cycle: A review of isotope effects and isotope modeling approaches. *Soil Biology and Biochemistry*, 105, 121-137.

Ding, C., Ohmori, H., Takamura, H., (2006). Relationship between water quality and land use in the Mamagawa river, Tokyo Metropolitan Area. *Journal of Japanese Association of* Hydrological Sciences 36 (4), 219e233.

Dyson, F. (2008). The question of global warning. New York review of books. http://www.nybooks.com/articles/archieves/2008/Jun/12/the-question-of-global-warming

Earth Systems Research Lab. (2005, October 01). ESRL Global Monitoring Division – Global Greenhouse Gas Reference Network. Retrieved December 2018, from https://www.esrl.noaa.gov/gmd/ccgg/trends/global.html

Franzluebbers, A.J. (1999). Microbial activity in response to water-filled pore space of variably eroded southern Piedmont soils. *Appl. Soil Ecol. 11*:91–101.

Gillis, Price, Stratton, & Gillis, J. (2014). Detection and degradation of organic contaminants in an agricultural soil amended with alkaline-treated biosolids. *Canadian Journal of Soil Science, 94*(5), 595-604.

Gregorich, Rochette, Vandenbygaart, & Angers. (2005). Greenhouse gas contributions of agricultural soils and potential mitigation practices in Eastern Canada. *Soil & Tillage Research, 83*(1), 53-72.

Groenigen, v.,J.W., Huygens, D., Boeckx, P., Kuyper, T. W., Lubbers, I. M., Rutting, L., et al. (2015). The soil N cycle: New insights and key challenges. *Soil*, 1, 235-256.

Guo, X., Drury, C., Yang, X., Reynolds, W., & Zhang, R. (2012). Impacts of Wet–Dry Cycles and a Range of Constant Water Contents on Carbon Mineralization in Soils under Three Cropping Treatments. *Soil Science Society of America Journal, 76*(2), 485-493.

Haei, Rousk, Ilstedt, Öquist, Bååth, & Laudon. (2011). Effects of soil frost on growth, composition and respiration of the soil microbial decomposer community. *Soil Biology and Biochemistry, 43*(10), 2069-2077.

Hardemink, A., & McSweeney, K. (Eds.). (2014). *Soil Carbon*. Dordrecht: Springer. doi:978-3-319-04084-4.

Health Canada (2017). Guidelines for Canadian Drinking Water Quality—Summary Table. Water and Air Quality Bureau, Healthy Environments and Consumer Safety Branch, Health Canada, Ottawa, Ontario.

Henry, H.A.L. (2007). Soil freeze-thaw cycle experiments: Trends, methodological weaknesses and suggested improvements. *Soil Biology &, 39*, 977-986.

Herrmann, A., & Witter, E. (2002). Sources of C and N contributing to the flush in mineralization upon freeze–thaw cycles in soils. *Soil Biology and Biochemistry, 34*(10), 1495-1505.

Hoorman, J. (2010, September 7). Understanding Soil Microbes and Nutrient Cycling. Retrived March 03, 2019, from https://ohioline.osu.edu/factsheet/SAG-16

Hursh, A., Ballantyne, A., Cooper, L., Maneta, M., Kimball, J., & Watts, J. (2017). The sensitivity of soil respiration to soil temperature, moisture, and carbon supply at the global scale. *Global Change Biology, 23*(5), 2090-2103.

International Plant Nutrition Institute. (2019). “Greenhouse Gas Reduction: Nitrous Oxide Emissions Reduction Protocol. *Fertilizer Canada.* fertilizercanada.ca/nutrientstewardship/greenhouse-gas-reduction/.

Jefferies, Walker, Edwards, Dainty. (2010). Is the decline of soil microbial biomass in late winter coupled to changes in the physical state of cold soils? *Soil Biology & Biochemistry, 42*, pp. 129-135.

Koch, H., Kessel, M.A.H.J. van, & Lücker, S. (2018). Complete nitrification: Insights into the ecophysiology of comammox Nitrospira. *Applied Microbiology and Biotechnology,* 1-13.

Kool, Müller, Wrage, Oenema, & Van Groenigen. (2009). Oxygen exchange between nitrogen oxides and H 2O can occur during nitrifier pathways. *Soil Biology and Biochemistry, 41*(8), 1632-1641.

Lai, T., & Denton, M. (2018). N2O and N2 emissions from denitrification respond differently To temperature and nitrogen supply. *Journal of Soils and Sediments, 18*(4), 1548-1557.

Lal, R. (2004). Soil carbon sequestration to mitigate climate change. Geoderma 123:1 22 Maag M, Vinther FP. (1996). Nitrous oxide emission by nitrification and denitrification in different soil types and at different soil moisture contents and temperatures. *Appl Soil Ecol 4*:5–14

Lasa, B., Quemada, M., Frechilla, S., Muro, J., Lamsfus, C. & AparicioTejo, P.M. (1997). Effect of digested sewage sludge on the efficiency of N-fertilizer applied to barley. Nutrient Cycling in *Agroecosystems*, *48*, 241–246.

Lee, Y., Choi, H., & Cho, K. (2019). Effects of carbon source, C/N ratio, nitrate, temperature, and pH on N2O emission and functional denitrifying genes during heterotrophic denitrification. *Journal of Environmental Science and Health*. Part A, Toxic/hazardous Substances & Environmental Engineering,54(1), 16-29.

Li, Sørensen, Olesen, & Petersen. (2016). Evidence for denitrification as main source of N2O emission from residue-amended soil. *Soil Biology and Biochemistry, 92*, 153-160.

Liu, Xinchao, Dong, Yunshe, Qi, Yuchun, Peng, Qin, He, Yating, Sun, Liangjie, . . . Liu, Xuehua. (2015). Response of N2O emission to water and nitrogen addition in temperate typical steppe soil in Inner Mongolia, China. *Soil & Tillage Research, 7*(1), 9-17.

Lorenz K, Lal R. (2005). The depth distribution of soil organic carbon in relation to land use and management and the potential of carbon sequestration in sub soil horizons. *Adv Agron* 88:36–66

Ma, Bedard-Haughn, Siciliano, & Farrell. (2008). Relationship between nitrifier and denitrifier community composition and abundance in predicting nitrous oxide emissions from ephemeral wetland soils. *Soil Biology and Biochemistry, 40*(5), 1114-1123.

Maggi, F., & Riley, W. (2015). The effect of temperature on the rate, affinity, and 15 N fractionation of NO3 − during biological denitrification in soils. *Biogeochemistry, 124*(1), 235-253.

Mahendrappa, M. K., R. L. Smith, and A. T. Christiansen. (1966). Nitrifying organisms affected by climatic region in western United States. *Soil Sci . Soc. Am. Proc* . 301'60,2.

Matzner, E., & Borken, W. (2008). Do freeze-thaw events enhance C and N losses from soils of different ecosystems? A review. *European Journal of Soil Science, 59*(2), 274-284.

McGill, W. B. (2007). The Physiology and Biochemistry of Soil Organisms. *In Soil Microbiology, Ecology, and Biochemistry* (3rd ed., pp. 245-250). Burlington, MA: Elsevier.

Morse, & Bernhardt. (2013). Using 15N tracers to estimate N2O and N2 emissions from nitrification and denitrification in coastal plain wetlands under contrasting land-uses. *Soil Biology and Biochemistry*, 57, 635-643.

Mueller, C., Kammann, C., Ottow, J. C. G., & Jaeger, H. J. (2003). Nitrous oxide emission from frozen grassland soil and during thawing periods. *Journal of Plant Nutrition and Soil Science*, 166(1), 46-53.

Nevison, C., & Holland, E. (1997). A reexamination of the impact of anthropogenically fixed nitrogen on atmospheric N sub(2) O and the stratospheric O sub(3) layer. *Journal of Geophysical Research, Washington, DC, 102*(D21), 25519-25536.

Nol, L., Verburg, P., & Moors, E. (2012). Trends in future N2O emissions due to land use change. *Journal of Environmental Management, 94*(1), 78-90.

Parkin, T.B., Sextone, A.J., & Tiedje, J.M. (1985). Adaptation of denitrifying populations to low soil pH. *Applied and Environmental Microbiology,* (5), 1053-0156.

Paul, K.I., P.J. Polglase, A.M. O'Connell, J.C. Carlyle, P.J. Smethurst, and P.K. Khanna. (2003). Defining the relation between soil water content and net nitrogen mineralization. Eur. *J. Soil Sci. 54*:39–47.

Phillips, R., Mcmillan, A., Palmada, T., Dando, J., & Giltrap, D. (2014). Temperature effects on N2O and N2 denitrification end-products for a New Zealand pasture soil. *New Zealand Journal of Agricultural Research, 58*(1), 1-7.

Picarro, Inc. (2019). Cavity Ring Down Spectrometer (CRDS). Retrieved from https://www.picarro.com/company/technology/crds

Pinto, A., Marcus, D., Ijaz, U., Bautista-de Lose Santos, Q., Dick, G., & Raskin, L. (2016). Metagenomic Evidence for the Presence of Comammox Nitrospira-Like Bacteria in a Drinking Water System. *MSphere, 1*(1), MSphere, 2016, Vol.1(1).

Poh, L., Jiang, X., Zhang, Z., Liu, Y., Ng, W., & Zhou, Y. (2015). N2O accumulation from Denitrification under different temperatures. *Applied Microbiology and Biotechnology, 99*(21), 9215-9226.

Price, G., Astatkie, T., Gillis, J., & Liu, K. (2015). Long-term influences on nitrogen dynamics and pH in an acidic sandy soil after single and multi-year applications of alkaline treated biosolids. *Agriculture, Ecosystems and Environment, 208*, 1-11.

Province of Nova Scotia. (2014, October 20). Climate Data for Nova Scotia. Retrieved June 02, 2019, from https://climatechange.novascotia.ca/climate-data?tid=10#climate-data-map

Raich, J., Potter, C., & Bhagawati, D. (2002). Interannual variability in global soil respiration, 1980–94. Global Change Biology, 8(8), 800-812.

Reddy, & Crohn. (2014). Effects of soil salinity and carbon availability from organic amendments on nitrous oxide emissions. Geoderma, 235-236, 363-371.Santoro, A. (2016). *MICROBIOLOGY*. The do-it-all nitrifier. *Science (New York, N.Y.),351*(6271), 342-343.

Risk, N., Snider, D., & Wagner-Riddle, C. (2013). Mechanisms leading to enhanced soil nitrous oxide fluxes induced by freeze-thaw cycles. *Canadian Journal of Soil Science*, 93(4), 401-414. doi:10.4141/cjss2012-071.

Robertson, G. P. (1989). Nitrification and denitrification in humid tropical ecosystems. *I* "Mineral Nutrients in Tropical Forest and Savanna Ecosystems" (J. Proctor, ed.), pp. 55–70. Blackwell Sci., Cambridge, UK.

Robertson, G P, and P M Groffman. (2007). Nitrogen Transformations – Nitrogen Mineralization and Immobilization. *Soil Microbiology, Ecology, and Biochemistry*, edited by E Paul, 3rd ed., Elsevier, pp. 344–346.

Rockström J, Steffen W, Noone K et al. (2009). A safe operating space for humanity. *Nature* 461:472–475

Roper, J.D., Burton, D.L., Madani, A. and Stratton, G.W. (2013). A simple method for quantifying dissolved nitrous oxide in tile drainage water. *Can. J. Soil Sci. 93*, 59-64.

Russow, R., Spott, O., & Stange, C.F. (2008). Evaluation of nitrate and ammonium as sources of NO and N2O emissions from black earth soils (Haplic Chernozem) based on 15N field experiments. *Soil Biology, 40*, 380-391.

San Emeterio, L., Canals, R., & Herman, D. (2014). Combined effects of labile and recalcitrant carbon on short-term availability of nitrogen in intensified arable soil. *European Journal of Soil Science, 65*(3), 377-385.

Savard, M. M., Paradis, D., Somers, G., Liao, S., & van Bochove, E. (2007). Winter nitrification contributes to excess NO3- in groundwater of an agricultural region: A dual-isotope study. *Water Resources Research, 43*, 6422-6433.

Schaufler, G., Kitzler, B., Schindlbacher, A., Skiba, U., Sutton, M.A., Zechmeister Boltenstern, S. (2010). Greenhouse gas emissions from European soils under different land use: effects of soil moisture and temperature. *Eur. J. Soil Sci*., 61 (5), pp. 683-696.

Schimel, Balser, Wallenstein. (2007). Microbial stress-response physiology and its implications for ecosystem function. *Ecology*, 88, pp. 1386-1394.

Schlüter, S., Henjes, S., Zawallich, J., Bergaust, L., Horn, M., Ippisch, O., . . . Dörsch, P. (2018). Denitrification in Soil Aggregate Analogues-Effect of Aggregate Size and Oxygen Diffusion. *Frontiers in Environmental Science, 6*, Frontiers in Environmental Science, Apr 11, 2018..

Signor, D., & Pellegrino Cerri, C. (2013). Nitrous oxide emissions in agricultural soils: A review. *Pesquisa Agropecuária Tropical, 43*(3), 322-338.

Soto Golcher, Arts, & Visseren-Hamakers. (2018). Seeing the forest, missing the field: Forests and agriculture in global climate change policy. *Land Use Policy, 77*, 627-640.

Soussana JF, Loiseau P, Vuichard N, Ceschia E, Balesdent J, Chevallier T, Arrouays D (2004). Carbon cycling and sequestration opportunities in temperate grasslands. *Soil Use Manag* 20:219–230

Stockdale, E.A., Hatch, D.J., Murphy, D.V., Ledgard, S.F. & Watson, C.J. (2002). Verifying the nitrification to immobilisation ratio (N/I) as a key determinant of potential nitrate loss in grassland and arable soils. *Agronomie, 22*, 831–838.

Sutka, R. L., Ostrom, N. E., Ostrom, P. H., Gandhi, H., & Breznak, J. A. (2003). Nitrogen isotopomer site preference of N 2 O produced by Nitrosomonas europaea and Methylococcus capsulatus Bath. *Rapid Communications in Mass Spectrometry, 17*(7), 738-745.

Sutka, R. L., Ostrom, N. E., Ostrom, P. H., Breznak, J. A., Gandhi, H., Pitt, A. J., & Li, F. (2006). Distinguishing Nitrous Oxide Production from Nitrification and Denitrification on the Basis of Isotopomer Abundances. *Applied and Environmental Microbiology, 72*(1), 638.

Tatti, Goyer, Chantigny, Wertz, Zebarth, Burton, & Filion. (2014). Influences of over winter conditions on denitrification and nitrous oxide-producing microorganism abundance and structure in an agricultural soil amended with different nitrogen sources. *Agriculture, Ecosystems and Environment, 183*, 47-59.

Tatti, E., Goyer, C., Burton, D., Wertz, L., Zebarth, S., Chantigny, B., & Filion, J. (2015). Tillage Management and Seasonal Effects on Denitrifier Community Abundance, Gene Expression and Structure over Winter. *Microbial Ecology, 70*(3), 795-808.

Teepe, R., Brumme, & Beese. (2001). Nitrous oxide emissions from soil during freezing and thawing periods. *Soil Biology and Biochemistry, 33*(9), 1269-1275.

Tisdale, S. (1993). *Soil fertility and fertilizers.* (5th ed. / Samuel L. Tisdale ... [et al.].. ed.). New York : Toronto : New York: Macmillan ; Maxwell Macmillan Canada ; Maxwell Macmillan International.

Toyoda, S., and N. Yoshida. (1999). Determination of nitrogen isotopomers of nitrous oxide on a modified isotope ratio mass spectrometer. *Anal. Chem*. *71*:4711-4718.

Toyoda, S., M. H. Mutobe, H. Yamagishi, N. Yoshida, and Y. Tanji. (2005). Fractionation of N2O isotopomers during production by denitrifier. *Soil Biol. Biochem*. 37:1535 1545.

Toyoda, S., Yano, M., Nishimura, S., Akiyama, H., Hayakawa, A., Koba, K., . . . Yoshida, N. (2011). Characterization and production and consumption processes of N2O emitted from temperate agricultural soils determined via isotopomer ratio analysis. *Global Biogeochemical Cycles*, 25(2), N/a.

Toyoda, S., Yoshida, N., Koba, K. (2015). Isotopocule analysis of biologically produced nitrous oxide in various environments. *Mass Spectrometry Reviews*. http://dx.doi.org/10.1002/mas.

van Kessel C, Nitschelm J, Horwath W et al. (2000). Carbon-13 input and turnover in a pasture soil exposed to long term elevated atmospheric pCO2. *Glob Chang Biol* 6:123–135.

Vargas, R., Detto, M., Baldocchi, D., & Allen, M. (2010). Multiscale analysis of temporal variability of soil CO2 production as influenced by weather and vegetation. *Global Change Biology, 16*(5), 1589-1605.

Waghmode, T. R., Chen, S., Li, J., Sun, R., Liu, B., & Hu, C. (2018). Response of Nitrifier and Denitrifier Abundance and Microbial Community Structure to Experimental Warming in an Agricultural Ecosystem. *Frontiers in microbiology*, *9*, 474. doi:10.3389/fmicb.2018.00474

Wagner-Riddle, C., Congreves, K. A., Abalos, D., Berg, A. A., Brown, S. E., Ambadan, J. T., Gao, X. P., and Tenuta, M. (2017). Globally important nitrous oxide emissions from croplands induced by freeze-thaw cycles. *Nature Geoscience 10*, 279-+.\

Wagner-Riddle, C., & Thurtell, G. W. (1998). Nitrous oxide emissions from agricultural fields during winter and spring thaw as affected by management practices. *Nutrient Cycling in Agroecosystems, 52*(2-3), 151-163.

Weintraub & Schimel. (2003). Interactions between carbon and nitrogen mineralization and soil organic matter chemistry in arctic tundra soils. *Ecosystems*, *6,* pp. 129-143.

Weiss and Price. (1980). Nitrous Oxide Solubility in Water and Seawater. *Marine Chemistry, 8*, 347-359.

Well, R., Kurganova, I., Lopes de Gerenyu, V., & Flessa, H. (2006). Isotopomer signatures of soil-emitted N2O under different moisture conditions—A microcosm study with arable loess soil. *Soil Biology and Biochemistry, 38*(9), 2923-2933.

Wertz, S., Goyer, C., Zebarth, B., Burton, D., Tatti, E., Chantigny, M., & Filion, M. (2013). Effects of temperatures near the freezing point on N2O emissions, denitrification and on the abundance and structure of nitrifying and denitrifying soil communities. *FEMS Microbiology Ecology, 83*(1), 242-254.

West TO, & Post WM. (2002). Soil organic carbon sequestration rates by tillage and crop rotation: a global data analysis. *Soil Sci Soc Am* J 66:1930–1946

Winiwarter, W., Erisman, J., Galloway, W., Klimont, J., & Sutton, N. (2013). Estimating environmentally relevant fixed nitrogen demand in the 21st century. *Climatic Change, 120*(4), 889-901.

Winogradsky, S. (1891). Researches sur les organisms de la nitrification. *Ann Inst Pasteur*. 5:577-616.

Wrage, Velthof, Van Beusichem, & Oenema. (2001). Role of nitrifier denitrification in the production of nitrous oxide. *Soil Biology and Biochemistry, 33*(12), 1723-1732.

Wrage-Mönnig, Horn, Well, Müller, Velthof, & Oenema. (2018). The role of nitrifier denitrification in the production of nitrous oxide revisited. *Soil Biology and Biochemistry,123,* A3-A16.

Xu, Xiaoya, Ran, Yu, Li, Yong, Zhang, Qichun, Liu, Yapeng, Pan, Hong, . . . Xu, Jianming. (2016). Warmer and drier conditions alter the nitrifier and denitrifier communities and reduce N2O emissions in fertilized vegetable soils. *Agriculture, Ecosystems and Environment, 231*, 133-142.

Yamamoto, Akiyama, Nakajima, & Hoshino. (2017). Estimate of bacterial and fungal N2O production processes after crop residue input and fertilizer application to an agricultural field by 15N isotopomer analysis. *Soil Biology and Biochemistry, 108,* 9-16.

Zhang, Jim, & Lu. (2016). Fingerprint natural soil N_2O emission from nitration and denitrification by dual isotopes (15N and 18O) and site preferences. *Acta Ecologica Sinica, 36*(5), 356-360.

Zhu, X., Burger, M., Doane, T., Horwath, W. (2013). Ammonia oxidation pathways and nitrifier denitrification are significant sources of N_2O and NO under low oxygen availability. . *Proceedings of the National Academy of Sciences of the United States of America, 110*(16), 6328-6333.

APPENDIX A: SOIL MAP

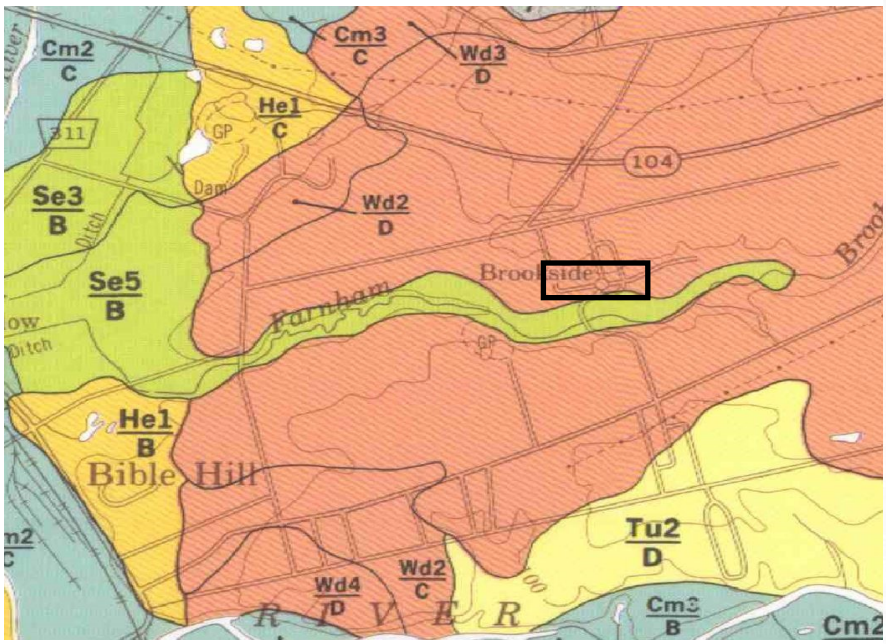

LEGEND

SOIL ASSOCIATION OR LAND TYPE	SOIL MATERIAL	COLOR & SYMBOL	MAP UNIT DESCRIPTION			
			SOIL COMPONENTS			
			DOMINANT SOILS	SIGNIFICANT SOILS	STONINESS	ROCKINESS
Rawdon	30 to 60 cm of gravelly sandy loam to gravelly loam over weakly compacted, olive brown, gravelly sandy loam to very gravelly loam, shallow, till derived from Cambrian slates and siltstones	Ra2	well drained soils	imperfectly drained soils (Ra3)	moderately to very stony	slightly rocky
		Ra3	imperfectly drained soils		moderately to very stony	non rocky
		Ra4	imperfectly drained soils (Ra3)	poorly drained soils (Ra5)	moderately to very stony	non rocky
		Ra5	poorly drained soils		moderately to very stony	non rocky
		Ra6	poorly drained soils (Ra5)	very poorly drained organic soils (Cl)	moderately to very stony	non rocky
Roseway	30 to 60 cm of gravelly loam to very gravelly sandy loam over dark brown, very gravelly sandy loam, shallow, stony, till derived from basalt	Ry1	rapidly to well drained soils		moderately stony	moderately rocky
		Ry2	rapidly to well drained soils (Ry1)	imperfectly drained soils	moderately stony	moderately rocky
		Ry4	imperfectly drained soils	poorly drained soils	moderately stony	non rocky
Salt Marsh	Grayish brown, silty clay loam marine sediments	SM	very poorly drained soils		non stony	non rocky
Stewiacke	Silt loam to silty clay loam, alluvium	Se3	imperfectly drained soils		non stony	non rocky
		Se4	imperfectly drained soils (Se3)	poorly drained soils (Se5)	non stony	non rocky
		Se5	poorly drained soils		non stony	non rocky
		Se6	poorly drained soils (Se5)	very poorly drained organic soils (Cl)	non stony	non rocky
Thom	60 to 80 cm of gravelly sandy loam to gravelly silt loam over compact, dark brown gravelly sandy loam to gravelly sandy loam till derived from hard sedimentary and metamorphic rocks	Tm1	well drained soils		very stony	slightly rocky
		Tm2	well drained soils (Tm1)	imperfectly drained soils (Tm3)	very stony	slightly rocky
		Tm3	imperfectly drained soils		very stony	non rocky
		Tm4	imperfectly drained soils (Tm3)	poorly drained soils (Tm5)	moderately stony	non rocky
		Tm5	poorly drained soils		moderately stony	non rocky
		Tm6	poorly drained soils (Tm5)	very poorly drained organic soils (Cl)	moderately stony	non rocky
Truro	60 to 80 cm of loamy sand to sandy loam over very friable to firm, red, glaciofluvial fine sands and loamy sands	Tu1	rapidly to well drained soils		non stony	non rocky
		Tu2	rapidly to well drained soils (Tu1)	imperfectly drained soils (Tu3)	non stony	non rocky
		Tu3	imperfectly drained soils		non stony	non rocky
		Tu4	imperfectly drained soils (Tu3)	poorly drained soils (Tu5)	non stony	non rocky
		Tu5	poorly drained soils		non stony	non rocky
Westbrook	50 to 70 cm of gravelly sandy loam to gravelly loam over compact, red gravelly sandy loam to very gravelly sandy loam, shallow, till derived from conglomerate	Wb1	well drained soils		moderately stony	slightly rocky
		Wb2	well drained soils (Wb1)	imperfectly drained soils (Wb3)	moderately stony	slightly rocky
		Wb3	imperfectly drained soils		slightly to moderately stony	non rocky
		Wb4	imperfectly drained soils (Wb3)	poorly drained soils	slightly to moderately stony	non rocky
Woodbourne	50 to 70 cm of gravelly loam to gravelly sandy loam over compact, dark reddish brown, gravelly loam to gravelly clay loam till derived from Carboniferous sandstone and shale	Wo1	moderately well drained soils		moderately stony	non rocky
		Wo2	moderately well drained soils (Wo1)	imperfectly drained soils (Wo3)	moderately stony	non rocky
		Wo3	imperfectly drained soils		moderately stony	non rocky
		Wo4	imperfectly drained soils (Wo3)	poorly drained soils (Wo5)	moderately stony	non rocky
		Wo5	poorly drained soils		moderately stony	non rocky
		Wo6	poorly drained soils (Wo5)	very poorly drained organic soils (Cl)	moderately stony	non rocky
Woodville	40 to 60 cm of sandy loam over firm, reddish brown, sandy loam to loam till derived from Triassic sandstone	Wd1	well drained soils		non to slightly stony	non rocky
		Wd2	well drained soils (Wd2)	imperfectly drained soils (Wd3)	non to slightly stony	non rocky
		Wd3	imperfectly drained soils		non to slightly stony	non rocky
		Wd4	imperfectly drained soils (Wd3)	poorly drained soils (Wd5)	non to slightly stony	non rocky
		Wd5	poorly drained soils		non to slightly stony	non rocky
		Wd6	poorly drained soils (Wd5)	very poorly drained organic soils (Cl)	non to slightly stony	non rocky
Wyvern	60 to 80 cm of gravelly sandy loam to very gravelly sandy loam over compact yellowish brown, gravelly sandy	Wn1	rapidly to well drained soils		very to excessively stony	moderately rocky
		Wn2	rapidly to well drained soils (Wn1)	imperfectly drained soils (Wn3)	very to excessively stony	moderately rocky
		Wn3	imperfectly drained		very to excessively	moderately rocky

APPENDIX B: EVENT THRESHOLD CONVERGENCE

REWETTING EVENTS

Change VOLUMETRIC WATER CONTENT over 15 minutes (m^3/m^3)	CELL NUMBER								
	1	**2**	**3**	**4**	**5**	**6**	**7**	**8**	**9**
0	132 98	128 42	74 36	58 02	35 93	70 62	48 46	20 38	65 91
0.005	166	233	12 8	14 2	17 9	13 3	76	91	52
0.01	46	100	57	59	52	64	27	35	23
0.015	21	50	34	34	22	39	15	22	16
0.02	11	31	21	20	5	33	8	17	9
0.025	9	23	14	16	4	24	7	11	4
0.03	7	19	13	13	1	21	5	9	4
0.035	4	16	11	11	1	16	1	6	4
0.04	4	15	7	10	1	14	1	6	1
0.045	4	13	7	6	1	13	1	6	1
0.05	3	11	5	5	**0**	11	1	4	1
0.055	2	11	5	4		10	1	2	1
0.06	2	10	3	4		9	1	2	1
0.065	2	9	2	4		6	1	2	1
0.07	2	8	1	3		5	1	2	1
0.075	2	8	1	3		5	1	2	1
0.08	2	7	1	3		4	1	2	1
0.085	2	7	1	3		4	1	2	1
0.09	1	7	**0**	2		4	1	2	1
0.095	1	6		2		3	1	2	1
0.1	1	4		1		2	1	2	1
0.105	1	4		**0**		2	1	2	1
0.11	1	4				1	1	2	1
0.115	1	3				1	1	2	1
0.12	1	2				1	1	2	1
0.125	1	2				1	1	2	1
0.13	1	2				1	1	2	1
0.135	1	2				1	1	2	1
0.14	1	2				1	1	2	**0**
0.145	1	1				1	1	2	
0.15	1	**0**				1	1	2	
0.155	1					1	1	2	

Change VOLUMETRIC WATER CONTENT over 15 minutes (m^3/m^3)	CELL NUMBER								
	1	**2**	**3**	**4**	**5**	**6**	**7**	**8**	**9**
0.16	**0**					1	1	2	
0.165						1	1	2	
0.17						1	1	**0**	
0.175						1	1		
0.18						1	1		
0.185						**0**	1		
0.19 – 0.885							1		
0.89							**0**		

APPENDIX C: WEATHER EVENT OBSERVATIONS

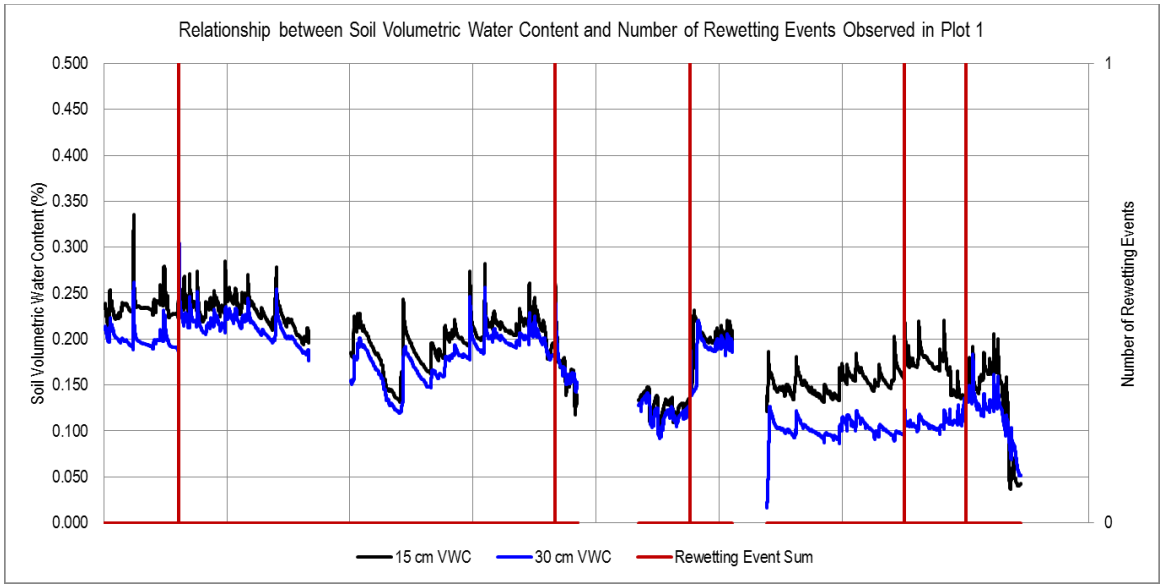

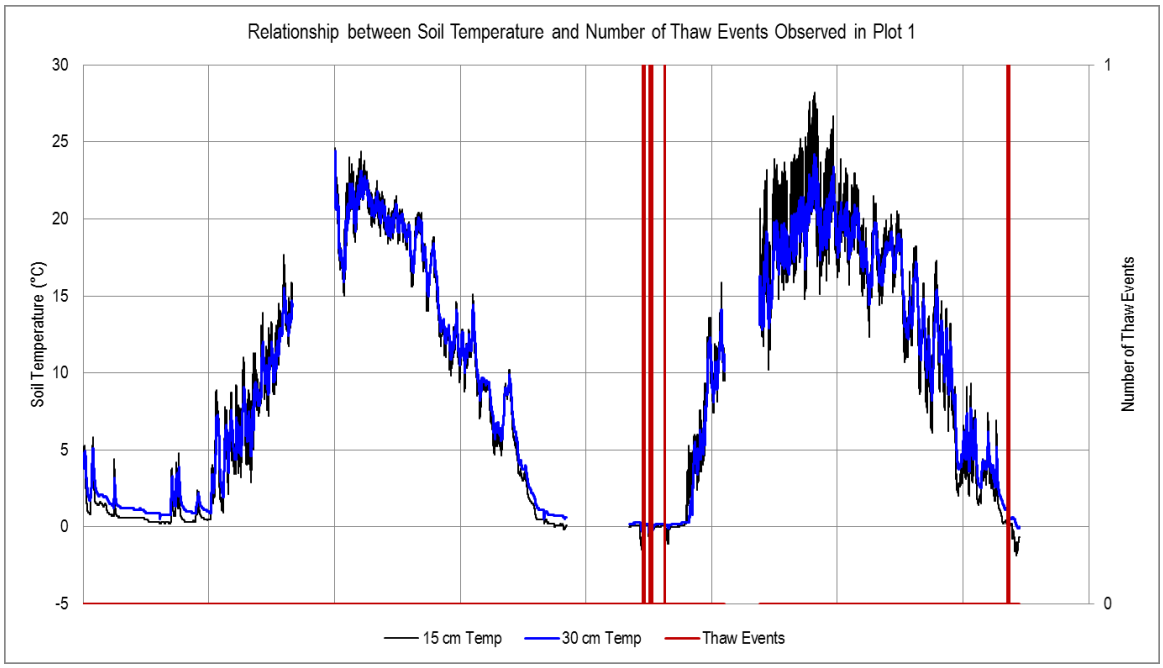

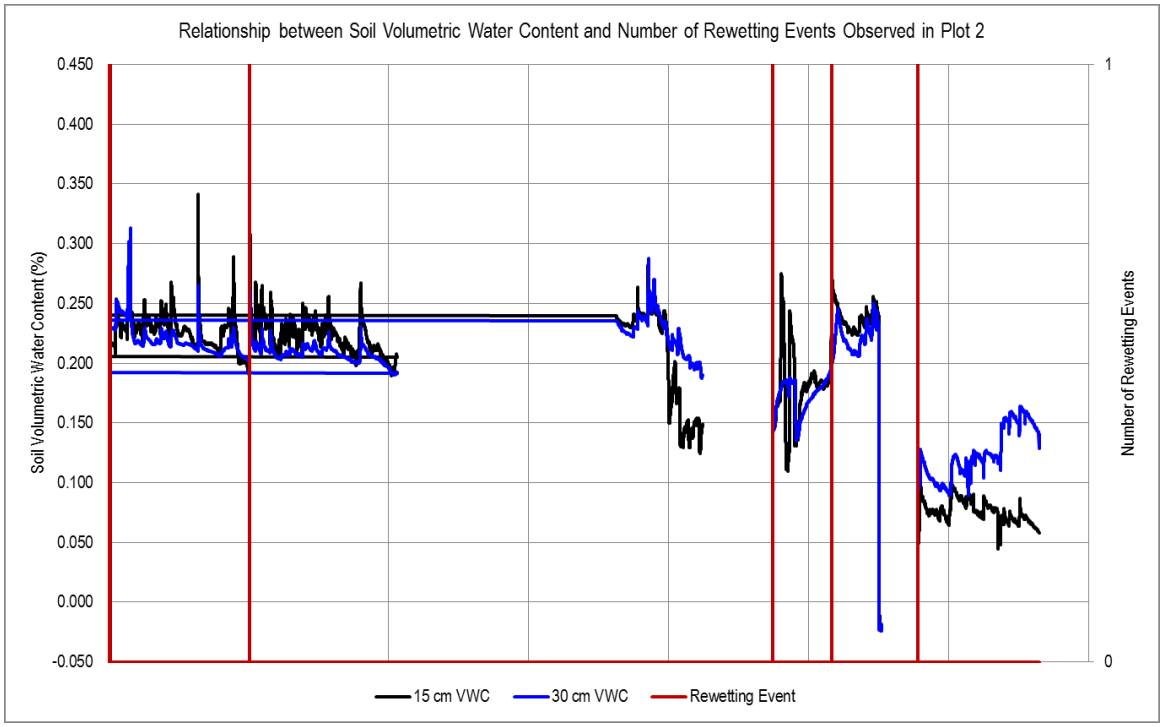
Relationship between Soil Volumetric Water Content and Number of Rewetting Events Observed in Plot 2
Soil Volumetric Water Content (%)
0.450
0.400
0.350
0.300
0.250
0.200
0.150
0.100
0.050
0.000
-0.050
Number of Rewetting Events
1
0
15 cm VWC
30 cm VWC
Rewetting Event

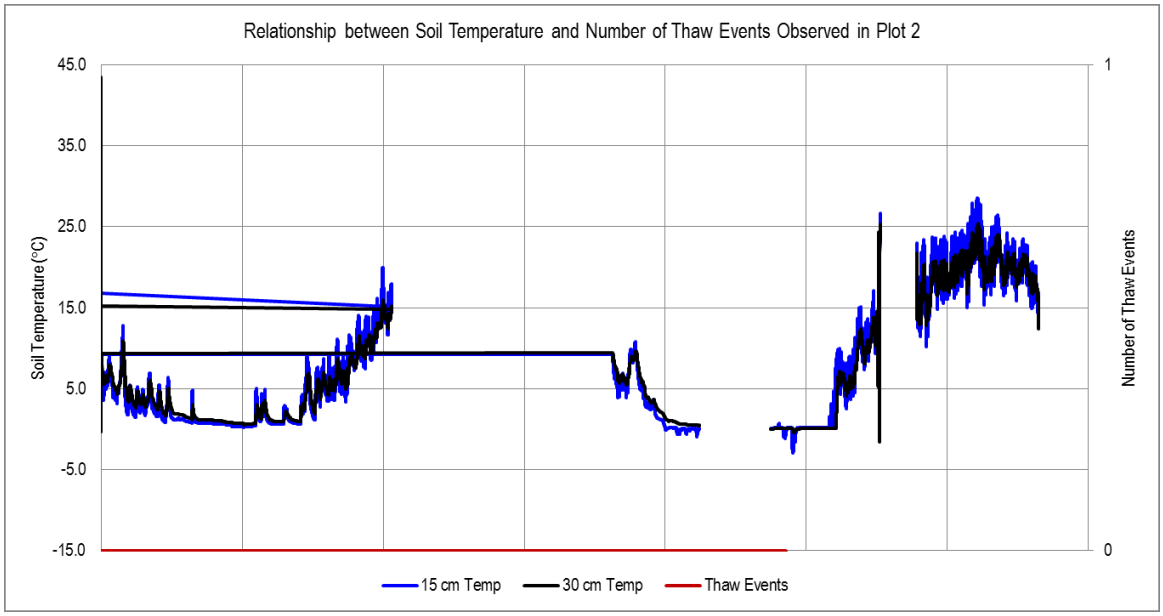
Relationship between Soil Temperature and Number of Thaw Events Observed in Plot 2
Soil Temperature (°C)
45.0
35.0
25.0
15.0
5.0
-5.0
-15.0
Number of Thaw Events
1
0
15 cm Temp
30 cm Temp
Thaw Events

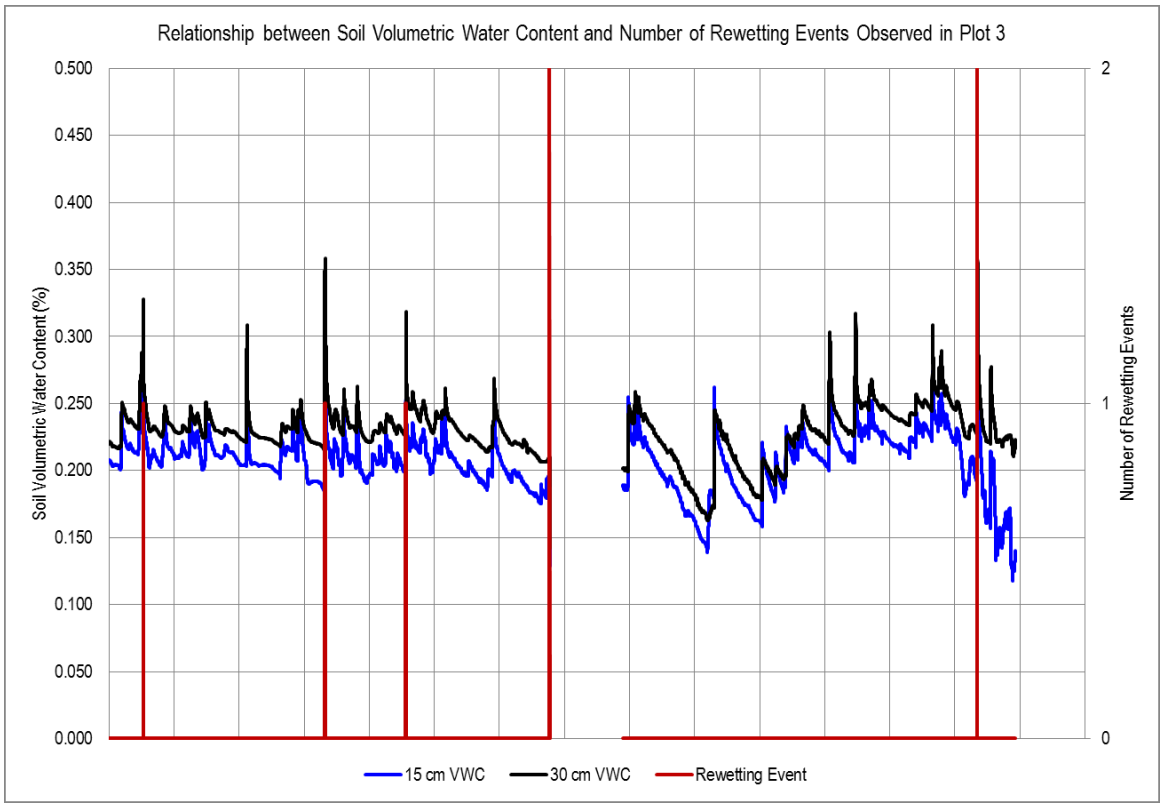
Relationship between Soil Volumetric Water Content and Number of Rewetting Events Observed in Plot 3
Soil Volumetric Water Content (%)
0.500
0.450
0.400
0.350
0.300
0.250
0.200
0.150
0.100
0.050
0.000
Number of Rewetting Events
2
1
0
15 cm VWC
30 cm VWC
Rewetting Event

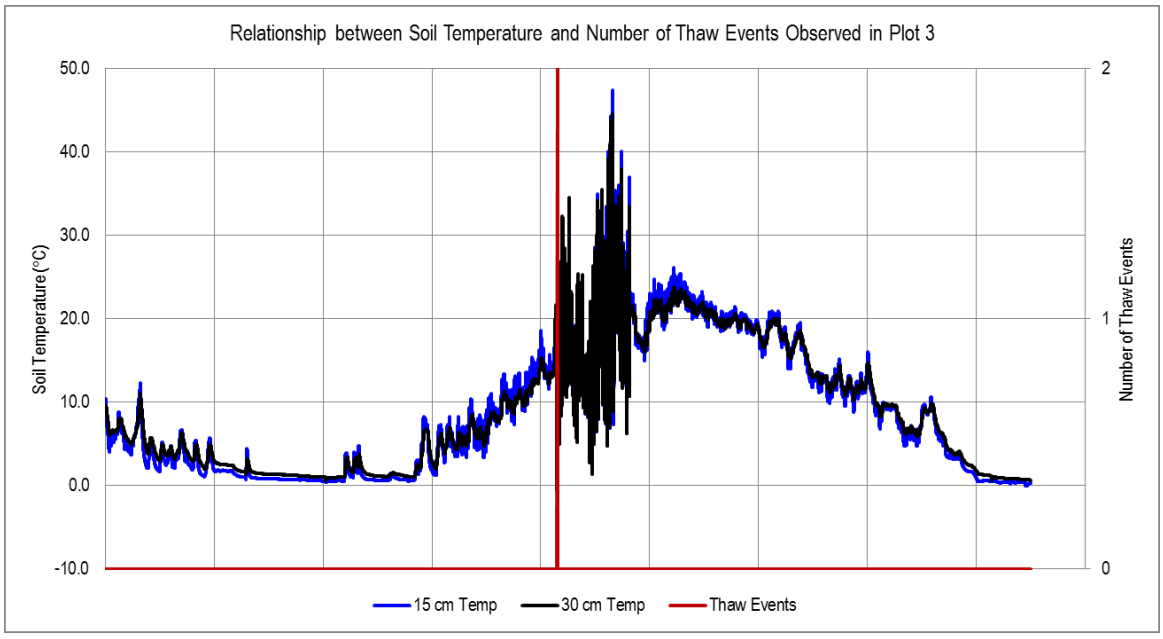
Relationship between Soil Temperature and Number of Thaw Events Observed in Plot 3
Soil Temperature (°C)
50.0
40.0
30.0
20.0
10.0
0.0
-10.0
Number of Thaw Events
2
1
0
15 cm Temp
30 cm Temp
Thaw Events

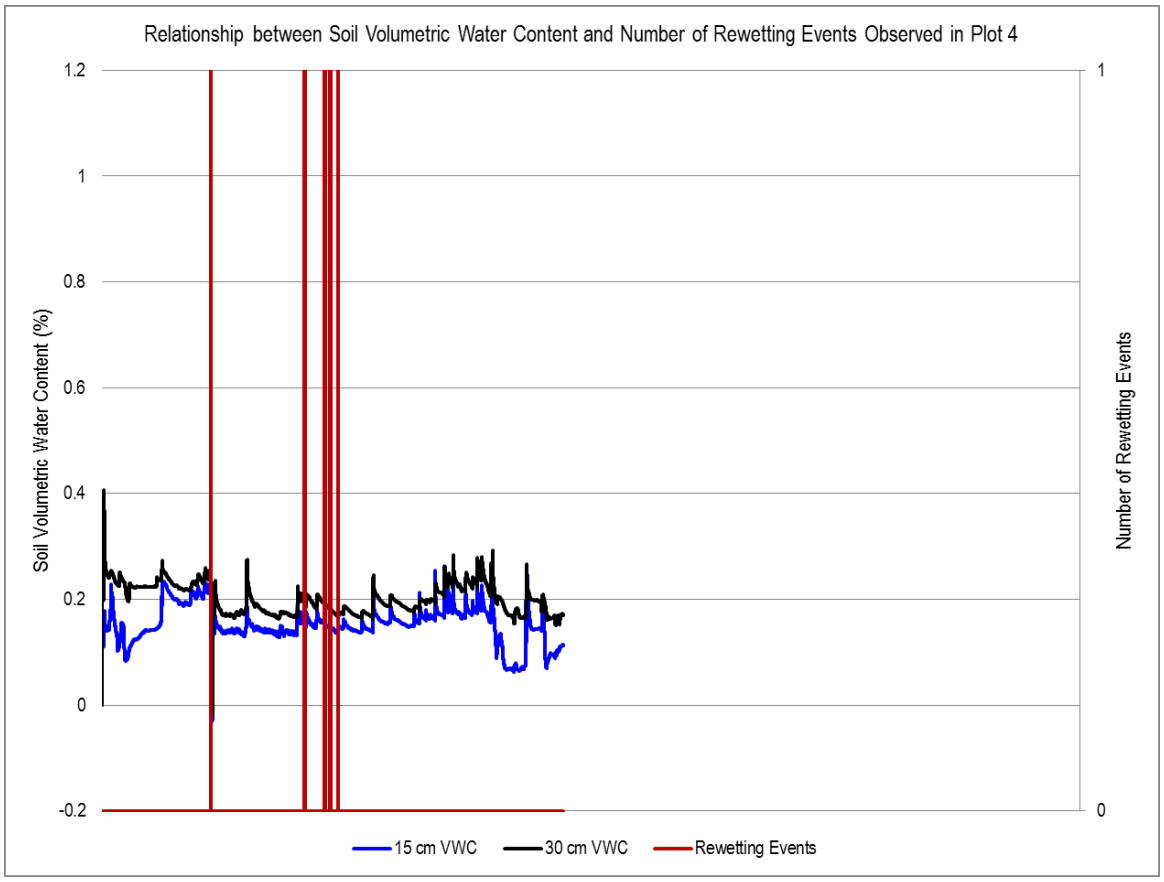
Relationship between Soil Volumetric Water Content and Number of Rewetting Events Observed in Plot 4
Soil Volumetric Water Content (%)
Number of Rewetting Events
1.2
1
0.8
0.6
0.4
0.2
0
-0.2
1
0
15 cm VWC
30 cm VWC
Rewetting Events

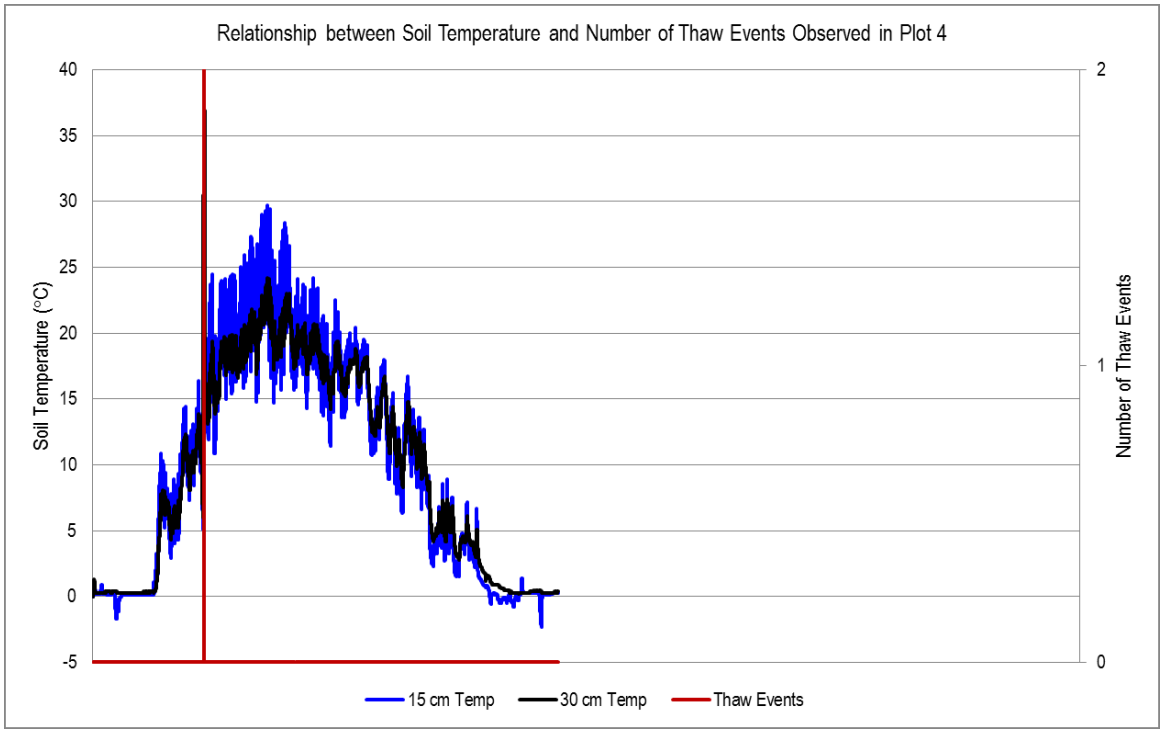
Relationship between Soil Temperature and Number of Thaw Events Observed in Plot 4
Soil Temperature (°C)
Number of Thaw Events
40
35
30
25
20
15
10
5
0
-5
2
1
0
15 cm Temp
30 cm Temp
Thaw Events

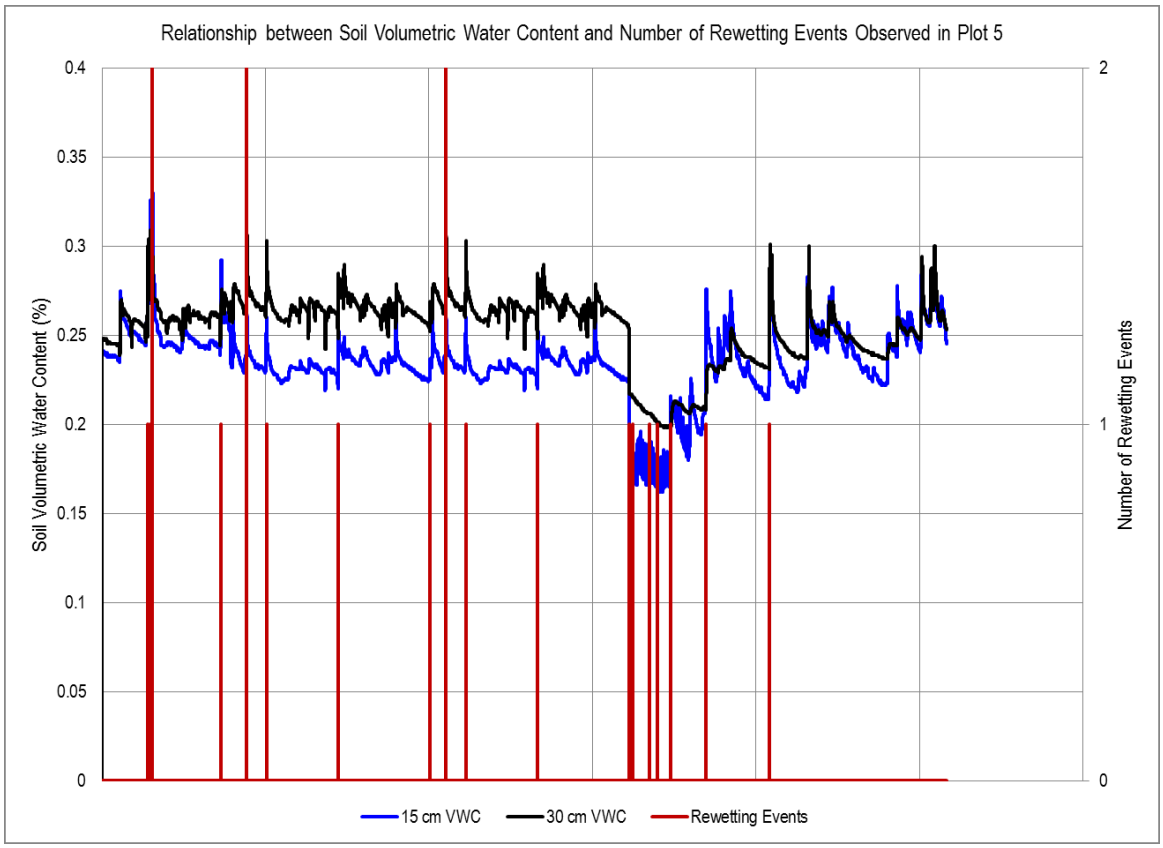
Relationship between Soil Volumetric Water Content and Number of Rewetting Events Observed in Plot 5
Soil Volumetric Water Content (%)
Number of Rewetting Events
0.4
0.35
0.3
0.25
0.2
0.15
0.1
0.05
0
2
1
0
15 cm VWC
30 cm VWC
Rewetting Events

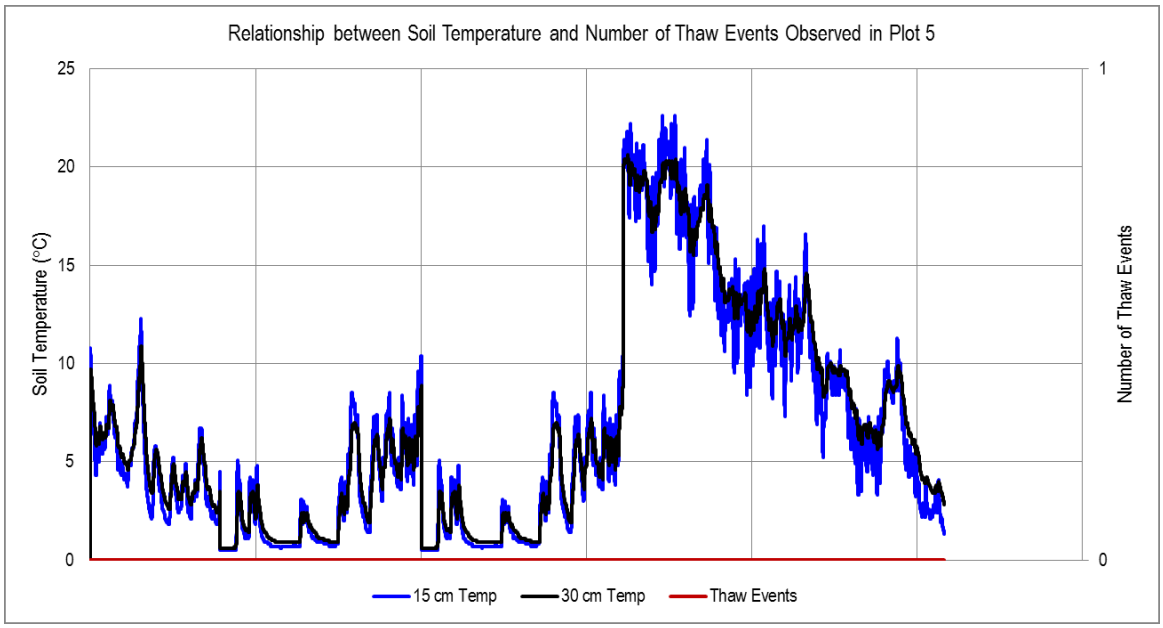
Relationship between Soil Temperature and Number of Thaw Events Observed in Plot 5
Soil Temperature (°C)
Number of Thaw Events
25
20
15
10
5
0
1
0
15 cm Temp
30 cm Temp
Thaw Events

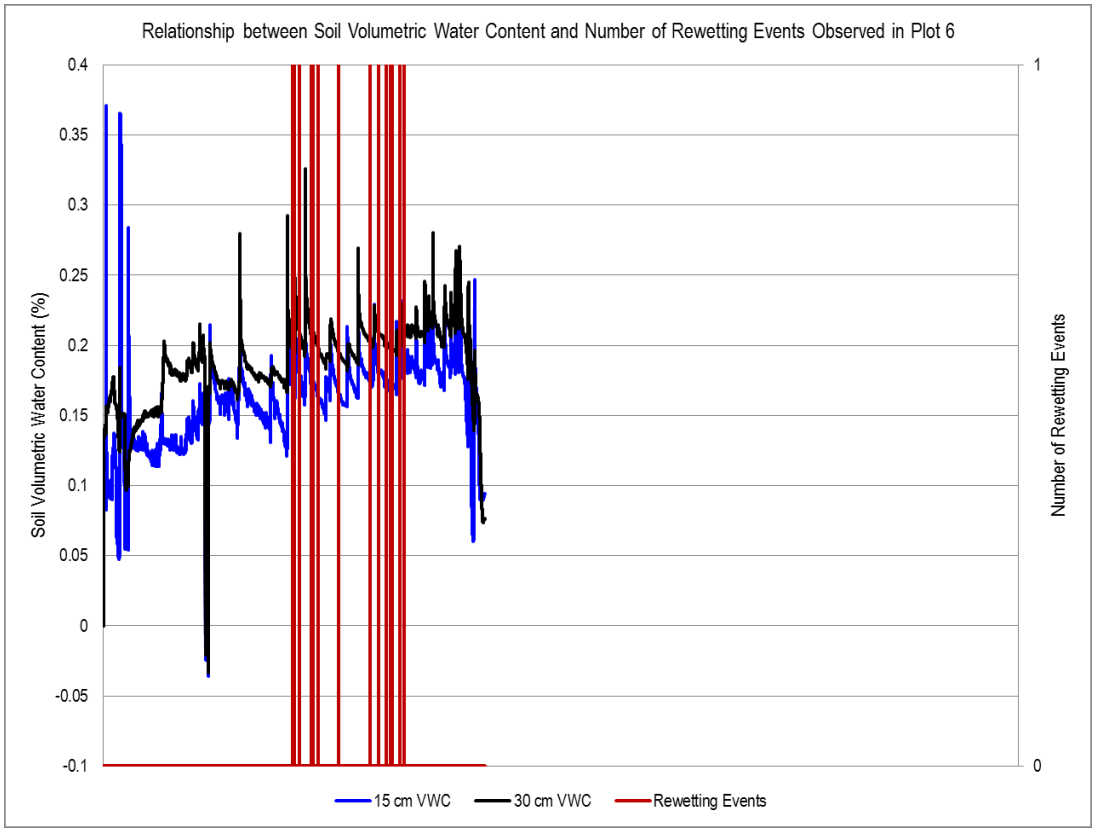
Relationship between Soil Volumetric Water Content and Number of Rewetting Events Observed in Plot 6
Soil Volumetric Water Content (%)
Number of Rewetting Events
0.4
0.35
0.3
0.25
0.2
0.15
0.1
0.05
0
-0.05
-0.1
1
0
15 cm VWC
30 cm VWC
Rewetting Events

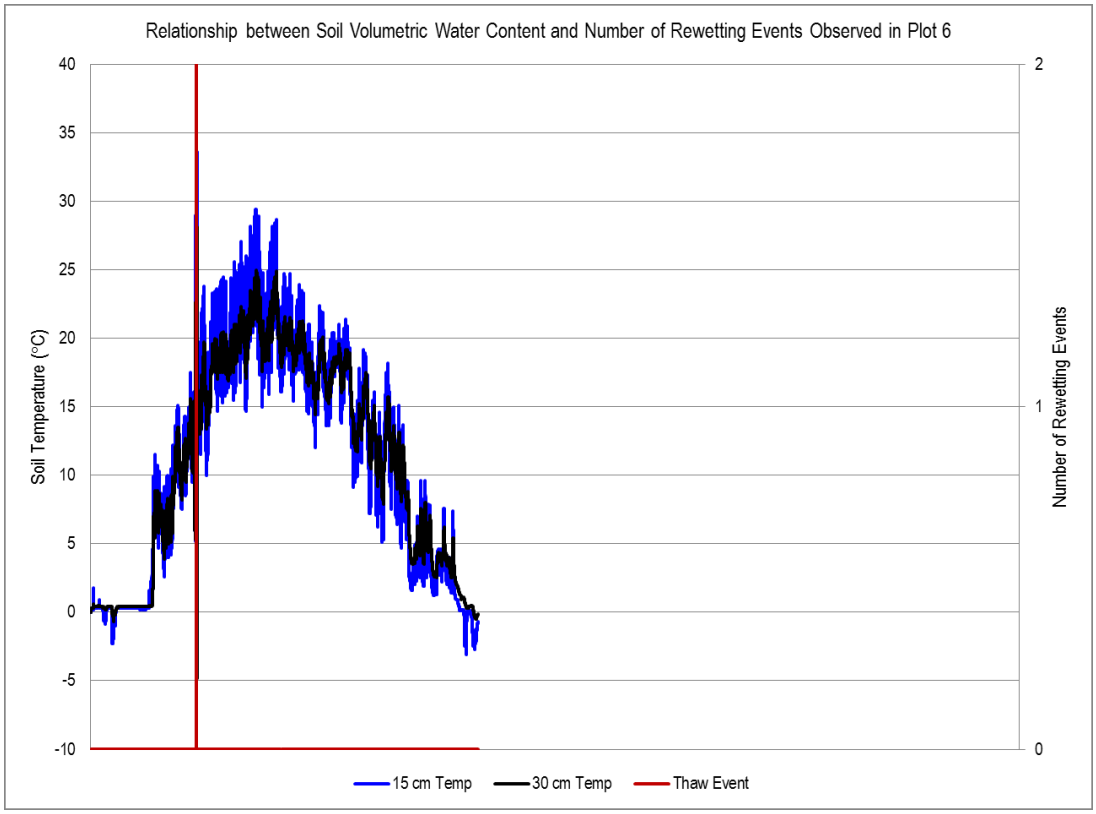
Relationship between Soil Volumetric Water Content and Number of Rewetting Events Observed in Plot 6
Soil Temperature (°C)
Number of Rewetting Events
40
35
30
25
20
15
10
5
0
-5
-10
2
1
0
15 cm Temp
30 cm Temp
Thaw Event

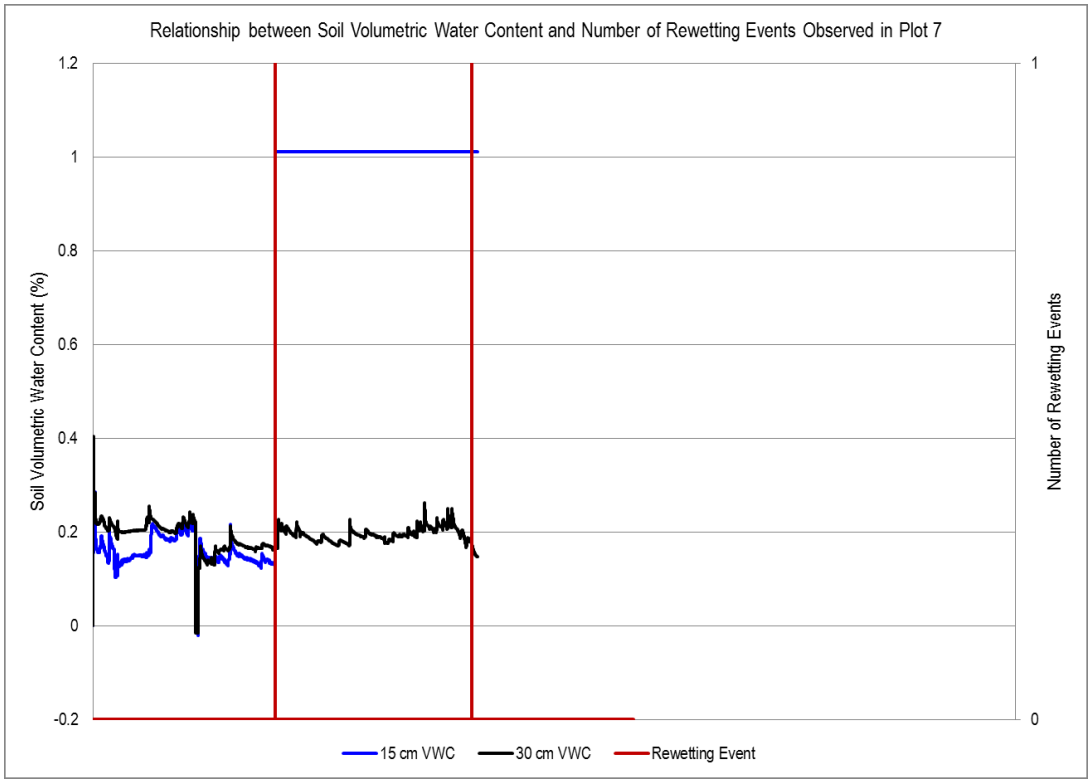
Relationship between Soil Volumetric Water Content and Number of Rewetting Events Observed in Plot 7
Soil Volumetric Water Content (%)
Number of Rewetting Events
1.2
1
0.8
0.6
0.4
0.2
0
-0.2
1
0
15 cm VWC
30 cm VWC
Rewetting Event

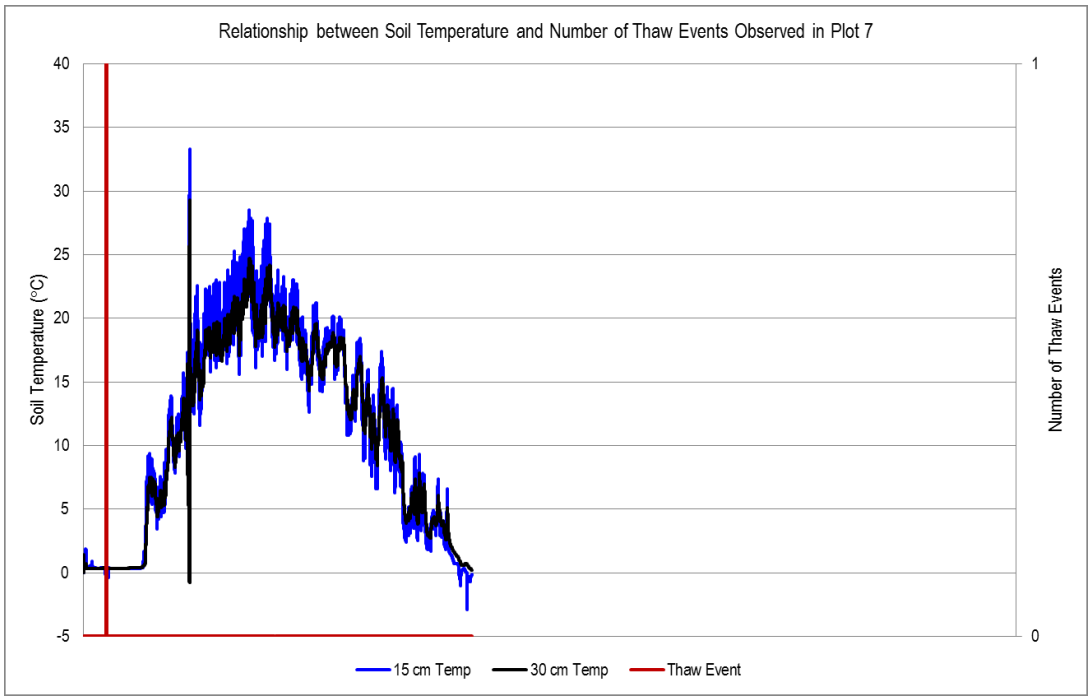
Relationship between Soil Temperature and Number of Thaw Events Observed in Plot 7
Soil Temperature (°C)
Number of Thaw Events
40
35
30
25
20
15
10
5
0
-5
1
0
15 cm Temp
30 cm Temp
Thaw Event

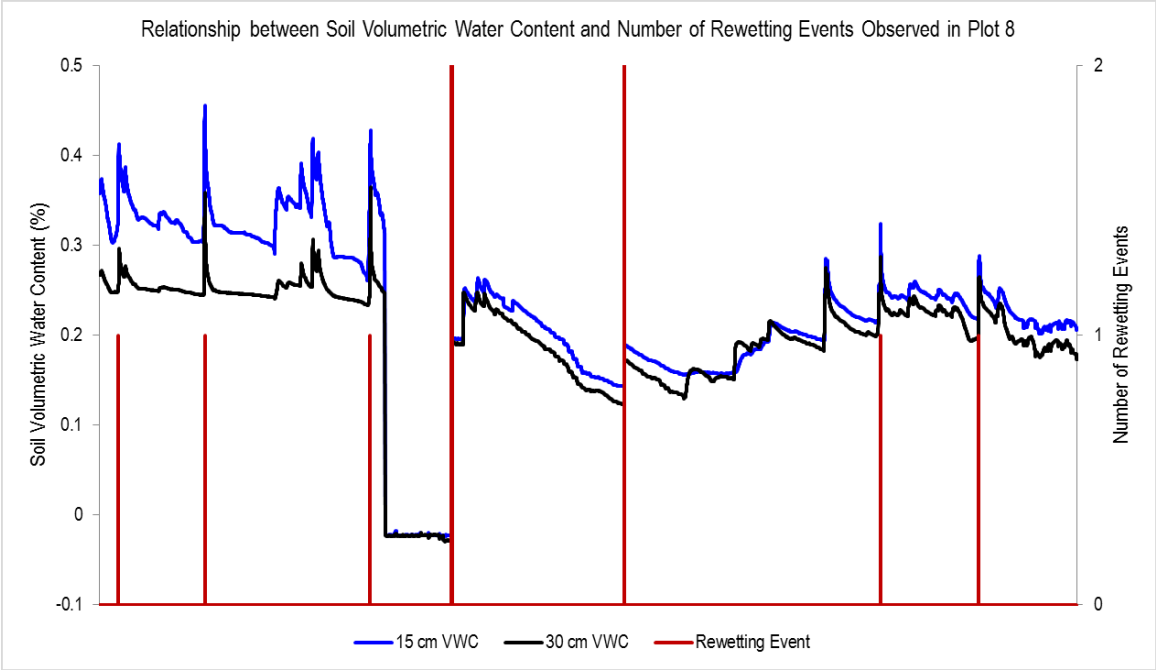
Relationship between Soil Volumetric Water Content and Number of Rewetting Events Observed in Plot 8
Soil Volumetric Water Content (%)
0.5
0.4
0.3
0.2
0.1
0
-0.1
Number of Rewetting Events
2
1
0
15 cm VWC
30 cm VWC
Rewetting Event

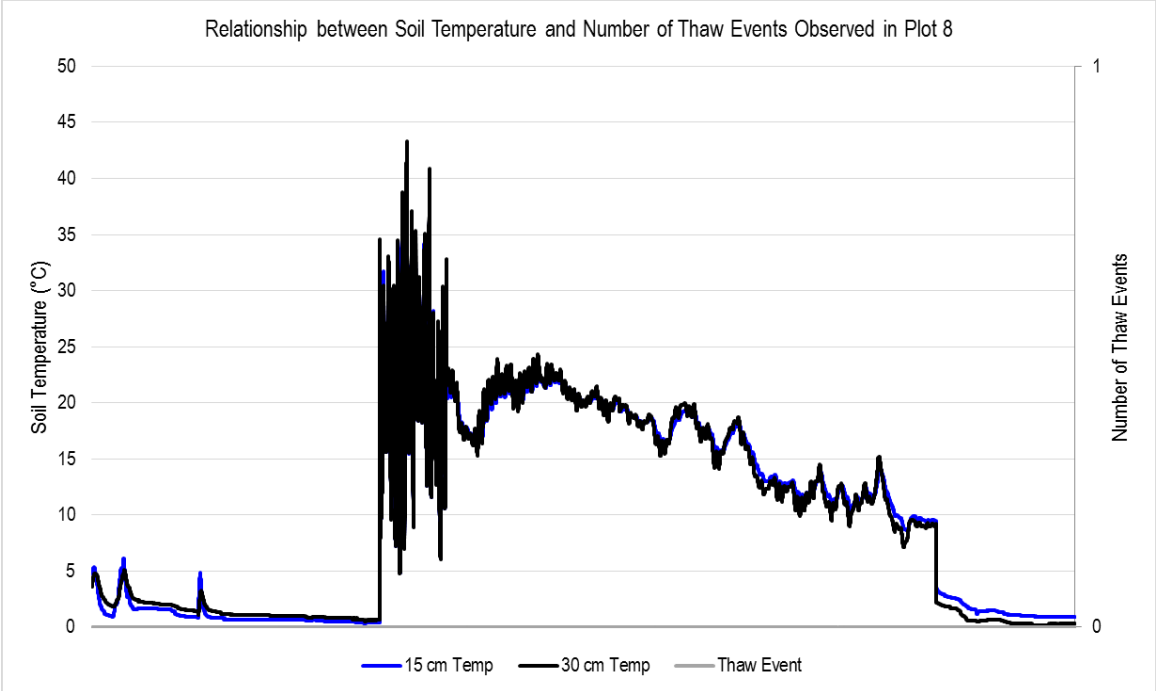
Relationship between Soil Temperature and Number of Thaw Events Observed in Plot 8
Soil Temperature (°C)
50
45
40
35
30
25
20
15
10
5
0
Number of Thaw Events
1
0
15 cm Temp
30 cm Temp
Thaw Event

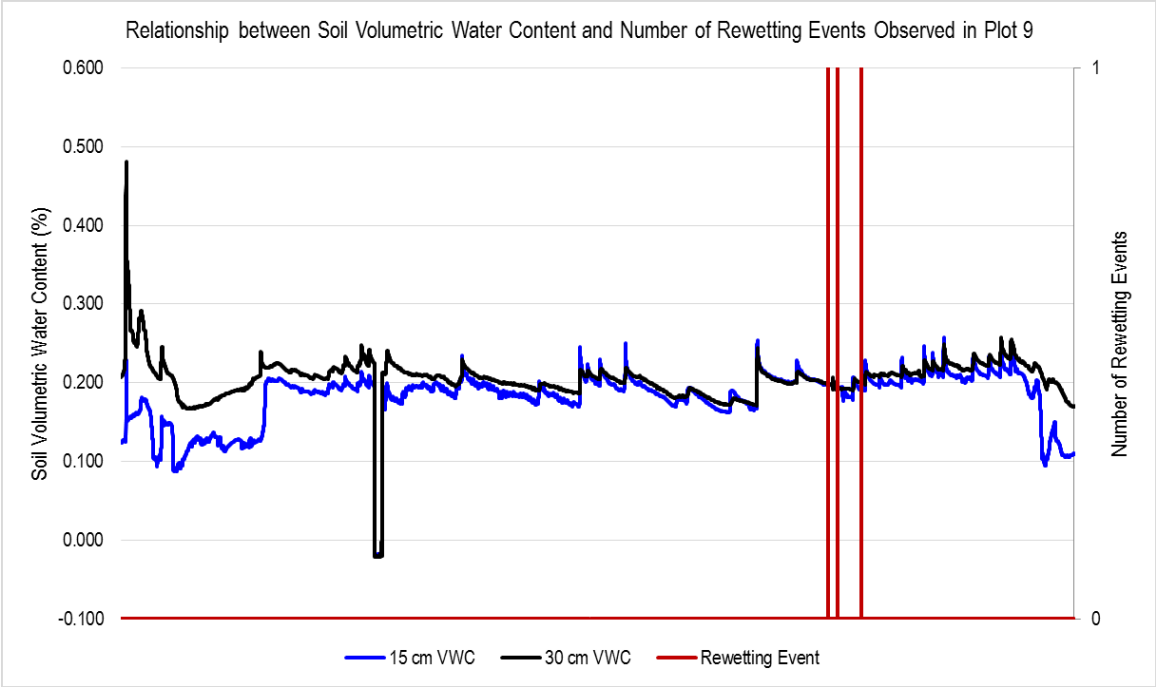
Relationship between Soil Volumetric Water Content and Number of Rewetting Events Observed in Plot 9
Soil Volumetric Water Content (%)
0.600
0.500
0.400
0.300
0.200
0.100
0.000
-0.100
Number of Rewetting Events
1
0
15 cm VWC
30 cm VWC
Rewetting Event

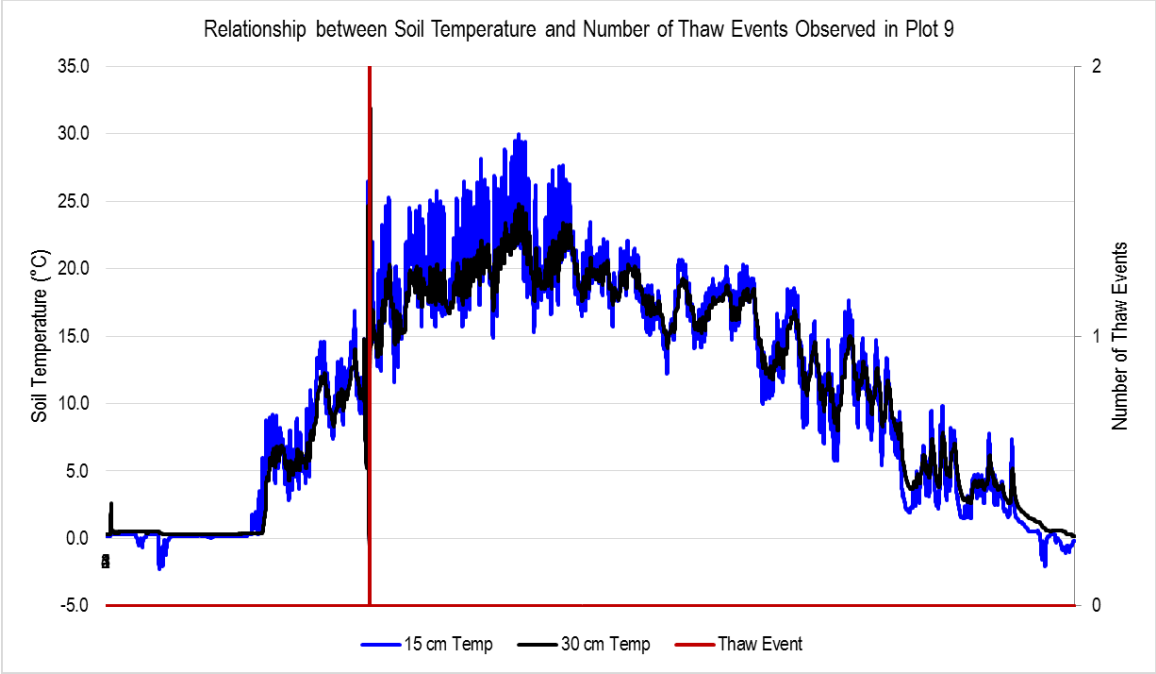
Relationship between Soil Temperature and Number of Thaw Events Observed in Plot 9
Soil Temperature (°C)
35.0
30.0
25.0
20.0
15.0
10.0
5.0
0.0
-5.0
Number of Thaw Events
2
1
0
15 cm Temp
30 cm Temp
Thaw Event

APPENDIX D: SOIL RESPIRATION RESPONSE TO EVENT DATES OF INTEREST

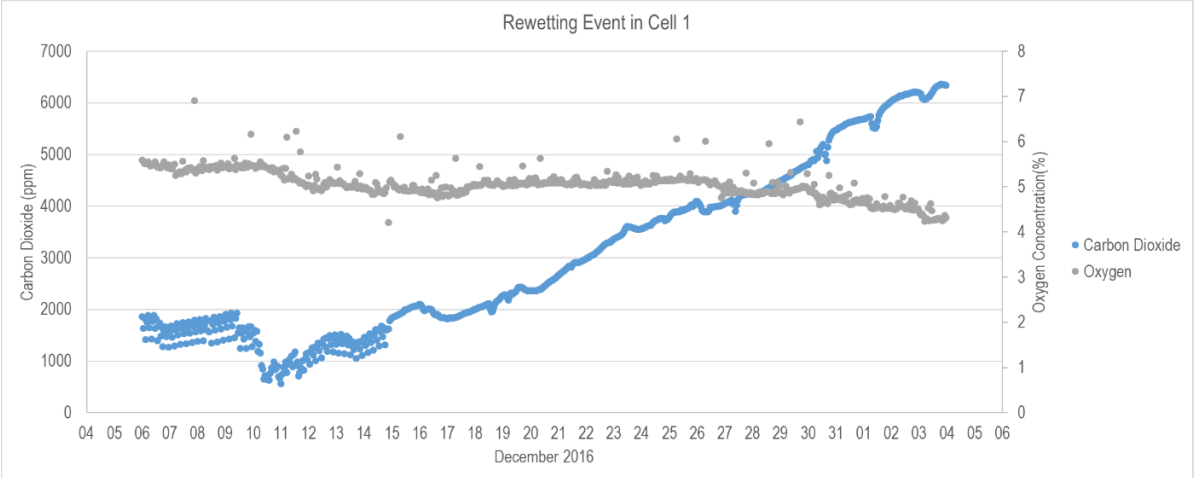

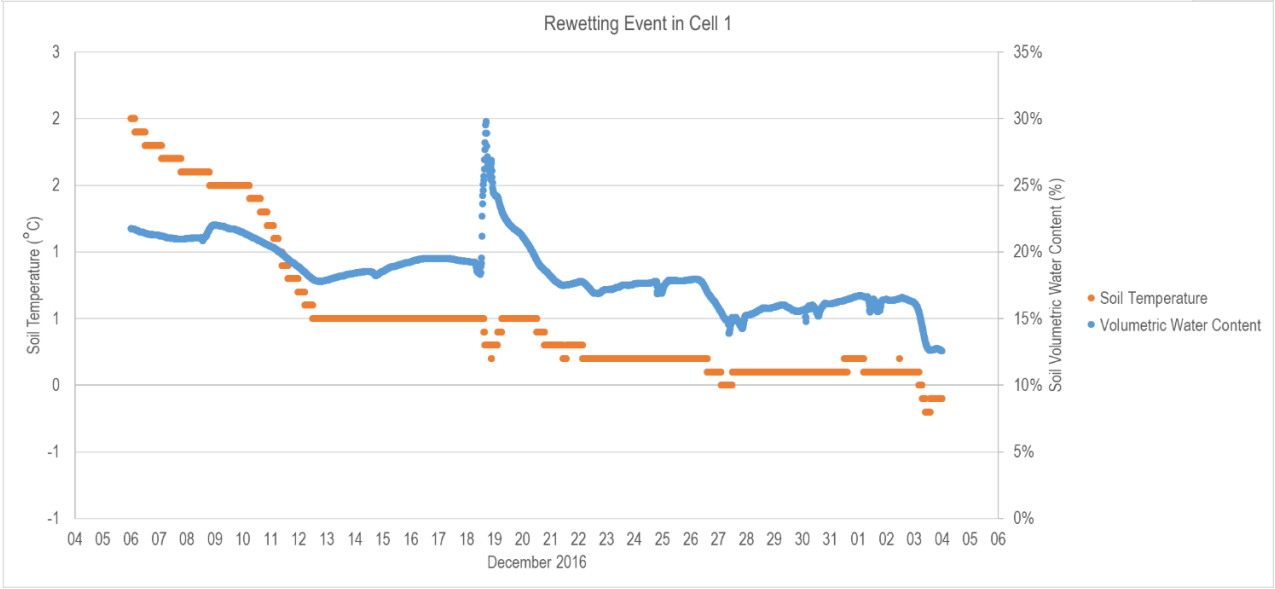

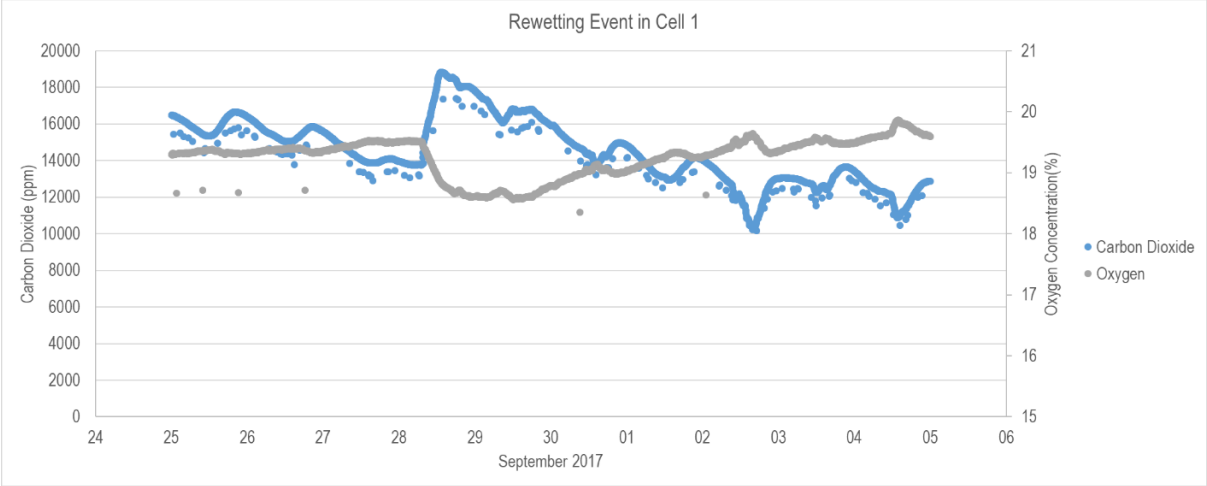
Rewetting Event in Cell 1
Carbon Dioxide (ppm)
Oxygen Concentration(%)
September 2017
Carbon Dioxide
Oxygen

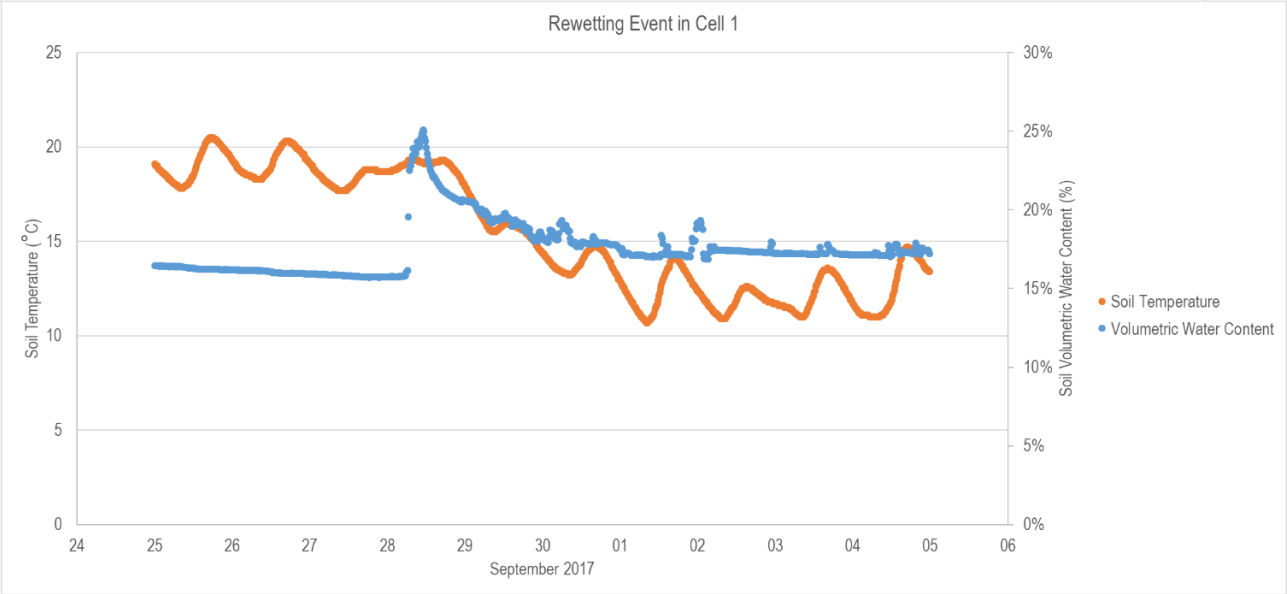
Rewetting Event in Cell 1
Soil Temperature (°C)
Soil Volumetric Water Content (%)
September 2017
Soil Temperature
Volumetric Water Content

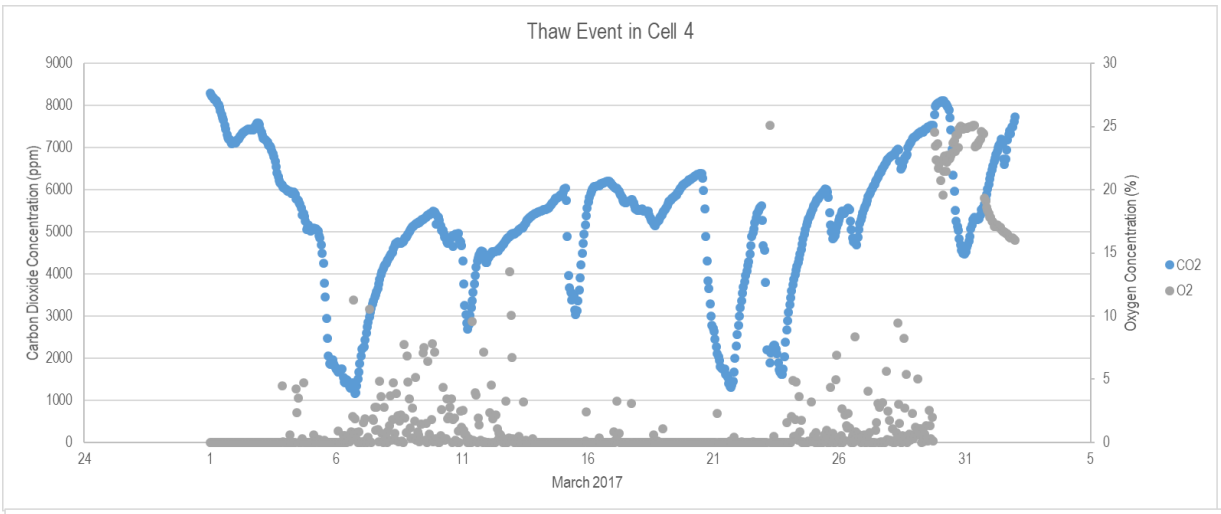
Thaw Event in Cell 4
Carbon Dioxide Concentration (ppm)
Oxygen Concentration (%)
CO2
O2
March 2017

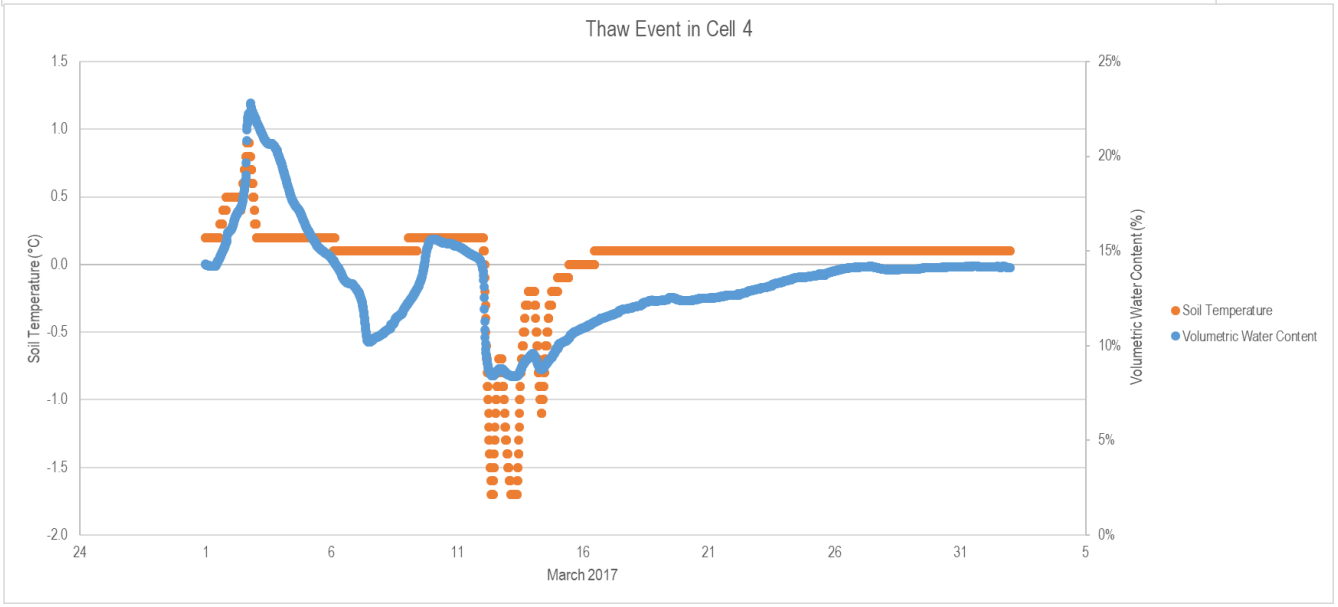
Thaw Event in Cell 4
Soil Temperature (°C)
Volumetric Water Content (%)
Soil Temperature
Volumetric Water Content
March 2017

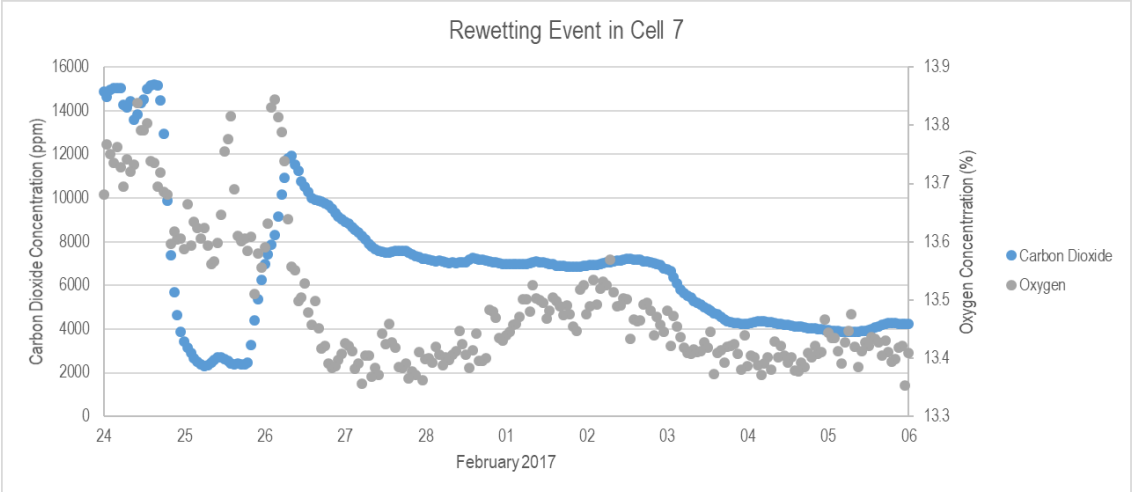
Rewetting Event in Cell 7
Carbon Dioxide Concentration (ppm)
Oxygen Concentration (%)
February 2017
Carbon Dioxide
Oxygen

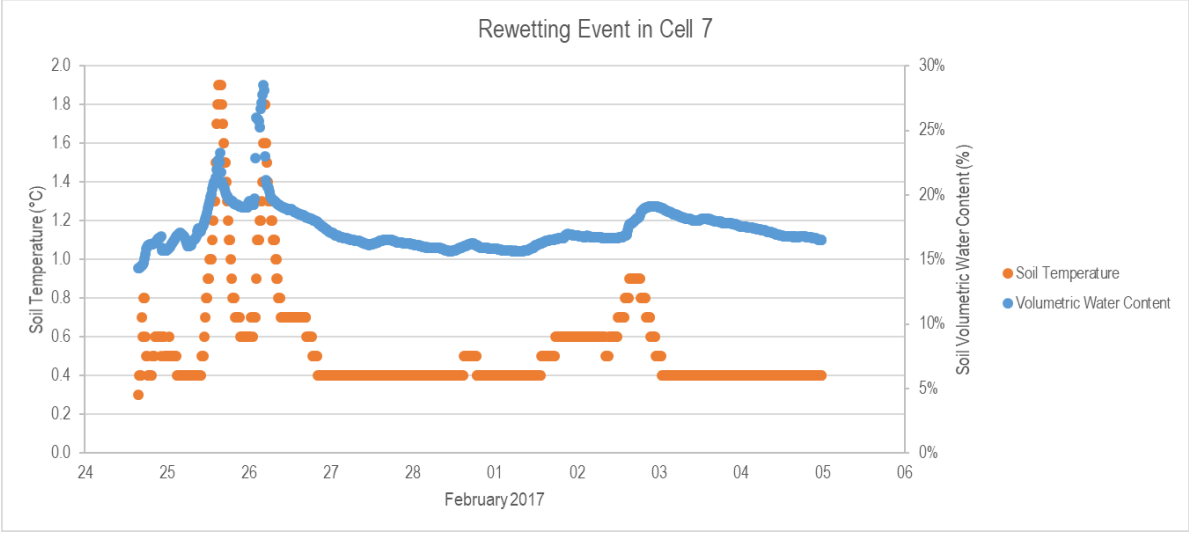
Rewetting Event in Cell 7
Soil Temperature (°C)
Soil Volumetric Water Content (%)
February 2017
Soil Temperature
Volumetric Water Content

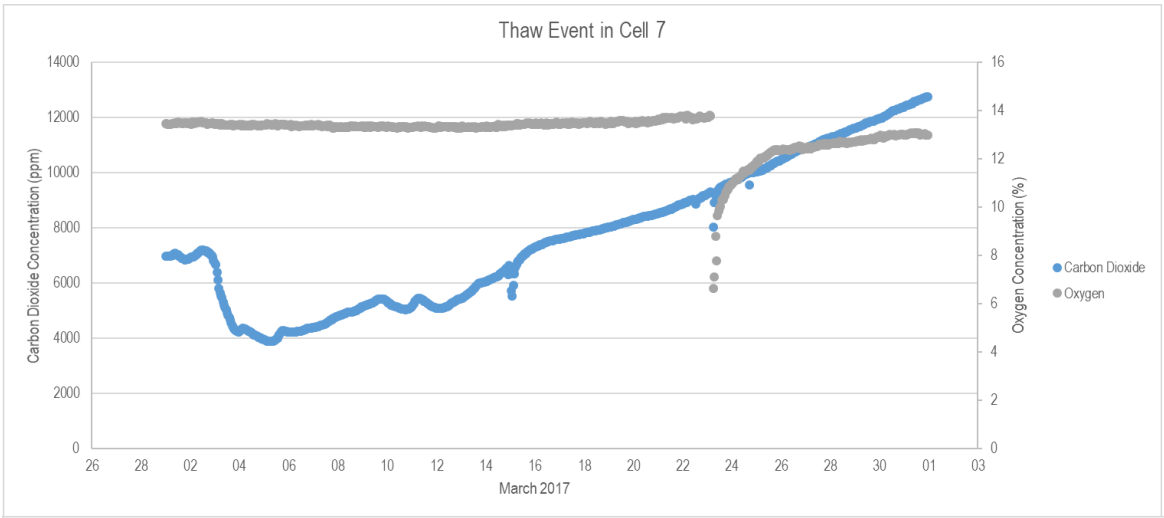
Thaw Event in Cell 7
Carbon Dioxide Concentration (ppm)
Oxygen Concentration (%)
March 2017
Carbon Dioxide
Oxygen

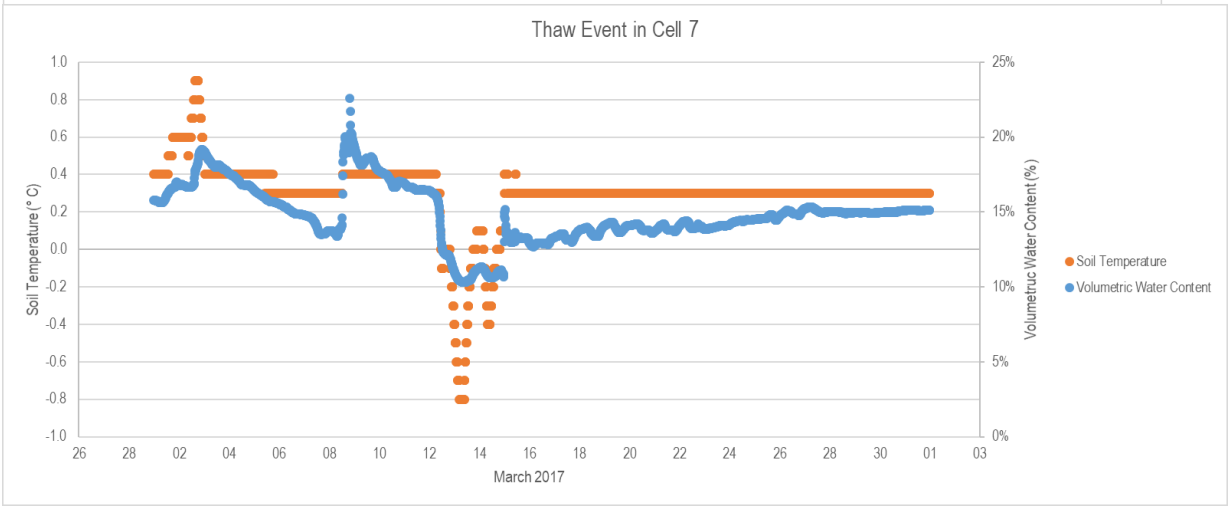
Thaw Event in Cell 7
Soil Temperature (° C)
Volumetruc Water Content (%)
March 2017
Soil Temperature
Volumetric Water Content

APPENDIX E: STANDARD OPERATING PROCEDURES

Anion Exchange Membranes

Membranes are cut from membrane fabric to dimensions of 5.2 cm by 6.0 cm. A small hole is placed at the end of the membrane with a needle and a fishing line is attached for marking.

Preparation:

1. Wash: Membranes are covered in 0.5 N HCl solution in a large bottle and are shaken for 30 minutes.

2. Rinse: Membranes are rinsed three times in distilled water.

3. Saturate: Membranes are covered with a 1 N NaCl solution and shaken for 2 hours on High.

4. Preserve: Membranes are stored in the NaCl solution in the refrigerator until they are needed in the field. Before transporting to the field, membranes are rinsed three times in distilled water and stored in distilled water for transport.

Field Installation and extraction:

Installation: Dig a hole to a depth of 15 cm. Use a scalpel to make a slot in the soil for installation. Ensure good soil-to-membrane contact. Attach a flag to the fishing lines and cover hole.

Extraction: After a two-week period (14 days), remove membranes from the soil carefully and rinse with distilled water. Store in a plastic bag for transport back to the laboratory.

Filtration:

Wash membranes with distilled water and ensure all soil particles are removed.

Place membranes in a DigiTube with 40 mL of 1M KCl.

Shake DigiTubes on reciprocal shaker at Low speed for one hour.

Gravity filter the solution from the DigiTubes through Whatman No. 5 filter papers into 20 mL plastic scintillation vials and freeze until NO_3 analysis on the Technicon Auto Analyzer.

Auto Analyzer: DETERMINATION OF NITRITE + NITRATE NITROGEN (0-10.0 mg/L)

INTRODUCTION

This SOP is to be used for the determination of the Nitrite NO_2-N + Nitrate NO_3 -Nitrogen concentrations in environmental samples such as surface, ground and wastewaters, soil leachates (0.01 M $CaCl_2$), soil extracts (2.0 M KCl).

SCOPE

This SOP is applicable to water samples and soil extracts with a Nitrite + Nitrate Nitrogen concentrations greater than MDL and less than 10.0 mg/L NO_2-N + NO_3-N/L. All technicians/users who perform this analysis are responsible for ensuring this SOP has been followed.

DEFINITIONS

DI Water - Deionized Water

MSDS - Material Safety Data Sheet

SUMMARY OF METHOD

In this procedure the entire Nitrate concentration of a sample is reduced to Nitrite utilizing a copper/cadmium reduction column. Thus the converted Nitrate to Nitrite plus the original Nitrite in the sample can be determined on the auto-analyzer using the Nitrite method. Nitrite reacts with sulfanilamide under acidic conditions to form a diazo compound. This compound then couples with N-1-naphythylenediamine dihydrochloride to form a reddish purple azo dye, which can be measured colorimetrically.

SAFETY

Due to the use of chemicals in this SOP the use of safety glasses is mandatory. Please consult the appropriate MSDSs relating to the chemicals used in the REAGENTS AND STANDARD PREPARATION (11.0) section to familiarize yourself with safe handling procedures.

SAMPLE HANDLING AND PRESERVATION

Samples (leachates, extracts) should be kept frozen until needed and thawed just prior to analyses.

PREPARATION OF GLASSWARE

Glassware should be cleaned and free of any organic matter and rinsed with DI water.

APPARATUS AND MATERIAL

Technicon Auto-Flow Analyzer, see Schematic

REAGENTS AND STANDARD PREPARATION

Note: All Reagents should be ACS Grade or Better

Stock Nitrate Solution (1000 mg/L-N): Dry 10 g of Potassium Nitrate at 105 degrees C for 2 hours and let cool in a dessicator. Dissolve 7.2180 g in 700 mL of DI water and make up to 1000 mL in a volumetric flask.

Note: Add 1 mL chloroform to preserve the stock solution and store at 4 degrees C. Solution is stable for 6 months.

Note: Make fresh standards with every batch of samples.

Working Standard (mg/L)	Volume of Stock (mL)	Volumetric Flask Size (mL)
0.00	0.00	100
1.00	0.10	100
2.00	0.20	100
5.00	0.50	100
10.00	1.00	100

Ammonium Chloride Buffer Solution: Dissolve 85 g NH_4Cl in 700 mL DI water and add 1.0 g EDTA (sodium salt). Adjust pH =6.60 with 1.0 N NaOH and make up to 1000mL.

Note: Buffer will last until used.

1 N NaOH Solution: Dissolve 40 g NaOH pellets in 700 mL DI water. Cool and make up to 1000 mL.

Colour Solution: To 700 mL DI water add 150 mL concentrated Hydrochloric Acid and 9.10 g Sulphanilamide. Dissolve completely (heat if necessary). Add 0.71 g N-1-naphthyl-ethylenediamine dihydrochloride and dissolve. Solution is stable for 1 month at 4 degrees C.

SAMPLE PREPARATION

If the samples are turbid or contain suspended solids or any particulate matter the sample should be filtered through a 0.45 um glass-fibre filter.

ANALYTICAL DETERMIANTION

Note: The use of the Copper/Cadmium coil is required. Attach the Copper/Cadmium coil into the system before introducing the solutions. Make sure that the flow of the system is into the Copper Coil first then the Cadmium Coil. Run a 1.00 mg/L NO_2 standard in order to calculate the percentage reduction of nitrate to nitrite with the Cu/Cd column. This should be between 95-105 % conversion.

Note: After running a batch of samples for Nitrite + Nitrate samples, clean the auto-analyzer system by putting the lines into a 0.1.N HCl solution and pumping the acid through the system for 15 minutes followed by another 15 minutes with DI water.

CALIBRATION OF INSTRUMENT

Multi-Point or Daily Calibration Procedures

Applicable – A six-point standard calibration curve is produced with each batch of samples.

DEMONSTRATION OF QUALITY CONTROL

Method Detection Limit (MDL) and Precision for Colorimetric Methods

Sample Concentration Range mg/L	Concentration Range	Method Detection Limit
0 – 10.0 mg/L	0 – 10.0 mg/L	0.05 mg/L

QC samples

A Blank is run with each set of samples.

A duplicate is run with each set.

Run an External Control Sample (ERA Sample) with each series of samples. Record values in corresponding logbook.

Performance Standards

With any default of the following performance standards, the Department Manager is informed, and the set is repeated, if necessary.

Repeatability

Duplicates should agree within tolerance levels set by validation or 10% of the relative value.

Reproducibility

External Control Standards should agree within 95% - 105% of true value.

REPORT FORMAT

All results are expressed in **mg/L**

REFERENCES

Standard Methods for the Examination of Water and Wastewater. 20th Edition.

K. Grasshof (Technicon International Conference 1969)

Federal Water Pollution Control Administration Methods for Chemical Analysis of Water and Wastewater.

Auto Analyzer: DETERMINATION OF AMMONIA NITROGEN (0-5.0 mg/L)

INTRODUCTION

This SOP is to be used for the determination of the Ammonia Nitrogen concentrations in environmental samples such as surface, ground and wastewaters, soil leachates (0.01 M $CaCl_2$), soil extracts (2.0 M KCl).

SCOPE

This SOP is applicable to water samples and soil extracts with Ammonia Nitrogen concentrations greater than MDL and less than 5.0 mg/L NH_3-N. All technicians/users who perform this analysis are responsible for ensuring this SOP has been followed.

DEFINITIONS

DI Water - Deionized Water

MSDS - Material Safety Data Sheet

SUMMARY OF METHOD

At the proper pH, ammonia ions are heated with sodium salicylate and sodium hypochlorite to produce blue colour, which is proportional to the ammonia ion concentration. The colour is then intensified by the addition of sodium nitro-prusside. The presence of EDTA in the buffer prevents the precipitation of calcium and magnesium ions.

SAFETY

Due to the use of chemicals in this SOP the use of safety glasses is mandatory. Please consult the appropriate MSDSs relating to the chemicals used in the REAGENTS AND STANDARD PREPARATION (11.0) section to familiarize yourself with safe handling procedures.

SAMPLE HANDLING AND PRESERVATION

Samples (leachates, extracts) should be kept frozen until needed and thawed just prior to analyses.

INTERFERENCES

PREPARATION OF GLASSWARE

Glassware should be cleaned and free of any organic matter and rinsed with DI water.

APPARATUS AND MATERIAL

Technicon Auto-Flow Analyzer, see Schematic

REAGENTS AND STANDARD PREPARATION

Note: All Reagents should be ACS Grade or Better

Stock Ammonia (Nitrogen) Solution (1000 mg/L-N): Dissolve 3.8207 g of anhydrous ammonium chloride (NH_4Cl) dried at 105 degrees for 2 hours in 700 mL DI water. Add 5 mL concentrated H_2SO_4 acid and make up to 1000 mL in a volumetric flask. Keep Ammonia stock bottle tightly stoppered. Note: Store in plastic bottle at 4 degrees C. Make up once per year.

Intermediate Standard Ammonia Solution (100 mg/L): Pipette 10 mL of Stock Ammonia solution into 100 mL volumetric flask. Add 1 mL 5 N H_2SO_4 and make up to the mark with DI water. Store in plastic bottle at 4 degrees C. Make up weekly.

Working Ammonia (Nitrogen) Standards: Make up standards in 100 mL volumetric flasks with DI Water or the matrix , i.e. 0.01 M $CaCl_2$ or 2.0 M KCl) of the samples. Note: Make fresh standards with every batch of samples.

Working Standard (mg/L-N)	Volume of Intermediate (mL)	5 N H_2SO_4 (mL)
0.25	0.25	0.5
0.50	0.50	0.5
1.00	1.00	0.5
2.00	2.00	0.5
5.00	5.00	0.5

Buffer Solution: Dissolve 50.0 g Potassium Sodium Tartrate Tetrahydrate and 20.0 g Di-Sodium Hydrogen Phosphate plus 10.0 g EDTA (sodium salt) in 700 mL DI water. Add 40.0 g NaOH and make up to 1000mL with DI water. Note: Buffer will last until used. Store at room temperature as precipitation will occur at cold temperatures.

Salicylate-Nitroprusside Solution: Dissolve 60.0 g Sodium Salicylate in 400 mL DI water. Add 0.25 g Sodium Nitro-prusside and 10 g NaOH pellets and make up to 500 mL. This solution will keep for 2 weeks at 4 degrees C.

Hypochlorite Solution (6 % Javex); Dilute 12 mL of Javex up to 200 mL. Make fresh daily.

5 N H_2SO_4 Solution: Carefully add 140 mL concentrated H_2SO_4 acid to 700 mL DI water. Cool and make up to 1000 mL. This solution will last until used.

5 N NaOH Solution: Carefully dissolve 200 g NaOH pellets in 700 mL DI water. Cool and make up to 1000 mL. This solution will last until used.

Wash water to Sampler: Dilute 5 mL 5 N H_2SO_4 solution to 1000 mL with DI water. Solution will keep until used.

SAMPLE PREPARATION

If the samples are turbid or contain suspended solids or any particulate matter the sample should be filtered through a 0.45 um glass-fibre filter. Dilute the sample id the Ammonia concentration appears to be high.

ANALYTICAL DETERMIANTION

CALIBRATION OF INSTRUMENT

Multi-Point or Daily Calibration Procedures

Applicable – A six-point standard calibration curve is produced with each batch of samples.

DEMONSTRAION OF QUALITY CONTROL

Method Detection Limit (MDL) and Precision for Colorimetric Methods

Sample Concentration Range mg/L	Ammonia Concentration Range	Method Detection Limit
MDL – 5.0 mg/L	MDL – 5.0 mg/L	<0.03 mg/L

QC samples

A Blank is run with each set of samples.

A duplicate is run with each set.

Run an External Control Sample (ERA Sample) with each series of samples. Record values in corresponding logbook.

Performance Standards

With any default of the following performance standards, the Department Manager is informed and the set is repeated, if necessary.

Repeatability
Duplicates should agree within tolerance levels set by validation or 10% of the relative value.

Reproducibility
External Control Standards should agree within 95% - 105% of true value.

REPORT FORMAT
All results are expressed in: mg/L

REFERENCES
Standard Methods for the Examination of Water and Wastewater. 20th Edition. 4500-NH_3-N (modified).

Collecting Water Samples Using Pipette Method for Determination of Dissolved N_2O

Equipment

Mercuric Chloride ($HgCl_2$)

Micropipette (0-200 µL range)

12 mL Exetainers *(Labco Limited 739W)*

Evacuation system with vacuum pump and UHP He source.

20 mL disposable syringes *(Fisher Scientific 14-826-2B)*

20 gauge x 12 inch Popper* Deflected Noncoring Septum Penetration Needles

25 gauge x 5/8 inch *(Fisher Scientific 14-826-AA)*

Reusable Class B 10 mL Volumetric Pipettes *(Fisher Scientific 13-650L)*

3-way Stopcock with Luer Connections, 2 male luer locks *(Cole-Parmer T-30600-23 and T-06464-90)*

Gloves

Procedure:

Preparation of Mercuric Chloride:

A 6.25% saturated solution of mercuric chloride should be prepared (0.4625 g $HgCl_2$ in 100 mL) of water. The mercuric chloride is used to inhibit any microbial activity (U.S. Department of Energy, 1994).

Note that this compound is poisonous and should be prepared with care. Consult with WHIMS Data sheet. Appropriate safety procedures should be observed. Wear gloves, masks, coat and goggles while preparing.

After preparation, transfer the $HgCl_2$ solution to a sealable bottle. Label the bottle according to WHIMS protocol. Keep it in a safe place until required.

Transferring the mercuric chloride into Exetainers:

Fifty µL of mercuric chloride should be transferred from the bottle containing $HgCl_2$ using a micropipette and injected in the Exetainer. (Note: The recommended minimum amount is about 0.02% by volume, of a saturated aqueous solution.)

Mercuric chloride is a highly toxic compound and, as any compound containing mercury, is an accumulative poison, and should therefore be handled very carefully. When initially handling the solid compound to prepare the dilute solution of $HgCl_2$ a protective mask is recommended to prevent dust inhalation. Once in a solution form prevent contact by wearing gloves and a laboratory coat, and wash your hands following use. All handling of this compound should be performed in a fume hood.

Purging headspace of Exetainers with helium (He):

Once the $HgCl_2$ has been introduced into the Exetainer, the headspace should be purged with an inert UHP Grade gas to remove any residual N_2O. An evacuation manifold equipped with a vacuum pump and a source of N_2 or He should be used. The headspace of the vial should be evacuated, achieving a vacuum of 2 Torr and back flushed with N_2 twice and then brought to atmospheric pressure. Following the last flush with nitrogen gas close the manifold and lead a tube from one of the manifold sites into water. Reopen the manifold allowing excess N_2 to escape from the Exetainers, while the N_2 remaining in the Exetainers are at atmospheric pressure. The Exetainers are now ready for short term storage or transport to the field and collection of water samples.

Storage and transport of Exetainers containing $HgCl_2$:

Keep in a tightly closed container and store in a cool, dry, ventilated area. Protect from physical damage and direct sunlight. Have a prior idea about the number of samples to

be collected and take the appropriate number to the field. Keep some additional Exetainers, syringes and needles as a reserve in case of emergency. Transport vials in a safe manner to the field by keeping the vials in a holder or a bag. Make sure you have all the essential equipment for collecting a sample before you leave for the field.

Mercuric chloride is expected to significantly bioaccumulate, posing extreme danger to the environment. It is very toxic to aquatic organisms and has the potential to cause long term adverse effects in an aquatic environment. In the occurrence of a spill, pick up/recover spilt material (using appropriate safety equipment) and place in a suitable container for reclamation or disposal. Sprinkle area with sulfur or calcium polysulfide to suppress mercury.

Using an ISCO auto sampler it is possible to attain consecutive sampling of tile drains with the use of pipettes. The pipettes limit the surface area exposed to the atmosphere, decreasing the potential of the water to degas. Place a reusable 10 mL volumetric pipet in the water sampling containers (1 L) (Note: the pipettes may need to be cut to properly fit in the containers). Ensure that the containers are filled to above the bulb of the pipette allowing for sufficient water to sample.

To fill the Exetainers collect 4 mL of water sample using a 20 mL disposable syringe. The syringe is attached to a 3-way stopcock, with one 5/8 inch needle attached and a 12 inch needle attached. Collecting the water sample is done by opening the valve between the 12 inch needle and the syringe, and inserting the needle into the pipette located in the auto sampler. The needle should reach the depth of the pipette bulb, from which a water sample will be drawn from (~5mL). Remove the needle from the syringe

and rotate the stopcock, opening the valve between the syringe and the 5/8 inch needle. Holding the syringe in a vertical position, tap the sides of the needle to free any air bubbles attached to the side of the syringe and then expel the water to the desired volume of 4 mL.

Transfer the 4 mL water sample to the prepared Exetainer. Following injection hold the barrel of the syringe down while withdrawing from the Exetainer to ensure positive pressure is retained in the vial.

Record the vial number and store in a cool location (e.g. a cooler with ice pack). Note that the samples do not have to be maintained at 4 ^{o}C, but elevated temperatures (> 25 ^{o}C) should be avoided.

The vials should be returned to the laboratory for headspace analysis via gas chromatography.

Vials should be allowed to equilibrate at the temperature of the room where the gas chromatographic analysis is to be performed for 24 hours prior to analysis. The temperature of the room during analysis should be recorded.

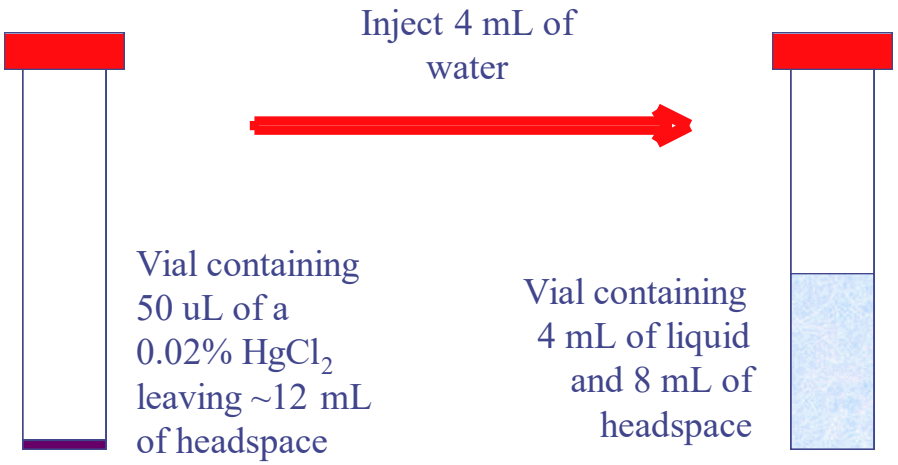

Calculations:

There are two components to the calculation of total dissolved N_2O in tile drainage waters: (i) N_2O accumulation in the headspace of the exetainer and (ii) accumulation of N_2O in the sampled water. The calculation for each component will be done separately and the amounts combined to determine the total original amount of dissolved N_2O.

(i) N_2O (mol) in the headspace (HS):

Volume N_2O_{HS} (µL) = Concentration (mole fraction) N_2O ($L \cdot L^{-1}$) x Volume HS Gas (L)

Since the analysis of the N_2O composition of the sample occurs on a sample that has been brought to atmospheric pressure (1 atm), the volume of the gas in the exetainer is equal to the volume of the exetainer (0.012 L). Alternatively, the increased pressure of

$$M_{N_2O} = \frac{P \times x' \times V_{sample}}{R \times T}$$

the compressed sample (0.012/0.008 atm) and the smaller headspace (0.008 L) can be used. The result is the same.

The temperature used should be that of the lab at the time of analysis in degrees K.

(ii) N_2O (mol) dissolved in water (DIS):

The method of Weiss and Price (1980) was used to calculate the amount of N_2O dissolved in the aqueous phase (C*).

$$C^* = x' * F$$

$$F = K_o * (P - pH_2O) * \exp\left[P * \left(\frac{B + 2\delta}{RT}\right)\right]$$

$$\ln\ pH_2O = 24.4543 - 67.4509 * (\frac{100}{T}) - 4.8489 * \ln(\frac{T}{100})$$

$$\frac{(B + 2\delta)}{RT} = \frac{-9.4563}{T} + 0.04759 - 6.427 * 10^{-5} T$$

The value for the nitrous oxide solubility (K_o) was adjusted for temperature according to the data presented by Weiss and Price (1980).

Total N_2O originally dissolved in tile water:

Total N_2O (mol) = N_2O_{DIS} (mol) + N_2O_{HS} (mol)

Amount of N_2O in L of water (M) = $\frac{\text{Total } N_2O \text{ (mol)}}{\text{Water volume (L)}}$

Safety

- All technicians are responsible for familiarising themselves with the Materials Safety Data Sheets for all chemicals used in this procedure.

• If WHMIS control products must be stored in containers other than their originals, a workplace label must be prepared for the new container. Control products include both pure decanted chemicals and prepared solutions.

Disposal Protocol:

The only regulation governing the disposal of toxic chemicals is that it is illegal to pour it down the drain and allow it to enter the sewage disposal system. Chemical waste disposal companies will dispose of the material for a fee which can be reduced if you provide the waste in the form of a solid instead of a liquid. Fortunately, $HgCl_2$ is fairly easy to convert into a less hazardous solid in the following manner.

In a fume hood, adjust the pH of your waste solution to a pH of 10 with 10% NaOH. Add 20% Na_2S with stirring until no further precipitation occurs. Allow the precipitate to settle. Check for further precipitation by withdrawing a small portion of the clear(er) liquid and adding 20% Na_2S. If a precipitate forms, continue to add 20% Na_2S until none occurs. Allow the precipitate to completely settle, decant or filter the liquid into the drain flushed with large amount soft water. The remaining precipitate is HgS, which can be disposed of with a chemical waste disposal company. HgS is insoluble in H_2O, alcohol and mineral acids and thus, poses a reduced level of risk while handling. Clearly mark the disposal container with a label indicating the contents and that it is a waste chemical.

Note: Any containers used in the preparation, transfer or storage of this material ($HgCl_2$) may be hazardous when empty, possibly retaining product residues.

Greenhouse Gas (CO_2, CH_4 and N_2O) Flux Measurement

Equipment:

chamber tops and collars

soil temperature probe (Cole-Parmer 90090-06)

air temperature and humidity gauge (Cole-Palmer 37952-00)

Hydrosense soil moisture gauge (Campbell Scientific CD620 and CS620)

20mL disposable syringes – One for each chamber (Becton-Dickinson 14-823-2B)

Luer-Lok tip needles – one for each syringe (+ spares) (Becton-Dickinson 14-826AA)

25 gauge

5/8" length

turquoise hub colour

data sheet & pen

stop watch

12mL Exetainers – 4 for each plot, 4 for standard gases and spares (Labco Limited 739W)

Freezer bag to store exetainers

5lb. Bags for soil samples

Procedure: Preparation of Exetainers

Evacuate all exetainers following the "Evacuation of Exetainers" SOP. Utilizing existing labelling codes contained on the exetainers.

Exetainers codes can be written on the data sheet prior to sampling

Insertion of Collars

Collars should be inserted at least 24 hours prior to the first measurement. The lower PVC collar is pressed into the soil at the sites by hand or through the use of a sledge hammer and a wooden block until about 5 cm remains above the soil surface.

If a sledge hammer must be used, place a piece of wood across the collar and hammer on the wood (to protect the edges of the collar from damage).

In cases where the soil is very dry or cemented, collar insertion may require excavation of soil around the outside of collar to ease insertion.

Initial Preparation Prior to Starting Flux Measurement

The objective of this procedure is to use the rate of gas accumulation in the headspace as a measure of the emission of the gas from the soil surface. Therefore, it is important that representative gas samples be collected at the time specified. Careful planning and organization will allow you to effectively move from chamber to chamber and collect samples on schedule. Prior to starting the flux measurement it is useful to layout the chamber tops, exetainers and syringes needed for each plot. Recording the exetainers numbers prior to starting the measurements is also an effective time saving measure. If you do this take care to ensure that the correct exetainers is used for each sampling interval. To ensure that samples are analysed sequentially on the gas chromatograph it is preferable to use sequential numbers for the sampling times for a chamber (e.g. use NS 506, NS 507, NS 508, NS 509 for t=0, t=10, t=20 and t=30 minute samples respectively). Before going out to sample, obtain four (4) exetainers and inject 20mL of the standard gas (0.5ppm N_2O) into each. Record the exetainers numbers on the sheet and store standard vials with sample vials.

Collection of Gas Samples

1. Place the chamber top on top of the collar

Record the time on a data sheet

2. Collect a headspace sample from each chamber immediately after it is sealed.

Insert the needle into the septum

Draw 20 mL of headspace into the syringe, pause 5 seconds to allow the gas to flow into the syringe.

Remove the needle and inject the sample into a previously evacuated 12mL exetainer. Keep the syringe plunger depressed until the needle is removed from the exetainer.

Record the vial number on the data sheet (if you have not already).

3. At the prescribed collection interval (e.g., 10, 20, 30 minutes) collect a headspace sample from each of the chambers using the procedure described above.

Record the exetainers number (if you have not already).

Record the exact time of sampling if it deviates from the planned time.

If one should come across a bad vial, use extra vials on hand or do an emergency evacuation of vial.

Gas Sample Transport and Storage

The samples should be placed in a plastic bag (Ziploc Bag) with their corresponding data sheet. Label the outside of the bag with the site name, person(s) responsible for collecting the samples and sampling date.

Samples should be transported back to the lab in a cooler to moderate temperature fluctuation and provide secure storage

Measurement of Associated Soil Properties

Volumetric Soil Moisture Content

• At each chamber location use the HydroSense soil moisture sensor to record the soil water content. Enter the 12cm probes evenly into the ground (no rocking back and forth) to prevent breakage of probes. This measurement can be made at anytime during

the flux measurement. If the soil is very hard use the guide probe block provided to establish the holes and then insert the HydroSense unit. Record this data on the data sheet.

Air temperature and humidity

- At collar location in the plot use the air temperature/humidity sensor provided to measure the air temperature and humidity at a 10cm elevation (chamber level) above the soil surface. Record this data on the data sheet.

Soil Temperature

- Using an electronic temperature probe insert to a depth 0f 5 cm, record the temperature. Take the soil temperature at each chamber location and record this data on the data sheet.
- This can be done at the time of sampling, or during the incubation period

Measurements to be done periodically (once a month).

Bulk Density

- Collect bulk density samples as per the “Bulk Density” SOP.

Measure the height of the collar

- Using the collar height measuring device, record the length of each of the metal bars protruding from the device once it has been fitted on top of the collar. Note also the number of the measuring device.

Samples Analysis and Calculations

- Headspace concentration of N_2O, CO_2 and CH_4 will be determined by gas chromatography

- For a complete description of calculations, see the "N_2O Standard Curve" or "CO_2 Standard Curve" SOPs

Notes

To facilitate easy location of collars, mark them with a brightly coloured flag or stake.

Incubation period can be made shorter or longer based on the anticipated magnitude of the flux event

Ideally, incubations should be started about five minutes apart

- This timing will be dependent upon the size of the site and the number of people working
- Thus, the ideal sampling strategy should be determined for each site individually

To save time on large sites, two people can work simultaneously such that two sets of incubations are set up at the same time. Alternatively one person can collect one time and the second (and/or third) can collect the next time(s). If this is to be done make sure the stop watches or other timing devices are synchronized.

Calculations

Nitrous Oxide Flux

$$\frac{1uL\,N_2O}{L \bullet hr} x \frac{323.7cm^2 \bullet (15+h)cm}{0.0324\,m^2} x \frac{1L}{1000cm^3} = 9.99 \bullet (15+h)cm \frac{uLN_2O}{m^2 \bullet hr}$$

$$9.99 \bullet h(cm) \frac{uLN_2O}{m^2 \bullet hr} x \frac{1umoleN_2O}{0.0821 \bullet T(K)\,uL\,N_2O} x \frac{44\,ugN_2O}{1umoleN_2O} = 5,353 \frac{(15+h)cm}{T(K)} \frac{ugN_2O}{m^2 \bullet h}$$

$$5,353 \frac{(15+h)cm}{T(K)} \frac{ugN_2O}{m^2 \bullet h} x \frac{10^3\,ngN_2O}{1ugN_2O} x \frac{1h}{60\min} x \frac{1\min}{60\sec} = 1487 \frac{(15+h)cm}{T(K)} \frac{ngN_2O}{m^2 \bullet \sec}$$

$$5,353 \frac{(15+h)cm}{T(K)} \frac{ugN_2O}{m^2 \bullet h} x \frac{1gN_2O}{10^6\,ugN_2O} x \frac{28gN}{44\,gN_2O} x \frac{10^4\,m^2}{1ha} x \frac{24h}{1d} = 817.6 \frac{(15+h)cm}{T(K)} \frac{gN_2O-N}{ha \bullet d}$$

Carbon Dioxide Flux

$$\frac{1uLCO_2}{L \bullet hr} x \frac{323.7(cm^2) \bullet (15+h)cm}{0.0324\,m^2} x \frac{1L}{1000cm^3} = 9.99 \bullet (15+h)cm \frac{uLCO_2}{m^2 \bullet hr}$$

$$9.99 \bullet (15+h)cm \frac{uLCO_2}{m^2 \bullet hr} x \frac{1umoleCO_2}{0.0821 \bullet T(K)uLCO_2} x \frac{44\,ugCO_2}{1umoleCO_2} = 5,353 \frac{(15+h)cm}{T(K)} \frac{ugCO_2}{m^2 \bullet h}$$

$$5,353 \frac{(15+h)cm}{T(K)} \frac{ugCO_2}{m^2 \bullet h} x \frac{1h}{60\min} x \frac{1\min}{60\sec} = 1.487 \frac{(15+h)cm}{T(K)} \frac{ugCO_2}{m^2 \bullet \sec}$$

$$5,353 \frac{(15+h)cm}{T(K)} \frac{ugCO_2}{m^2 \bullet h} x \frac{1kgCO_2}{10^9\,ugCO_2} x \frac{12\,kgC}{44\,kgCO_2} x \frac{10^4\,m^2}{1ha} x \frac{24\,h}{1d} = 0.3504 \frac{(15+h)cm}{T(K)} \frac{kgCO_2 - C}{ha \bullet d}$$

Methane Flux

$$\frac{1uLCH_4}{L \bullet hr} x \frac{323.7(cm^2) \bullet (15+h)cm}{0.0324\,m^2} x \frac{1L}{1000cm^3} = 9.99 \bullet (15+h)cm \frac{uLCH_4}{m^2 \bullet hr}$$

$$9.99 \bullet (15+h)cm \frac{uLCH_4}{m^2 \bullet hr} x \frac{1umoleCH_4}{0.0821 \bullet T(K)\,uLCH_4} x \frac{16ugCH_4}{1umoleCH_4} = 1{,}947 \frac{(15+h)cm}{T(K)} \frac{CH_4}{m^2 \bullet h}$$

$$1{,}947 \frac{(15+h)cm}{T(K)} \frac{ugCH_4}{m^2 \bullet h} x \frac{10^3\,ngCH_4}{1ugCH_4} x \frac{1h}{60\min} x \frac{1\min}{60\sec} = 540.8 \frac{(15+h)cm}{T(K)} \frac{ngCH_4}{m^2 \bullet \sec}$$

$$1{,}947 \frac{(15+h)cm}{T(K)} \frac{ugCH_4}{m^2 \bullet h} x \frac{1gCH_4}{10^6\,ugCH_4} x \frac{12gC}{16gCH_4} x \frac{10^4\,m^2}{1ha} x \frac{24h}{1d} = 350.5 \frac{(15+h)cm}{T(K)} \frac{gCH_4 - C}{ha \bullet d}$$

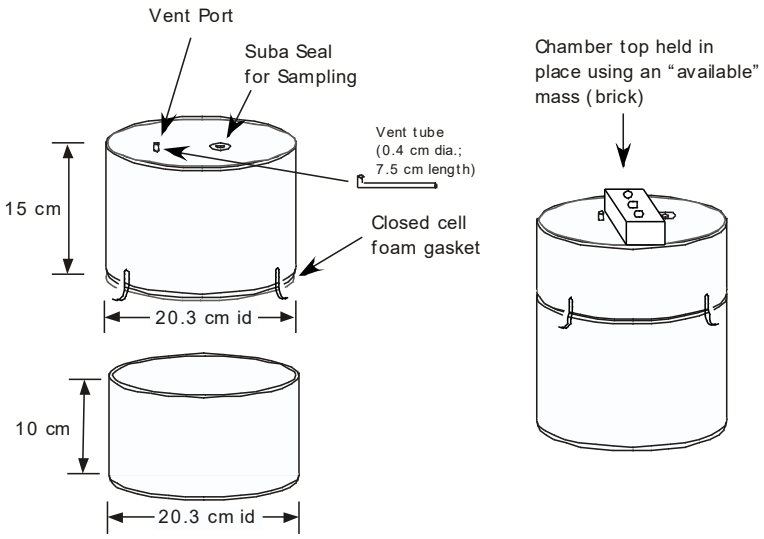

$$Upperchambervolume = \pi \bullet r^2 \bullet h = \pi(10.15)^2 \bullet 15$$

$$volume(L) = \frac{323.7(cm^2) \bullet 15(cm)}{1000} = 4.856L$$

$$Collarvolume = \pi \bullet r^2 \bullet h = \pi(10.15)^2 \bullet h$$

$$volume(L) = \frac{323.7(cm^2) \bullet h(cm)}{1000}$$

$$collararea = \pi \bullet r^2 = \pi(10.15)^2 = 0.0315\,m^2$$

Inorganic N (NH_4^+, NO_2^- and NO_3^-) Extraction

Equipment

4oz. French Square bottles (Fisher Scientific cat# 0332714D)

Whatman No. 42 filter papers (Fisher Scientific cat# 09-855C)

20mL scintillation vials (Fisher Scientific Cat# FS58501-20)

2M KCl solutionExtraction

Prepare 2 M KCl solution by dissolving 150g KCl crystals in 1L distilled water (or 1500g KCL made up to 10L).

Soil

Weigh out a 20g portion of soil into the square French bottles.

Add 100mL of 2M KCl to the square French bottle using a repipettor. Cap the bottles ensuring they are on tight to prevent leaking.. For each set of extractions, prepare a solution blank containing only KCl

Place the bottles on a lateral shaker set at low speed for 1 hour.

After shaking, pass the soil suspension through Whatman No. 42 filter paper.

Funnels are not necessary; filter paper is folded and placed in the funnel rack directly.

Filter paper should be rinsed with extractant prior to filtration.

Collect filtrate in 20mL scintillation vials.

Cap vials and placed in the freezer as soon as possible. The B set may be left overnight if the filtration time prolonged.

To determine soil moisture content, approximately weigh out ~10g fresh soil into pre-labelled aluminium tins. Be sure to record the weight of the tin and tare it prior to

weighing the soil in it. Place tins in oven @ 60°C for 24 hours. Take out tins to cool, record weights of dry soil, and discard soil.

Analysis

Analyse filtrate for NO_3^-, and NH_4^+ using the Technicon Auto-Analyser.

Calculations

1. Calculate the mass of NH_4^+, NO_3^- (µg N g^{-1} soil)

$$\frac{ug\ \ N}{g\ \ soil} = \frac{\left(\frac{ug\ \ N}{mL}\ \ extract - \frac{ug\ \ N}{mL}\ \ blank\right) \bullet (mL\ \ extract + (g\ \ wet\ \ soil \bullet GWC)}{\left(\frac{g\ \ wet\ \ soil}{1 + GWC}\right)}$$

- µg mL^{-1} N comes from the Auto-Analyser
- mass of wet soil/(1 + GMC) gives the mass of oven dry soil
- mass wet soil • GMC gives the mass of water in the sample

Safety

- All technicians are responsible for familiarising themselves with the Materials Safety Data Sheets for all chemicals used in this procedure.
- If WHMIS control products must be stored in containers other than their originals, a workplace label must be prepared for the new container. Control products include both pure decanted chemicals and prepared solutions.

Notes

- Square French bottles should be acid-washed, then rinsed with distilled water and allowed to dry prior to use.
- If more or less soil is used in the analysis, adjust the amount of KCl added so that the ratio of soil:solution remains 1:5.

Eluting the PRS™-Probes (Western Ag Innovations)

PRS™-probes are eluted using a 0.5N HCl solution for 1 hour, following which the eluent is analyzed colourimetrically or with an ICP.

1) Elute the PRS™-probes by adding 17.5 mL (corresponds to 17.5 cm2 surface area of the PRS™-probe membrane) of a 0.5N HCl solution for each PRS™-probe in the bag. If several PRS™-probes are being bulked for analysis, then place all of them in the same bag and add 17.5 mL to the bag for each PRS™-probe in the bag. , i.e., if three PRS™-probes are being bulked in on bag, then 3 x 17.5 mL = 52.5 mL HCl should be added to the bag). Cation and anions PRS™-probes can be combined in the same bag.

2) Remove as much air as possible from the bag (push air bubbles up and away from the membrane surface), thereby ensuring the PRS™-probe is completely immersed in the acid solution. The most effective way of doing this is to hold the bag against the edge of a bench-top and then push the PRS™-probe and eluant against the bench-top – this forces the air up and out of the bag (Figure 3). As much air should be removed out of the bag WITHOUT LOSING ANY OF THE LIQUID. As long as the PRS™-probe is completely immersed and there are no air pockets touching the membrane, the eluant should proceed along fine. Losing a portion of the liquid will alter the ion concentrations and final results and requires adjustment of the elution volume in the supply rate calculation (p. 7). In this case, the amount of acid remaining in the bag will need to be determined. © Western Ag Innovations Inc. http://www.westernag.ca/innov/index.php

3) Be sure to seal the bag properly to eliminated HCl leakage. Loss of HCL from the gab will change the concentration of the eluting solution and artificially increase supply rate results.

4) Let stand for one hour.

5) Transfer the eluate to a separate, clean, labelled 20-dram vial for analysis.

6) Remove the PRS™-probes from the elution bag and return to the soaking container for PRS™-probe regeneration.

Note: Due to the sensitivity of some types of analyses to an acid matrix, some researchers find it more practical to use 1 M KCl or 1 M NaCl as the eluting solution. If doing so however, it is very important that the solutions be stored at 4º C and analysed as quickly as possible due to the potential for microbial activity. To ensure that the PRS™-probes are clean and/or to account for ions that were not cleaned off the PRS™-probes prior to measurements, it is desirable to elute a few "blank" PRS™-probes that have been regenerated but have not been buried in soil as described earlier under "PRS™-probe Blank and Quality Control". The PRS™-probes used as blanks should come from the same "batch" of PRS™-probes that were buried. The eluate from these PRS™-probes should then be analysed for ions in a similar manner as regular sample eluates. If contamination is detected and it is known that there was no contamination of the blank PRS™-probes during burial of the sample PRS™-probes, it may be necessary to subtract the value of the blank eluate from the sample eluates. It may also be necessary to increase the number of wash/regeneration steps prior to the next analyses.

PRS™-Probe Preparation/Regeneration (Western Ag Innovations)

PRS™-probes must be cleaned and regenerated prior to each use. It is very important that PRS™-probes not be contaminated with ions prior to making measurements, as this will confound the results.

1) To begin the wash / regeneration, secure approximately two to four litres of deionized water. Distilled or deionized water should provide reasonable accuracy under normal use.

2) Prepare a soaking solution of 0.5 N HCl

3) Clean ‘used’ PRS™-probes by soaking in the HCl solution for one hour. The mixture should be stirred or agitated every 15 minutes or if possible, shaken continuously at slow speed on a rotary-bench or side to side shaker.

4) Prepare a soaking solution of 0.5 N sodium bicarbonate (NaHCO3).

5) Regenerate ‘cleaned” PRS™-probes by submerging and soaking in the bicarbonate solution. This solution should be changed a minimum of four times, typically at one-hour intervals and should also be stirred on a regular basis or slowly shaken.

6) Rinse ‘regenerated’ PRS™-probes with deionized water.

Note: With each wash, approximately 95% of the soil ions on the PRS™-probe membrane surface are replaced with ions from the wash solution. If you are measuring high nutrient supply rates, there will be a relatively large amount of ions present even after several washes and it may be necessary to increase the number of HCl (and potentially NaHCO3) wash/regeneration steps. Also, if blank PRS™-probe have levels of contamination it can be an indication that the PRS™-probes need more HCl washes.